

November 7, 2001

U. S. Nuclear Regulatory Commission
ATTN: Document Control Desk
Mail Station P1-137
Washington, D.C. 20555-0001

Gentlemen:

ULNRC- 04558



**DOCKET NUMBER 50-483
CALLAWAY PLANT
UNION ELECTRIC COMPANY
RESPONSE TO REQUEST FOR ADDITIONAL INFORMATION
ON REVISION TO TECHNICAL SPECIFICATION 5.5.9
"STEAM GENERATOR (SG) TUBE SURVEILLANCE PROGRAM"**

References: 1) ULNRC-4391, dated February 15, 2001
2) NRC letter dated October 16, 2001

AmerenUE transmitted an application for amendment to Facility Operating License No. NPF-30 for the Callaway Plant in Reference 1. The NRC Staff requested additional information regarding the submittal in the NRC's Request for Additional Information (RAI) as discussed in Reference 2. The requested information is provided in the Attachments to this letter as are additional changes to Technical Specification (TS) 5.5.9 as identified during a meeting held on September 26th and 27th, 2001 with AmerenUE, Framatome ANP, and the NRC Staff.

The additional changes to TS 5.5.9d.1.j) 2) are as follows: 1) The revision level and date for Framatome ANP's Topical Report BAW-10219P has been changed to "Revision 4, dated 12/00," and a reference to the responses to the NRC's RAI's has been added. 2) A statement has been added with regards to the 20% through wall plugging limit to state that all sleeves with ID flaws will be removed from service upon detection. 3) A statement has also been added with regards to locked tubes to state that no sleeves will be installed in the periphery where potentially locked tubes could cause high axial loads.

It has been determined that these additional changes to TS 5.5.9 are still bounded by the significant hazards consideration submitted in Reference 1 and therefore do not involve a significant hazards consideration as determined by 10 CFR 50.92, and also an environmental assessment need not be prepared pursuant to 10 CFR 51.22(b).


Attachments 1 through 5 provide the required affidavit, the description and assessment, the marked-up TS page, the retyped TS page, and the RAI responses.

AP01

Framatome ANP has determined that certain information associated with the installation process for Electrosleeves is proprietary, and is thereby supported by an affidavit signed by Framatome ANP, the owner of the information. The affidavit sets forth the basis on which the information may be withheld from public disclosure by the Commission and addresses with specificity the considerations listed in paragraph (b)(4) of 10 CFR 2.790. Accordingly, it is respectfully requested that the information that is proprietary to Framatome ANP be withheld from public disclosure in accordance with 10 CFR 2.790.

If you have any additional questions on this amendment application, please contact Mr. Dave Shafer at (314) 554-3104.

Very truly yours,



John D. Blosser
Manager, Regulatory Affairs

JMC/

- Attachments:
- 1) Affidavit
 - 2) Description and Assessment
 - 3) Marked-up Technical Specification Page
 - 4) Retyped Technical Specification Page
 - 5)
 - a) RAI Questions and Responses (Proprietary)
 - b) RAI Questions and Responses (Non-proprietary)
 - c) Proprietary Affidavit

STATE OF MISSOURI)
)
CITY OF ST. LOUIS)

S S

John D. Blosser, of lawful age, being first duly sworn upon oath says that he is Manager Regulatory Affairs, for Union Electric Company; that he has read the foregoing document and knows the content thereof; that he has executed the same for and on behalf of said company with full power and authority to do so; and that the facts therein stated are true and correct to the best of his knowledge, information and belief.

By *Blosser*
John D. Blosser
Manager Regulatory Affairs

SUBSCRIBED and sworn to before me this 7th day
of November, 2001.

Melissa L. Orr

MELISSA L. ORR
Notary Public - Notary Seal
STATE OF MISSOURI
City of St. Louis
My Comm. Expires June 23, 2003

cc: M. H. Fletcher
Professional Nuclear Consulting, Inc.
19041 Raines Drive
Derwood, MD 20855-2432

Regional Administrator
U.S. Nuclear Regulatory Commission
Region IV
611 Ryan Plaza Drive
Suite 400
Arlington, TX 76011-8064

Senior Resident Inspector
Callaway Resident Office
U.S. Nuclear Regulatory Commission
8201 NRC Road
Steedman, MO 65077

Mr. Jack Donohew (2)- **OPEN BY ADDRESSEE ONLY**
Office of Nuclear Reactor Regulation
U.S. Nuclear Regulatory Commission
1 White Flint, North, Mail Stop OWFN 7E1
11555 Rockville Pike
Rockville, MD 20852-2738

Manager, Electric Department
Missouri Public Service Commission
P.O. Box 360
Jefferson City, MO 65102

Ron Kucera
Department of Natural Resources
P.O. Box 176
Jefferson City, MO 65102

Denny Buschbaum
TU Electric
P.O. Box 1002
Glen Rose, TX 76043

Pat Nugent
Pacific Gas & Electric
Regulatory Services
P.O. Box 56
Avila Beach, CA 93424

bcc: Phyllis Murdock/A160.761
/QA Record (CA-758)
E210.01
J. V. Laux
G. L. Randolph
R. J. Irwin
S. Gallagher
J. D. Blosser
D. E. Shafer (2)
S. Wideman (WCNOC)
Gerald Falibota, (Bechtel)
J. D. Schnack
NSRB (Susan Klang, CA460)
J. M. Chapman
T. E. Herrmann
B. S. Humphries (Framatome ANP)
A140.0001 (1216)

ULNRC-04558

ATTACHMENT 2

DESCRIPTION AND ASSESSMENT

DESCRIPTION AND ASSESSMENT

1.0 INTRODUCTION

- 1.1** These additional changes to the original License Amendment Request (LAR), submitted by ULNRC-4391, dated February 15, 2001, are requests pursuant to 10 CFR 50.90 to revise Technical Specification (TS) 5.5.9, "Steam Generator (SG) Tube Surveillance Program" for Callaway Plant to provide correction and clarification to the TS based on discussions and meetings with the NRC Staff.

1.2 Final Safety Analysis Report (FSAR) Section

There are no changes to the Callaway Plant FSAR associated with this LAR submittal.

2.0 DESCRIPTION

These additional changes would revise Administrative Controls TS 5.5.9d.1.j) 2) to make the following changes: 1) The revision level and date for Framatome ANP's Topical Report BAW-10219P has been changed to "Revision 4, dated 12/00," and a reference to the responses to the NRC's Request for Additional Information (RAI) has been added. 2) A statement has been added with regards to the 20% through wall plugging limit to state that all sleeves with ID flaws will be removed from service upon detection. 3) A statement has also been added with regards to locked tubes to state that no sleeves will be installed in the periphery where potentially locked tubes could cause high axial loads.

3.0 BACKGROUND

ULNRC-4391, dated February 15, 2001 submitted a proposed LAR to remove the two operating cycle limit for steam generator tubes repaired with Electrosleeves. This LAR was based on Framatome ANP's Topical Report BAW-10219P, Revision 4. Revision 4 of this topical report addressed the issues discussed in Section 3.10 of the NRC Staff's Safety Evaluation for Amendment No. 132 and provided the evaluation and justification for the proposed LAR. The NRC reviewed the proposed LAR and developed a set of questions with regard to the submittal. Responses to the NRC's Request for Additional Information were prepared by AmerenUE and Framatome ANP and a meeting was held with the NRC on September 26-27, 2001 to discuss the RAI's and responses. At this meeting it was noted that TS 5.5.9d.1.j) 2) did not contain the correct revision number and date for Revision 4 of Topical Report BAW -10219P. It was also decided at this meeting to add statements to the TS to state that all sleeves with ID pits will be removed from service upon detection and that no sleeves will be installed in the periphery of the steam generators.

4.0 TECHNICAL ANALYSIS

These additional changes to TS 5.5.9 are based on agreements reached in meetings held on September 26-27, 2001 between AmerenUE, Framatome ANP, and the NRC Staff. These additional changes are to correct the date and revision level of the latest Framatome ANP topical report and to add statements to the TS imposing additional restrictions which would removing from service upon detection, sleeves with ID flaws and not allow the installation of sleeves in the periphery of the steam generators. These

additional changes are providing only correction and clarification to the TS and any additional technical analysis other than that already provided in ULNRC-4391 is not warranted.

5.0 REGULATORY ANALYSIS

5.1 No Significant Hazards Determination

The significant hazards determination submitted in Attachment 2 to ULNRC-4391 is still valid for these additional proposed changes since they represent clarification or additional restrictions to that originally proposed, therefore no additional significant hazards consideration has been performed.

5.2 Regulatory Safety Analysis

The regulatory safety analysis submitted in Attachment 2 to ULNRC-4391 is still valid for these additional proposed changes since they represent clarification or additional restrictions to that originally proposed, therefore no additional regulatory safety analysis has been performed.

6.0 ENVIRONMENTAL EVALUATION

The environmental evaluation submitted in Attachment 2 to ULNRC-4391 is still valid for these additional proposed changes since they represent clarification or additional restrictions to that originally proposed, therefore no additional environmental evaluation has been performed.

7.0 REFERENCES

1. ASME Code Case N-504-1, "Alternative Rules for Repair of Class 1, 2, and 3 Austenitic Stainless Steel Piping."
2. ULNRC-03910, dated October 27, 1998.
3. ULNRC-4391, dated February 15, 2001.
4. NRC Letter, dated October 16, 2001.

ULNRC-04558

ATTACHMENT 3

MARKUP OF TECHNICAL SPECIFICATION PAGE

5.5 Programs and Manuals

5.5.9 Steam Generator (SG) Tube Surveillance Program (continued)

- j) Tube Repair refers to a process that reestablishes tube serviceability. Acceptable tube repairs will be performed by the following processes:
- 1) Laser welded sleeving as described in Westinghouse Technical Report WCAP-14596-P, "Laser Welded Elevated Tube Sheet Sleeves For Westinghouse Model F Steam Generators." March 1996 (W Proprietary)
 - 2) Electrosleeving as described in Framatome Technical Report BAW - 10219P, Revision 4, ~~12/003-10/98~~, "Electrosleeving Qualifications for PWR Recirculating Steam Generator Tube Repair, -" **and as supplemented by the information provided by ULNRC-04558, dated November 7, 2001.** The plugging or repair limit for the pressure boundary portion of Electrosleeves is determined to be 20% through wall of the nominal sleeve wall thickness (as determined by NDE). The 20% plugging or repair limit will apply to inner diameter pits in Regions B and C, **however all sleeves with detected ID flaw indications will be removed from service upon detection.**

Electrosleeves will not be installed in the outermost periphery tubes of the steam generator bundles where potentially locked tubes would cause high axial loads.

~~All steam generator tubes containing an Electrosleeve will be removed from service within 2 cycles following installation of the first Electrosleeve.~~
- k) Degraded Sleeve means a sleeve containing imperfections greater than 0% but less than 20% of the nominal wall thickness caused by degradation.

2. The steam generator status shall be determined after completing the corresponding actions (plug or repair by sleeving all tubes exceeding the plugging or repair limit and all tubes containing through-wall cracks) required by Tables 5.5.9-2 and 5.5.9-3.

(continued)

5.5 Programs and Manuals

Reports

The contents and frequency of reports concerning the steam generator tube surveillance program shall be in accordance with Specification 5.6.10.

(continued)

ULNRC-04558

ATTACHMENT 4

RETYPE TECHNICAL SPECIFICATION PAGE

5.5 Programs and Manuals

5.5.9 Steam Generator (SG) Tube Surveillance Program (continued)

- j) Tube Repair refers to a process that reestablishes tube serviceability. Acceptable tube repairs will be performed by the following processes:
- 1) Laser welded sleeving as described in Westinghouse Technical Report WCAP-14596-P, "Laser Welded Elevated Tube Sheet Sleeves For Westinghouse Model F Steam Generators." March 1996 (W Proprietary)
 - 2) Electrosleeving as described in Framatome Technical Report BAW - 10219P, Revision 4, 12/00, "Electrosleeving Qualifications for PWR Recirculating Steam Generator Tube Repair," and as supplemented by the information provided by ULNRC-04558, dated November 7, 2001. The plugging or repair limit for the pressure boundary portion of Electrosleeves is determined to be 20% through wall of the nominal sleeve wall thickness (as determined by NDE). The 20% plugging or repair limit will apply to inner diameter pits in Regions B and C, however all sleeves with detected ID flaw indications will be removed from service upon detection.
- Electrosleeves will not be installed in the outermost periphery tubes of the steam generator bundles where potentially locked tubes would cause high axial loads.
- k) Degraded Sleeve means a sleeve containing imperfections greater than 0% but less than 20% of the nominal wall thickness caused by degradation.

2. The steam generator status shall be determined after completing the corresponding actions (plug or repair by sleeving all tubes exceeding the plugging or repair limit and all tubes containing through-wall cracks) required by Tables 5.5.9-2 and 5.5.9-3.

Reports

The contents and frequency of reports concerning the steam generator tube surveillance program shall be in accordance with Specification 5.6.10.

(continued)

**REQUEST FOR ADDITIONAL INFORMATION
REVIEW OF THE CALLAWAY PLANT APPLICATION
FOR REVISION TO TECHNICAL SPECIFICATION 3/4.4
TAC NUMBER: MB1214**

On May 21, 1999, the NRC granted a limited, two-cycle approval to Union Electric (UE) for Electrosleeve repairs at Callaway Plant, based on some unresolved technical issues that restricted the period of approval. The staff expected that UE would address the remaining technical issues, discussed below, in order to seek approval without limitations during the two-cycle period. These issues were discussed in detail in a letter from the NRC staff to UE dated May 20, 1998. Some of the technical issues pertained to weaknesses in the UT qualification data and lack of experience with nanocrystalline nickel material in the steam generator. The staff also had concerns about the UT technique's ability to inspect dented intersections. To remove the two-cycle restriction, the staff was expecting UE to provide additional technical basis to show that the UT technique could reliably size stress corrosion cracks (SCC). UE was also asked to provide additional UT data on pits and disbonds. Based on the staff's evaluation of data that had been previously submitted by UE, the staff was concerned that a safety significant flaw could be undersized.

The staff also told UE that for a permanent approval, the licensee needed to provide additional details on the exclusion of tubes due to locked tube effects and propose specific text to incorporate exclusion requirements into the license for the Callaway Plant.(See Response RAI #A) In addition, the staff requested additional data to support the equivalency of a one-directional approach to sizing flaws by UT examinations, as compared to the two-directional UT approach. The staff indicated that the depth to which these issues would need to be addressed is dependent on how the licensee addresses the UT depth sizing of the SCC issued described above.

The NRC staff held a public meeting on June 7, 2001 with UE and Framatome Technologies Inc. (FTI) to discuss a UE license amendment request dated February 15, 2001. This proposed license amendment would revise Technical Specification 5.5.9 to remove the two cycle operating limit and allow all steam generator tubes repaired with Electrosleeved tubes to remain in service. The proposed change is based on the evaluations and justifications presented in a FTI topical report, BAW-10219P, Revision 4, "Electrosleeving Qualification for PWR Recirculating Steam Generator Tube Repair."

The NRC staff indicated at the meeting that they would develop request for additional information questions, based on the material presented and discussed at the June 7, 2001 meeting and from their review of the FTI topical report. The letter from UE to the NRC, dated February 15, 2001, conveying the FTI topical report, requested that the NRC staff focus their review on Section 11.0 of the report and the Appendix J qualified NDE techniques for examination of the Electrosleeves that will remain in service. The staff acknowledges that Section 11.0 pertains to the technical justifications of the NDE techniques requested by the NRC, and accordingly, has focused most of its review on this section. However, a few questions regarding changes to repair limits, discussed in Section 12.0, have been included. In addition, the staff noted in its review of the report that some issues, such as the one-directional versus two-directional UT approach to sizing flaws, were addressed. Others, such as the specific details on tubes that would be included in an exclusion zone due to locked tube effects, were not explicitly addressed.

The staff developed a set of questions, which are presented below. Some general themes emerged while developing the questions. These themes include concerns about the qualification data set, detecting and sizing primary water stress corrosion cracking (PWSCC)/outside diameter stress

corrosion cracking (ODSCC)/pits/disbonds, specifics about the use of UT techniques and data analysis, and cited repair limits. In the current revision to the topical report, the PWSCC flaws from the previously submitted data sets have been removed. The staff has continuing concerns about UE's ability to detect PWSCC flaws, due to issues raised during the previous license amendment review about the UT technique undersizing PWSCC flaws. Based on the past review, the staff was expecting additional data and analysis on detection of ID flaws to support the current license amendment review, which was not provided.

Additionally, the FTI report often provides summaries of the data, without providing the actual analyst data sets. This prevents the staff from making an independent review and finding that the techniques are adequate to detect and size the range of possible flaws before they result in reductions of required margins. In a similar manner, different factors and values are presented throughout the report without discussing how they were derived.

The staff noted that a number of the data sets have been changed since the last revision of the topical report, and some data has been deleted. For example, new data sets have been added for dent detection and sizing, combined wall thickness measurements, and ODSCC detection and sizing to Revision 4 of BAW-10210P. The staff would like to understand the basis for selecting the data sets and the applicability of the data sets to Callaway. The content of the data sets was discussed briefly in the June 7, 2001 meeting, and is also discussed in the questions below. The staff also has concerns about the applicability of the data sets to the field conditions at Callaway. The basis for the staff concerns is that the qualification of the examination technique needs to demonstrate the ability to detect and size flaws that are representative of those that are expected to be in tubes that are sleeved at Callaway.

NRC Concerns from Introduction

RAI #A "The staff also told UE that for a permanent approval, the licensee needed to provide additional details on the exclusion of tubes due to locked tube effects and propose specific text to incorporate exclusion requirements into the license for the Callaway Plant."

Response:

Section 8.5 of BAW-10219P, Rev. 4 provides discussion on the locked tube issue. In addition locked tubes are identified for evaluation in Section 12. Figure 8.2.1 provides direction for identification of tubes to be excluded for installation of an Electrosleeve **if circumferential degradation is defined**. Appendix B provides direction for utility identification of tubes to be excluded.

No sleeves were installed within 7 tube rows/pitches of the wedge supports at Callaway. AmerenUE will add a statement to the Technical Specification prohibiting the installation of Electrosleeves in any outermost periphery tube.

Data Sets Used for Qualification

RAI #1. In reviewing the qualification program described in Section 11.9, the staff had overlying concerns about how well the sample set represented the conditions at Callaway. The staff identified the following concerns about the data set used in Section 11.9.1:

A “thin Electrosleeve repair” that was “typically 0.012 inch” was applied for the tubes used in the qualification program sample set, rather than the nominal thickness used at Callaway. How does the use of a thinner sleeve impact the qualification, and how is this demonstration representative of the actual conditions at Callaway? (Page 11-59, BAW-10219P, Rev. 4)

Section 11.8.5 states that inner diameter profilometry is used to detect and size dented regions located in the parent tube to sufficient accuracy to determine if the Electrosleeve operation can be performed. The staff believes it is also necessary to demonstrate that dents do not affect the ability of the UT technique to detect and size flaws. What was the range of dent sizes in the sample set presented in Section 11.9.1? Are they representative of the full range of dents sizes that could be Electrosleeved? (Pages 11-57 to 11-63, BAW-10219P, Rev. 4)

What were the maximum depths for the axial and circumferential cracks listed in Tables 11.9.1 to 11.9.4? Relatively long flaws were used in this data set. Are these flaw lengths representative of those that would be sleeved at Callaway? Are there a range of flaw depths, similar to what you would identify at Callaway? (Pages 11-57 to 11-63, BAW-10219P, Rev. 4)

Response:

Representation of Conditions at Callaway

ECT results are used to identify indications in Steam Generator Tubing, which must either be removed from service by plugging or repaired using a Tech. Spec. Amendment approved "sleeve". For UT qualification purposes, corrosion induced flaws were produced in the laboratory and ECT detection was used to assist in the selection of flaws. The known degradation modes in a steam generator tube are associated with top-of-tube sheet expansions and support plate locations. Use of these geometry conditions is consistent with the EPRI guideline (J2.2.1) where in “the influence of extraneous test variables associated with each of the damage mechanisms (e.g., denting, deposits, tube geometry changes) shall be assessed.” Top-of-tube sheet expansion transition samples and dented samples were used as a method of inducing axial and circumferential ODSCC.

Due to geometry, the axial flaw lengths for an expansion transition are relatively short, typically less than 0.5 inch, and consequently extent (length) sizing these flaws by themselves did not fulfill the sample set requirements for the extent sizing qualification. The longer laboratory environment ODSCC flaws may represent conditions that exceed plant technical specification tube plugging margins, but these flaws were used to represent a sleeved tube that may have additional service induced degradation within the parent tube material. See pgs. 8-19, 11-58, BAW-10219P-Rev.4.

The sleeve installation at Callaway was performed at the top of the tube sheet expansion. Structurally significant flaw lengths and depths were selected to span the expected structural limits for the qualification sample set(s). These samples would not necessarily represent the degradation at Callaway, but could represent continued degradation, should it occur. Callaway has not detected denting and denting is not expected at Callaway due to stainless steel quatrefoil support plates, periodic chemical cleaning, and controls for the secondary side chemistry.

Impact of Using a Thinner Sleeve

The "use of a thinner sleeve" was included in the qualification as a variable. Although the sleeve thickness contributes to the "time-of-flight" of the ultrasonic sound energy within the combined wall thickness, the detection of the half skip reflection is used to determine "flaw length" for ODSCC. Based upon the results of the extent sizing qualification, specifically the circumferential crack set, the addition of sleeve material did not affect detection of the half skip reflection. In addition, the length sizing is based on the accuracy of the axial or circumferential encoder, which are not affected by sleeve thickness. As presented in BAW-10219P-Rev 4, pg. 11-58: "Typically, axial cracks in the tube-sheet expansion transition region are less than 0.5 inch length and are not structurally challenging after the Electrosleeve repair. Long circumferential cracks at the expansion transition were chosen to demonstrate the ability of the technique to accurately extent size a circumferential crack after the application of the structural (thick) Electrosleeve repair." The axial cracks, in the extent sizing crack set, had axial extents of sufficient length and mix to meet the requirements of EPRI Appendix J. The lengths measured with and without the sleeve are the same, based upon a comparison of the average errors and standard deviations for the pre-sleeve data versus the post-sleeve data (Table 11.10.2). Therefore the sleeve thickness does not make a significant difference in the detection and length sizing performance of the UT technique.

Dented Samples Used in Qualification Data Sets

As discussed on page 11-59, both the axial and circumferential detection and extent sizing data sets contained dented samples. Table R1-1 summarizes the dented samples used in the extent sizing data sets, and the maximum measured depth (by destructive examination) of the corresponding crack. The results of the extent sizing qualification presented in Tables 11.9.1 through 11.9.4 support the statement that "the dent does not effect the ability...to detect cracking" (pg. 11-15).

Since the slope of an expansion transition is more severe than the slopes associated with denting at support structures, the inclusion of dented tubes in the depth sizing sample set was not necessary, although some dented samples were included in the peer review as documented in ETSS 303. A slope angle as large as 6 degrees would still produce traverse shear waves, in the material, at an angle between 30 degrees and 65 degrees, which is sufficient for detection and sizing in accordance with the procedures. The profilometry plots in Figures R1-1 through R1-4 present the slopes associated with dents and expansion transitions.

The variables considered in ODSCC flaw extent (length) sizing qualification (pg. 11-59):

Tube size:	7/8" x 0.050", 3/4" x 0.043"	
Sleeve thickness:	[] ^{b,c,d,e}
Flaw Type:	Axial (18 samples), Circumferential (18 samples).	
Geometry:	Dents (in 7/8"), Expansion transitions (in 3/4").	

Maximum Depths for Samples in Tables 11.9.1 to 11.9.4

Section 11.9.1, BAW-10219P-Rev.4 is qualification of **Extent (flaw length)** measurement. Thus the Acquisition Parameters, pg. 11-16, BAW-10219P-Rev 4, associated with axial and circumferential position encoder(s) were qualified. The analysis and destructive evaluation that was performed for the extent qualification did not include detailed depth sizing, nor was the destructive examination intended to define the maximum depth. The maximum **observed** depth for each sample ranged from 0.015 to 0.062 inch, as shown in Table R1-1. The dent sizes ranged from 0.000 to 0.033 inch.

Note that eight (8) circumferential crack samples were utilized in both the extent sizing and depth sizing data sets. These samples are 013-8, 013-9, 022-14, 022-15, 023-16, 023-17, 024-18, and 024-19. The maximum crack depths for these samples are reported in Table 11.9.7 in the Topical Report.

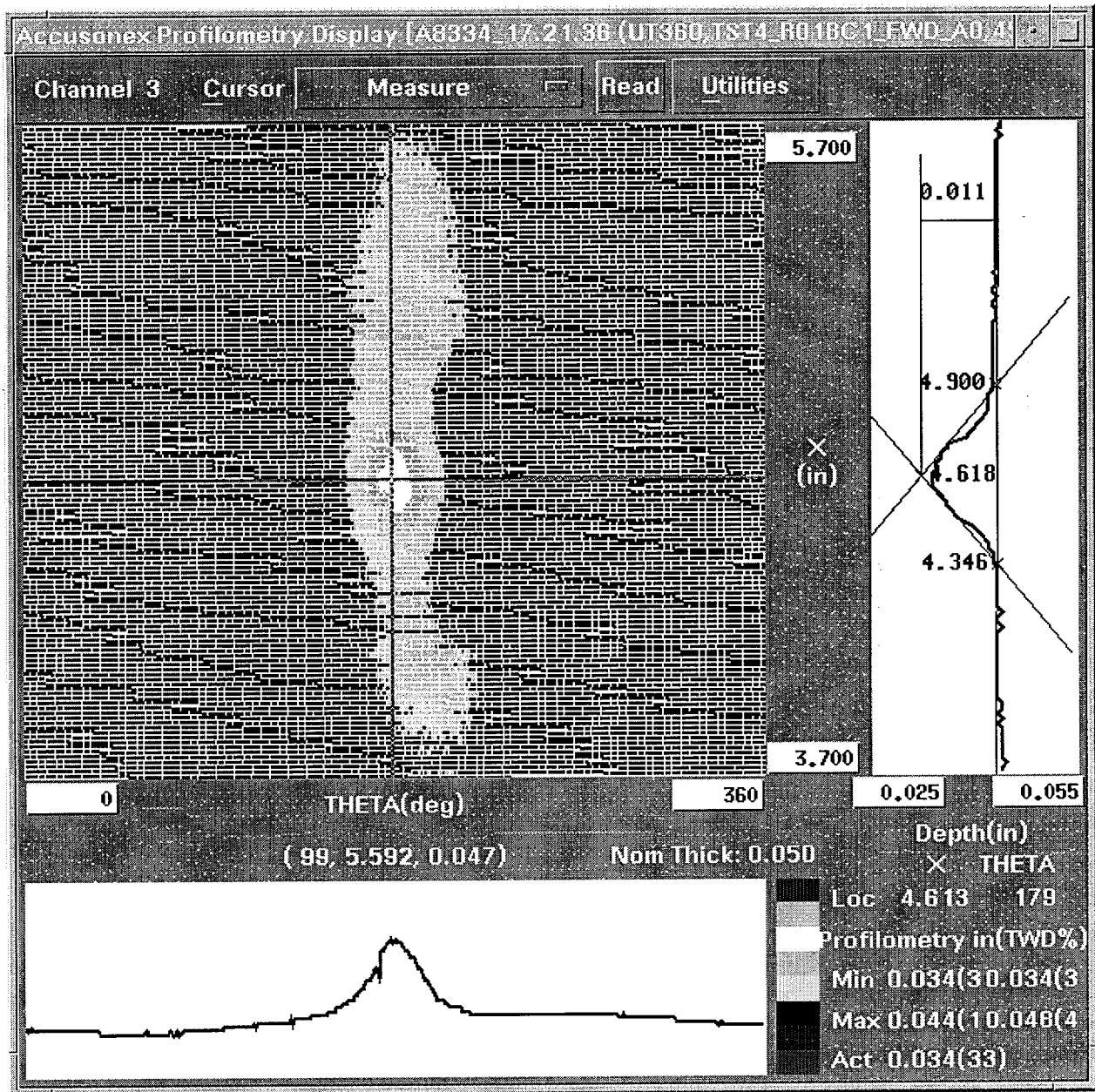


Figure R1-1

This is the profilometry plot for the dented tube TST4-018-1. This tube has a 0.010 inch dent (Table 11.8.12). From this plot, the various slopes associated with this dent can be computed. For example, the axial slopes would be computed as $\text{ATAN}(0.011/(4.900 - 4.618))$ or 2.2 degrees and $\text{ATAN}(0.011/(4.618 - 4.346))$ or 2.3 degrees.

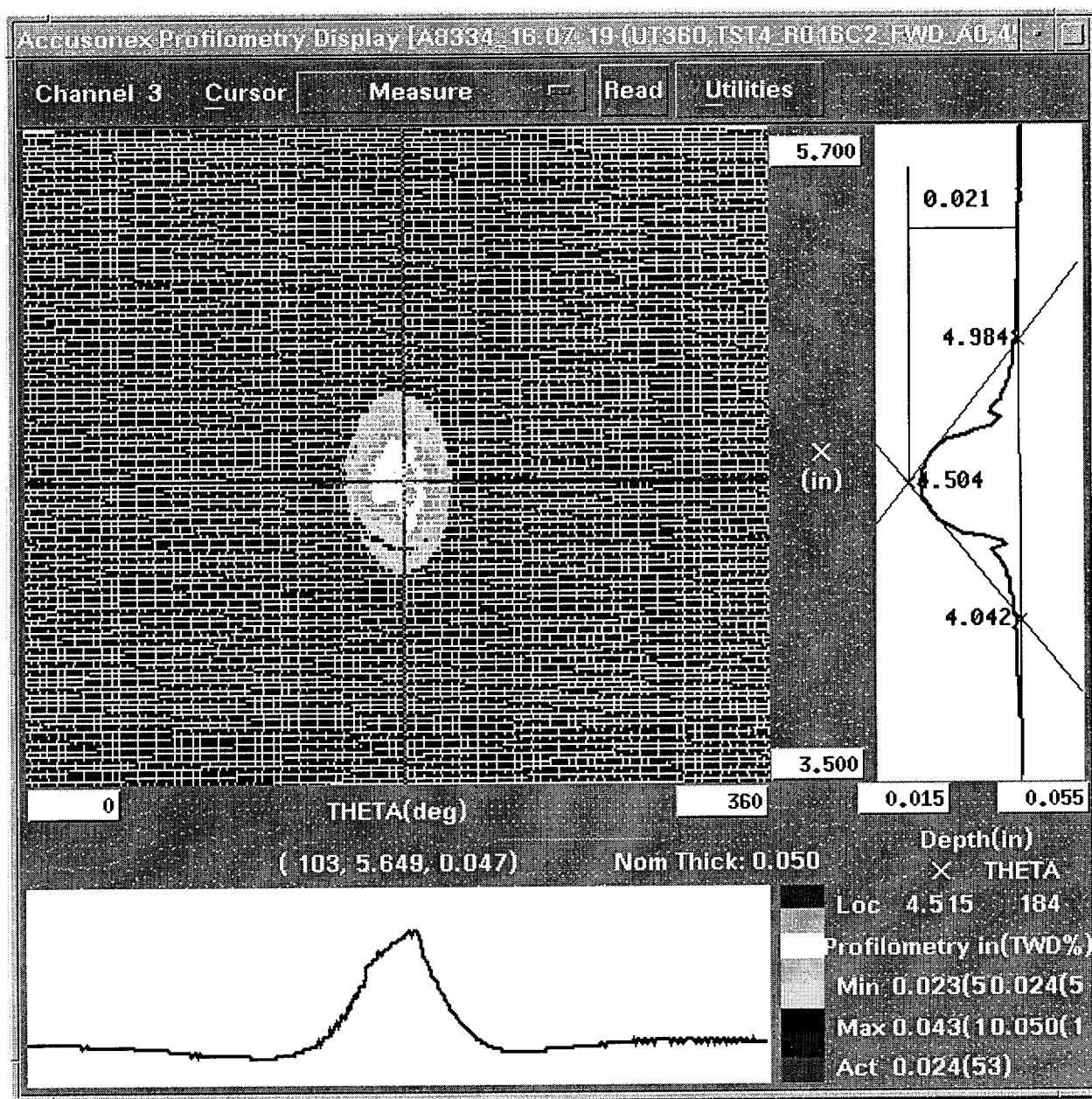


Figure R1-2

This is the profilometry plot for the dented tube TST4-016-2. This tube has a 0.021 inch dent (Table 11.8.12). From this plot, the various slopes associated with this dent can be computed. The axial slopes would be computed as $\text{ATAN}(0.021/(4.984 - 4.504))$ or 2.5 degrees and $\text{ATAN}(0.021/(4.504 - 4.042))$ or 2.6 degrees.

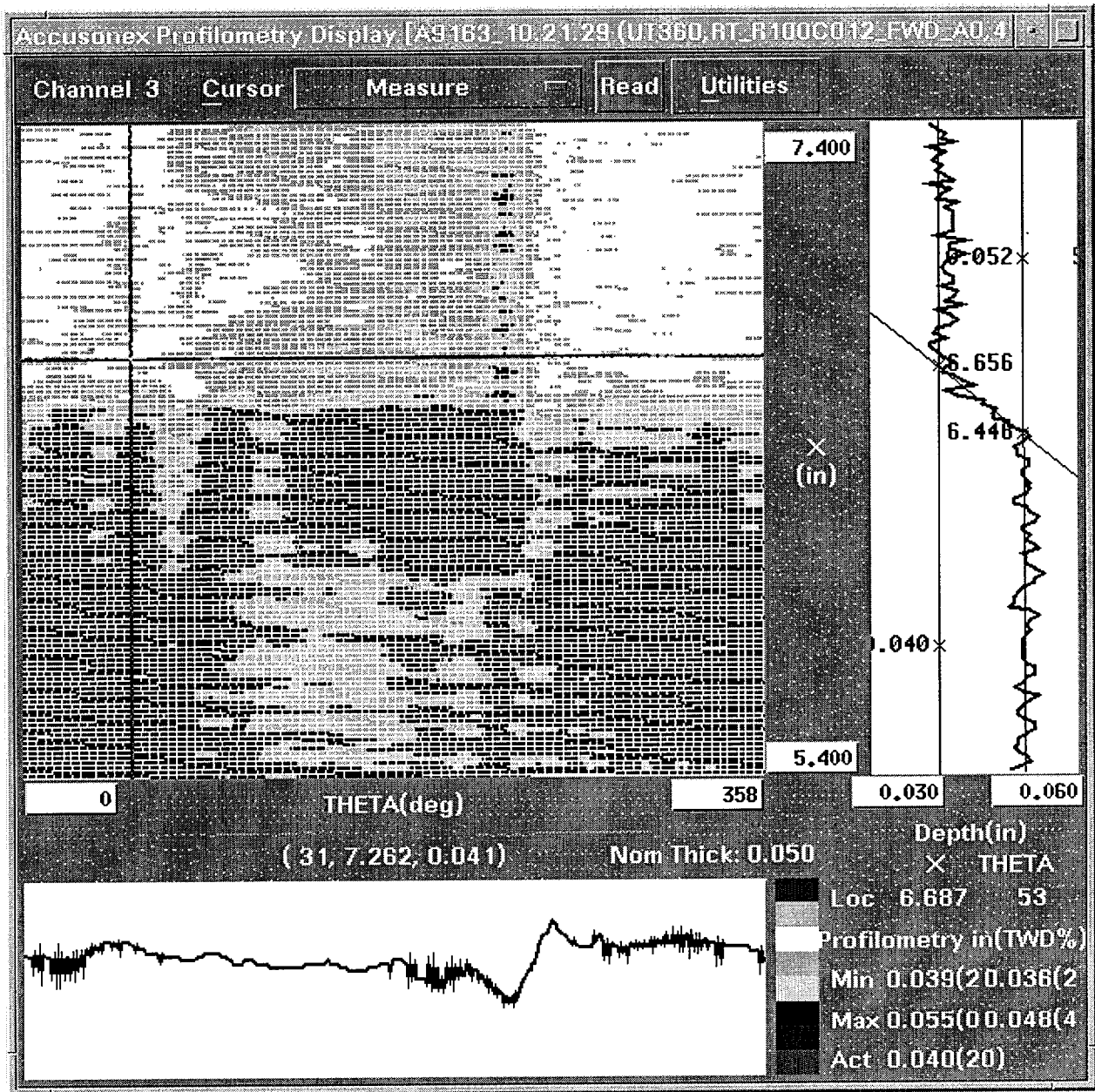


Figure R1-3

This is the profilometry plot for the expansion transition tube RT100-012. The profile shown is for the transition and circumferential location associated with axial crack A12. Axial crack A12 has a DE reported maximum depth of 0.011 inch. This crack was detected and depth sizing from the pre-sleeve data. This is the pre-sleeve acquisition. The axial slope would be computed as $\text{ATAN}((0.052 - 0.040)/(6.656 - 6.446))$ or 3.3 degrees

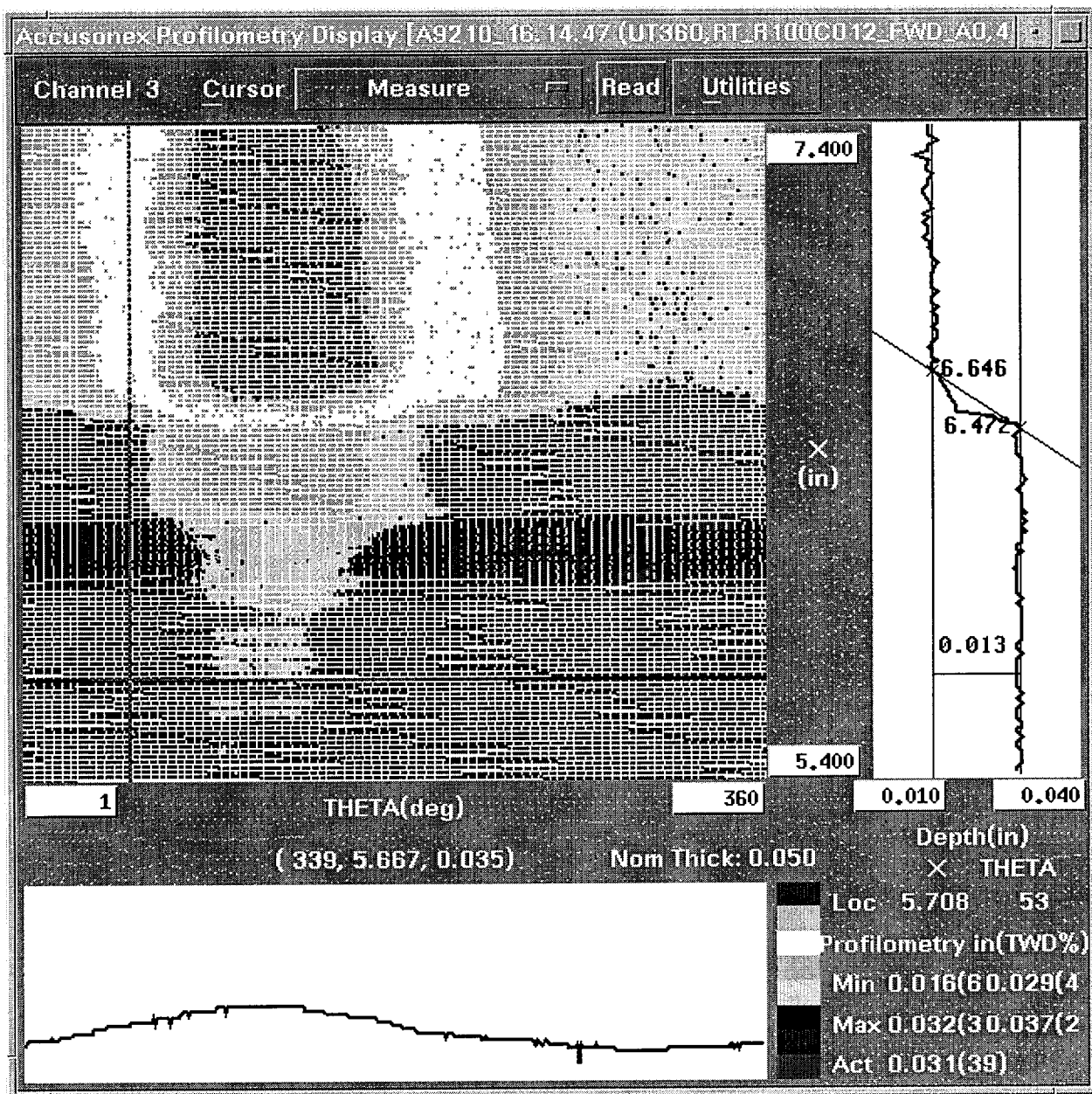


Figure R1-4

This is the profilometry plot for the expansion transition tube RT100-012. The profile shown is for the transition and circumferential location associated with axial crack A12. Axial crack A12 has a DE reported maximum depth of 0.011 inch. This crack was detected and depth sizing from the post sleeve data. This is the post sleeve acquisition. The axial slope would be computed as $\text{ATAN}(0.013/(6.646 - 6.472))$ or 4.3 degrees

The table below contains the dented tube samples that appear in Tables 11.9.1 through 11.9.4 in the Topical Report. The "UT Measured Dent Deformation" is presented in accordance with the profilometry procedure. The "DE Measured Crack Depth" is the maximum recorded crack depth from the flaw extent destructive evaluation. These samples were cut to follow the crack along the length and "find" the crack end points.

Table R1-1

Tube	UT Measured Dent Deformation (inch)	DE Measured Crack Depth (inch)
009-1	0.003	0.045
009-3	0.004	0.050
011-3	0.011	0.048
012-3	0.009	0.036
013-2	0.005	0.050
017-1	0.000	0.037
020-1	0.008	0.048
021-1	0.004	0.049
023-1	0.011	0.047
025-3	0.010	0.050
027-1	0.016	0.049
028-1	0.008	0.047
030-1	0.033	0.019
031-1	0.007	0.049
032-2	0.006	0.018
034-1	0.008	0.047
035-1	0.012	0.045
040-1	0.003	0.049
039-3	0.018	0.049
044-2	0.020	0.023
044-10	0.009	0.023
044-14	0.003	0.023
046-1	0.007	0.033
053-1	0.014	0.027
063-1	0.011	0.014
064-1	0.004	0.047
070-1	0.003	0.047
072-1	0.007	0.062

Note:

Sample 072-1 is a sleeved tube that was pressure cycled to propagate the ODSCC crack through the tube wall and then propagate a fatigue crack into the sleeve. Therefore the "DE Measured Crack Depth" exceeds the parent tube wall thickness.

RAI # 2. Prior to the June 7, 2001 meeting, the staff compared the UT data sets from the current proposed license amendment request with the UT data sets provided for the license amendment review for the 5/21/99 safety evaluation. The staff noted that the new data sets appeared to contain only a portion of the data from the old data sets. During the 6/7/01 meeting, the Framatome discussed the differences in the data sets. They indicated that the UT data collection procedures had become more proceduralized over time, so they did not feel it was appropriate to utilize the old data that may have been collected using different procedures (and was no longer available because it had been destructively examined).

However, following the meeting the staff further reviewed the data sets and it appears that some of the old data (which was also destructively examined) was included in the new data sets. For example, flaw designations A1-A5, A8-A11, and C1 which are listed in Table Q2.1, provided to the staff in a letter dated 2/24/98 from Ameren UE to the NRC, are also listed in Table 11.8.15 of BAW-10219P, Rev. 4, provided to the staff by letter dated 2/15/01. In both tables, the flaws have been destructively analyzed. This appears to negate the explanation provided by the licensee at the 6/7/01 meeting. Please clarify this discrepancy (e.g., does this indicate that the numbering scheme is not unique?).

In addition to the above information, please provide the list of all flaws removed from each of the data sets, and a detailed explanation as to why the data from the prior and current sets could not be combined. (Question from the 6/7/01 meeting held with UE, FTI, and the NRC staff)

Response:

No "old" samples were used in the crack extent and depth sizing qualifications presented in BAW-10219P-Rev 4. An abbreviated sample numbering scheme was used in portions of the topical report. For example, the combined wall thickness samples in Table 11.8.15 are described in Section 11.9.2 which provides the full description of the sample sets in Tables 11.9.5, .6, .7, and .8. For example, flaw A2 (Table 11.8.15, pg. 11-56) is Sample RT-100-001 Axial crack number 2 as listed in Table 11.9.5, pg. 11-66. Axial flaw A1 in Table 11.8.15 is not listed in Table 11.9.5. This flaw was the Axial crack number 1 of RT-100-001. Flaw A1 was not detected by ET but was detected by UT. The DE depth was recorded as 0.015 inch.

The Table Q2.1 data contained in the 2/24/98 letter was obtained from several non-sleeved steam generator pulled tubes. The flaw designations were assigned to remove the operating plant identity while retaining some form of cross-reference for later source identification. The flaws came from five sources, hence the letter designations A, B, C, D, and E. The numbers following the letter designation represented the flaw. The Table Q2.1 flaws were presented as part of the crack depth sizing set for revision 3 of the topical report, Table 11.9.10. The Table Q2.1 flaws are not presented in revision 4 of the topical report.

For the topical report (revision 4) crack depth sizing data set, the letter designation A, is used to identify an axial crack, and the letter designation C, is used to identify a circumferential crack.

RAI # 3. The staff did not identify any dents included in the sample set discussed in Section 11.9.2. The staff is just as interested in the effect denting has on the ability to reliably depth size flaws, as only dented intersections were used for the probability of detection data set. Discuss the impact of not including dents in the ODSCC depth sizing data set, as it pertains to the expected field conditions of Callaway's SG tubes. (Pages 11-64 to 11-69, BAW-10219P, Rev. 4)

Response:

The sample set for crack depth sizing qualification contains tube expansion transitions with laboratory induced corrosion cracking and installed sleeves (pg. 11-64 through 11-70, BAW-10219P-Rev 4), which is consistent with the top-of tubesheet installation at Callaway. Two sets of stress corrosion cracks were produced, axial and circumferential. The EPRI Appendix J review(s) evaluated the data set, analysis of the data, DE documentation, and the procedures and found the sample sets to be an adequate basis for the qualification.

Depth sizing of eight dented samples were evaluated during the EPRI peer review of the ODSCC depth sizing technique. These samples, containing 4 axial cracks and 4 circumferential cracks, are not included in the qualification sample set discussed in Section 11.9.2 of the topical report. They were, however, included in ETSS 303 (pages 5 and 6) to determine if their inclusion would affect the statistical uncertainties associated with the depth sizing. The result was that including these samples in the axial and circumferential depth sizing sample sets did not change the RMSE values that are reported in Tables 11.9.5 through 11.9.8 in the Topical Report.

The additional dented samples listed in ETSS 303 are:

Axial ODSCC:	009-1, 017-1, 030-1, & 040-1
Circumferential ODSCC:	044-10, 046-1, 053-1, & 063-1

The dent sizes and maximum crack depth for each of these samples is reported in the answer to Question #1, Table R1-1.

No denting has been observed at Callaway, and is not expected due to the use of stainless steel quatrefoil support plates, periodic chemical cleaning, and controls for secondary side chemistry.

RAI # 4. Please provide the associated flaw lengths in Tables 11.9.5 - 11.9.8, and discuss whether the flaw morphology and sizes are consistent with what is found in Callaway's SG tubes. (Pages 11-64 to 11-69, BAW-10219P, Rev. 4)

Response:

For the axial flaws, Tables 11.9.5 and 11.9.6, the flaw extent range is 0.1 to 0.6 inch, with an average flaw extent of 0.4 inch. For the circumferential flaws, Tables 11.9.7 and 11.9.8, the flaw extent range is 20 ° to 240 °, with an average flaw extent of 100 °. Based on ECT indications, the "typical" flaw extents observed at Callaway are on the smaller end of this range. The qualification samples therefore provide ample margin to envelop the potential flaw morphology growth at Callaway.

RAI # 5. How does the sample set in Section 11.9.2 achieve the stated objective of UT demonstrating a high probability of detection of service induced cracks that have depths of penetration exceeding 40% through-wall of the parent tube, when the sample set contains just 4 flaws (out of 20) that are less than 60% through wall? (Pages 11-64 to 11-69, BAW-10219P, Rev. 4)

Response:

For the pre-sleeve examination, Eddy Current did not detect flaws C13 (circumferential crack number 13, Table 11.9.7), A11, A12, A17, and A18 (axial cracks, Table 11.9.5). Since the ultrasonic technique detected the flaws in the pre-sleeve and post sleeve conditions, the high probability of detection argument has been demonstrated. There was no loss of sensitivity to the flaw population after the addition of the sleeve material.

After the sleeve application, the percent through wall crack depths become significantly less given the combined wall thickness. For example, a 60% through wall in a 0.050 inch wall parent tube would become $(0.030 / (0.050 + 0.038))$ or 34% through wall after the installation of the nominal 0.038 inch sleeve. A 60% through wall in a 0.042 inch wall parent tube would become $(0.025 / (0.042 + 0.034))$ or 33% through wall after the installation of the nominal 0.034 inch sleeve. This is significant in that for region B of the sleeve there is a plug on detection requirement. The flaws, A12, A20 and A22 are less than 30% TW pre-sleeve and are less than 16% TW post sleeve. Since the amplitude of the reflected sound energy (sensitivity) is a function of distance traveled in the material, it can be inferred that the technique would detect flaws less than 40% TW (parent tube) for both region B and region A. For region A, there is a requirement for detection at the utility's technical specification, which typically is 60% through wall for actual flaw depth.

PWSCC

RAI # 6. During the meeting, FTI indicated that PWSCC detectability in the sleeve could be inferred from the ID notches in the UT calibration standards and the data sets containing pits. It is not clear to the staff how detecting EDM notches in the calibration standards or another degradation morphology such as pits would infer an ability to detect tight flaws such as PWSCC. Explain the basis for the statement that sleeve PWSCC ID defects will be detected, and the resulting sensitivity and POD, since the peer review (ETSS # 98404) only covers volumetric defects. Please provide additional discussion or, preferably, additional data to support the claims of the capability of the technique to detect PWSCC in the sleeve. (Question from the 6/7/01 meeting held with UE, FTI, and the NRC staff)

Response:

"Substantial experimental data are available to indicate that the nanophase Electrosleeve material is highly resistant to corrosion and SCC in PWR primary and secondary water environments, Particularly under neutral and caustic conditions." (plus additional uncertainties). D.R. Diercks, Argonne National Laboratory, July 15, 1999. Pages 9-21, 9-33, and 9-51, BAW-10219P-Rev.4 provide the test results to support the evaluation that PWSCC is very unlikely in the Electrosleeve material.

Although it may be possible to produce fatigue cracks on the ID surface of the sleeve, the only way to produce the crack would be to install an initiation site, such as an EDM notch. In this case, the UT technique would be sensitive to the EDM notch, so reporting an indication at that location would not prove anything with respect to detection of cracks. For this reason we believe the use of fatigue cracks to address UT detection of sleeve PWSCC is not appropriate.

ASME Code Case N-569-1 [3.0(d)(1)] (BAW-10219P-Rev.4, Reference 13.4) references Section NB-2552.3 that defines the requirements for a Reference (Calibration) Specimen. It states that the standard defects shall be axial notches or grooves on the outside and inside surfaces of the reference specimen, whose depth is not greater than the larger of 0.004 in. or 5% of the nominal wall thickness. The use of the Calibration Standard is included in the inspection procedures. (This EDM notch is a structurally insignificant flaw.)

The assertion about the calibration standard and the inner diameter sleeve pit was to demonstrate sensitivity of the ultrasonic technique to inner diameter initiated flaws. The inner diameter pit provides a difficult cross-sectional target due to its cylindrical shape. This was felt to be a more challenging test of the detection capability of the shear wave transducers than the broad side of an EDM notch. The staff is correct in their opinion that neither of these flaws fully represent PWSCC, but these are the only morphologies available for evaluation since sleeve SCC cannot be fabricated.

To support the assertion that the system, (probe and technique) are sensitive to inner diameter flaws, three separate presentations will be offered. The first will show the sensitivity of the system to the inner diameter EDM notches in a calibration standard. The data was acquired in accordance with the

procedure where in the 10% outer diameter notch reflection amplitudes are set between 50% and 80% full screen height. This equates to a minimum of 128 analog-to-digital converter counts for an eight bit digitizer. The presentation consists of C-Scan and A-Scan plots of the EDM notches in the UT 0.750 by 0.043 Nickel Sleeve Qualification Sample #1246536C-1 as acquired with the 0.750 three channel probe. The presentation uses EDM notches located in two specific regions of typical calibration standards. For amplitude comparison, sleeved region outer diameter notches are presented in addition to sleeve inner diameter notches. The 10%, 0.004 inch, typical depth, parent tube outer diameter notches are presented to show that the equipment sensitivity was established in accordance with the acquisition and analysis procedures used for the Appendix J qualifications for crack extent and depth sizing.

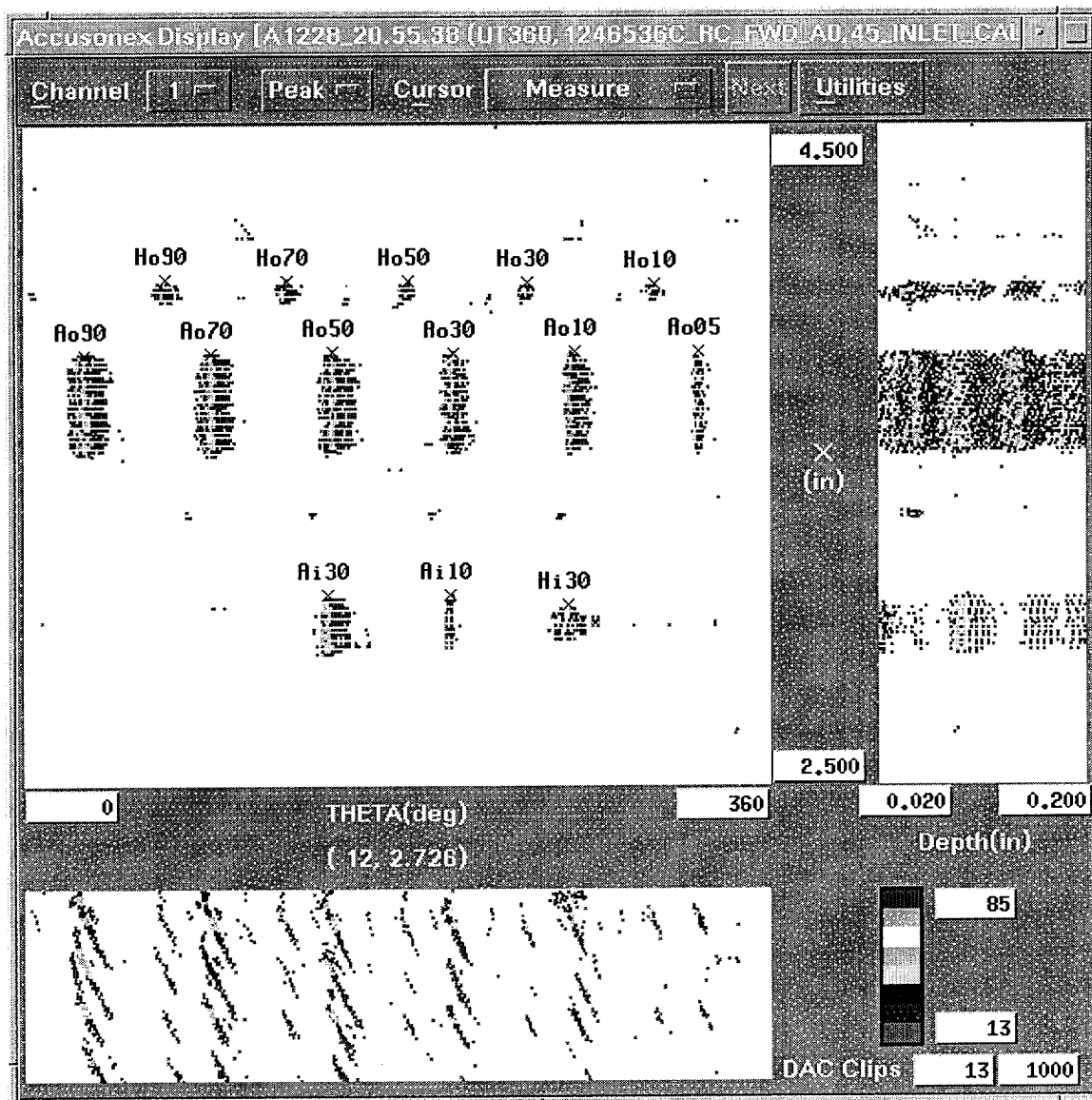


Figure R6-1. Calibration Standard 1246536C-1: Parent Tube Region Flaws
Axial Shear Wave Detection

The flaws labeled "Ai" are parent tube inner diameter axial EDM notches. The flaws labeled "Ao" are parent tube outer diameter axial EDM notches. The flaws labeled with the first character "H" are EDM contoured bottom holes. Of interest is the detection of "Ai10", the 0.004 inch deep inner diameter notch.

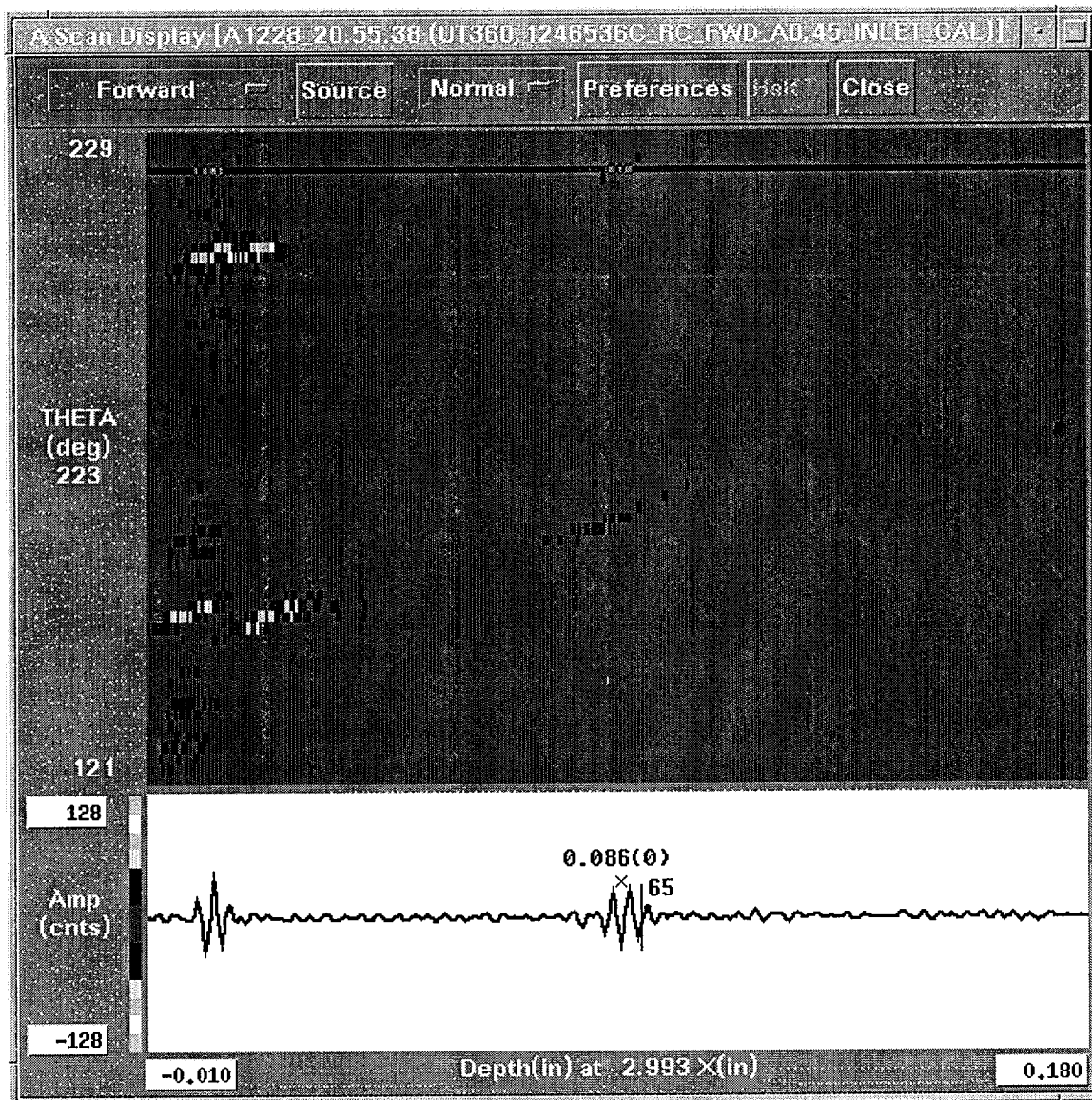


Figure R6-2. EDM Notch Ai10: Parent Tube Inner Diameter, 0.004" depth

This is the A-Scan plot showing the inner diameter corner reflection, (full skip) for the notch "Ai10". The notch is at the expected depth for the full skip, (two times the wall thickness) 0.086 inch. The peak to peak amplitude of this reflection is 65 counts out of a possible 256 counts or 25% full screen height.

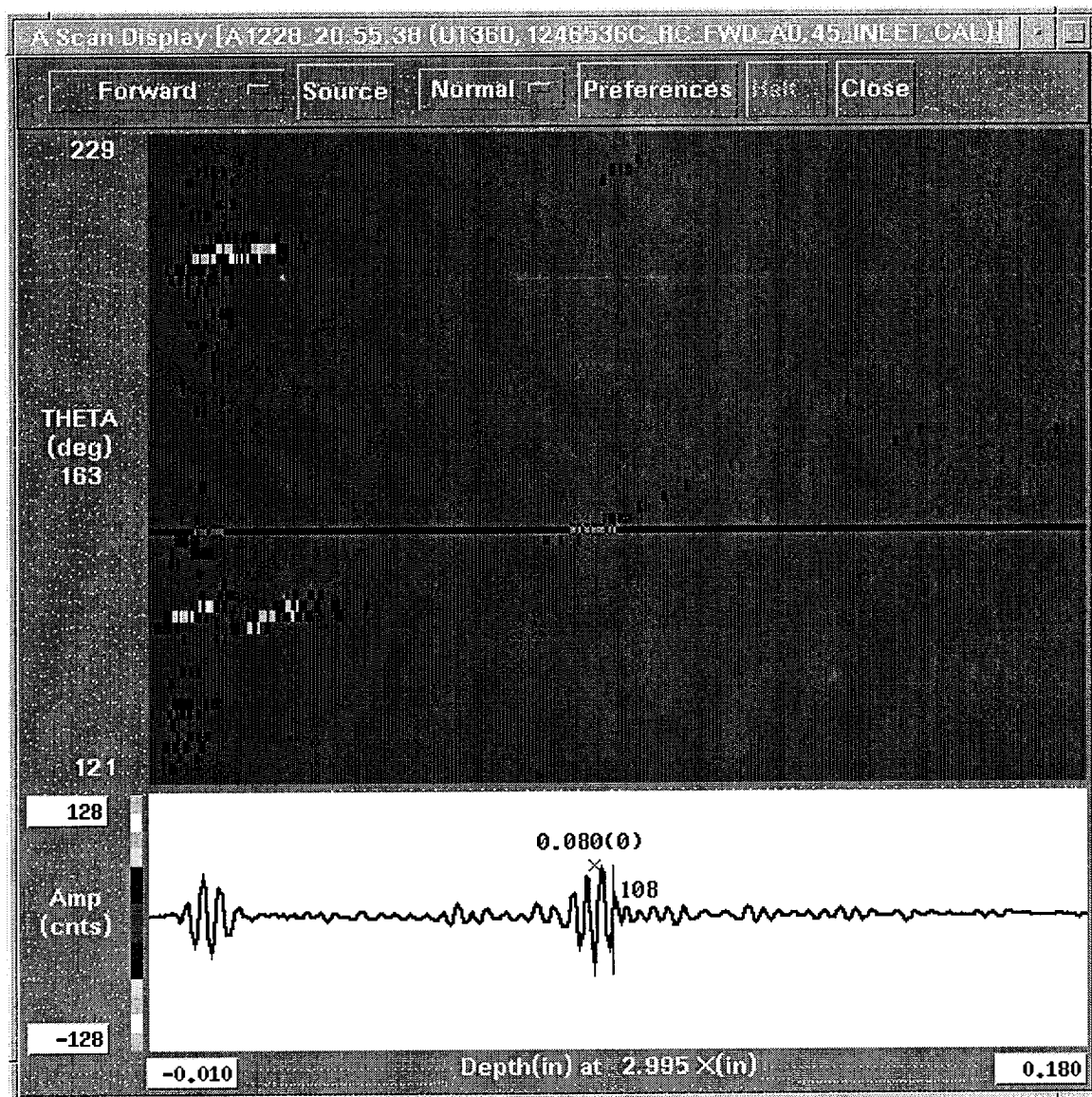


Figure R6-3. EDM Notch Ai30: Parent Tube Inner Diameter, 0.012" depth

This is the A-Scan plot showing the inner diameter corner reflection, (full skip) for the notch "Ai30". The peak to peak amplitude of this reflection is 108 counts or 42% full screen height.

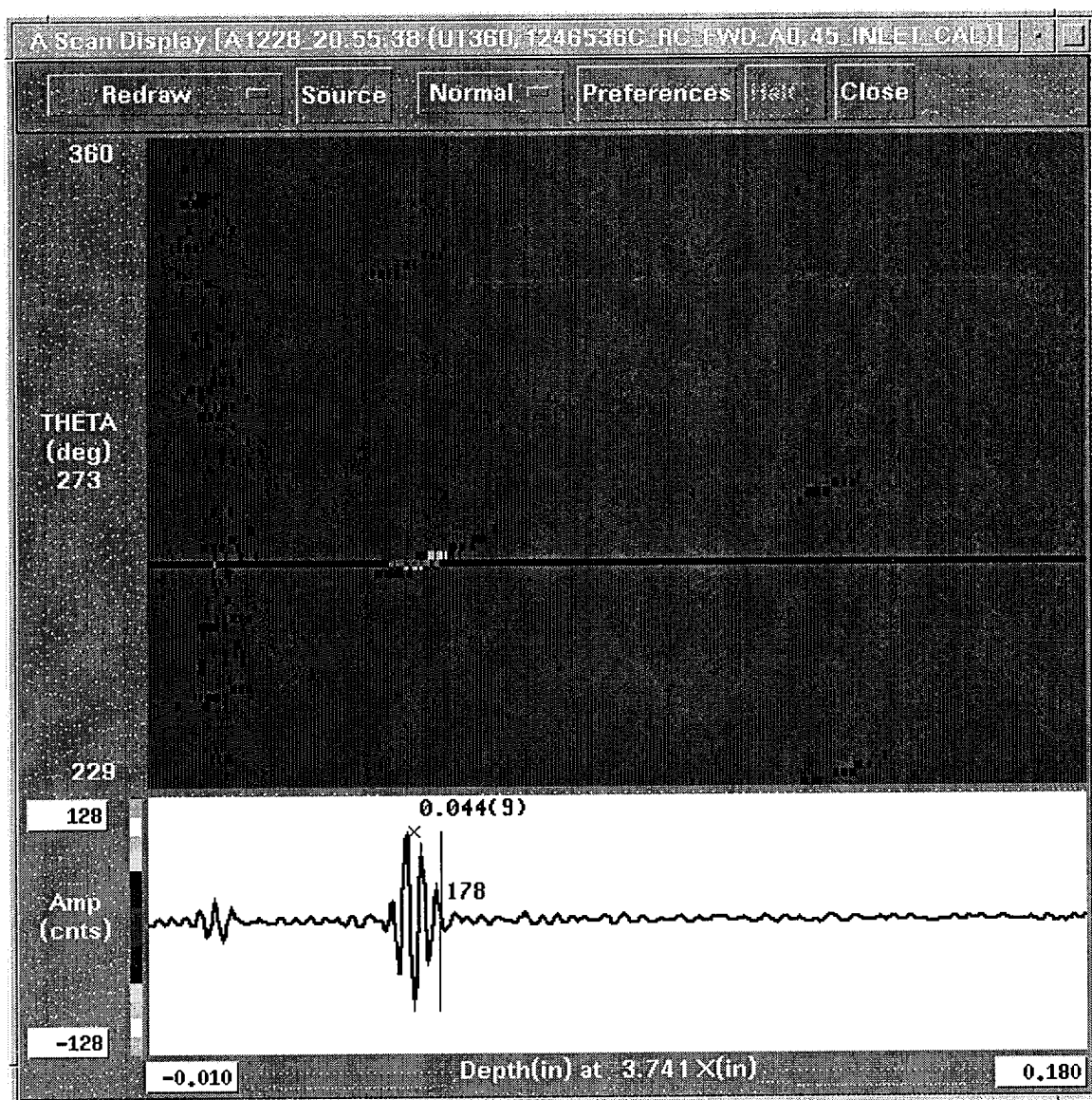


Figure R6-4. EDM Notch Ao10: Parent Tube Outer Diameter, 0.003" depth

This is the axial EDM notch that is used to establish the sensitivity and time-of-flight to depth calibration. The sensitivity must be set between 50% and 80% of the digitizer full scale. For an eight bit digitizer, the full scale is 256 counts (cnts). The amplitude of this reflection is 178 counts or (178/256), 70%.

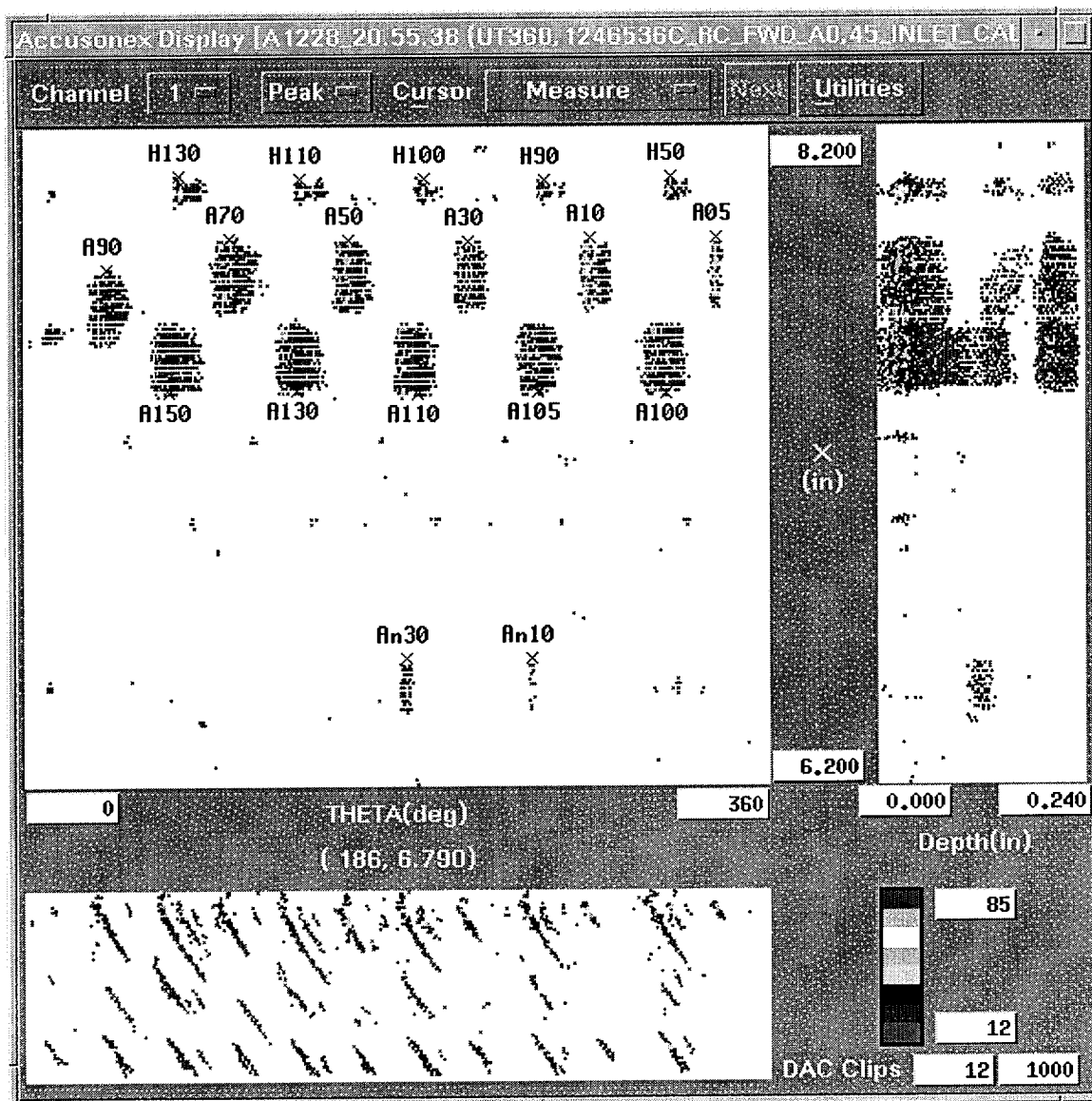


Figure R6-5. Calibration Standard 1246536C-1: Sleeved Tube Region Flaws
Axial Shear Wave Detection

The flaws labeled “An” are sleeve inner diameter axial EDM notches. The flaws labeled “A” are combined wall outer diameter axial EDM notches. The flaws labeled with the first character “H” are outer diameter EDM contoured bottom holes. Of interest is the detection of “An10”, the 0.004 inch deep inner diameter notch.

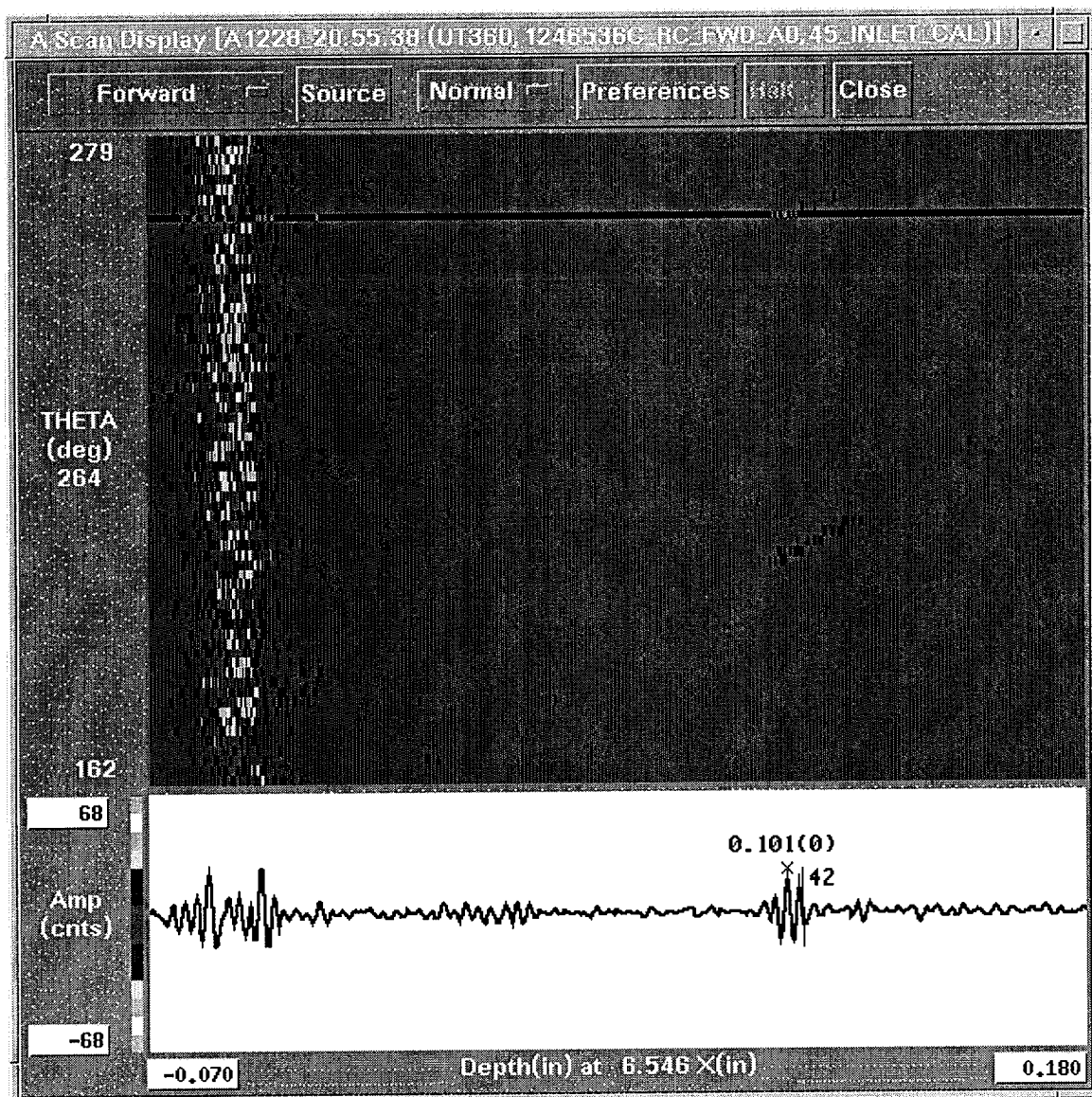


Figure R6-6. EDM Notch An10: Sleeve Inner Diameter, 0.004" depth

This is the A-Scan plot showing the inner diameter corner reflection, (full skip) for the notch "An10". The peak to peak amplitude of this reflection is 42 counts or 16% full screen height.

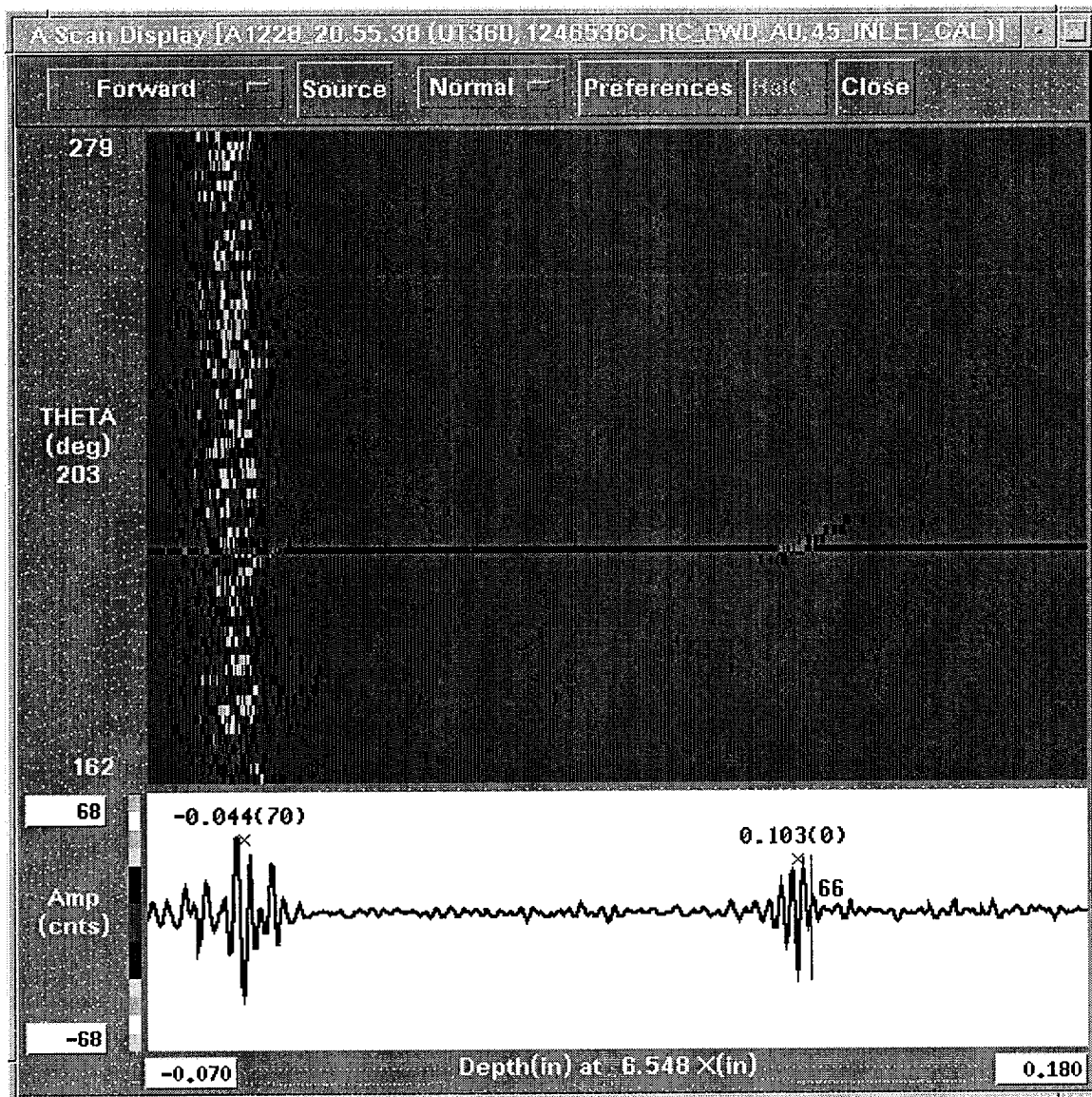


Figure R6-7. EDM Notch An30: Sleeve Inner Diameter, 0.012" depth

This is the A-Scan plot showing the inner diameter corner reflection, (full skip) for the notch "An30". The peak to peak amplitude of this reflection is 66 counts or 26% full screen height.

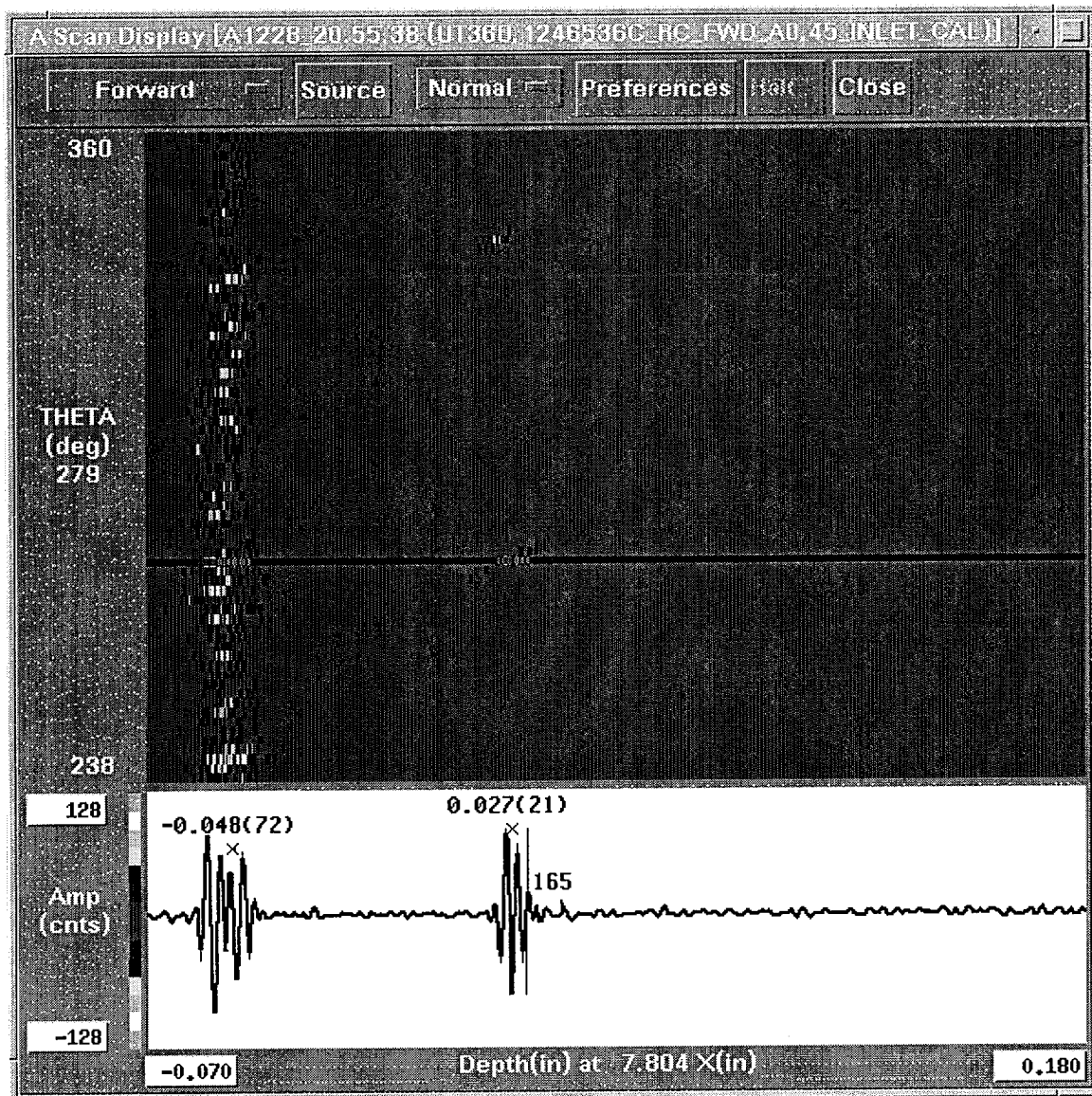


Figure R6-8. EDM Notch A10: Sleeved Region Outer Diameter, 0.003" depth

This is the A-Scan plot showing the outer diameter corner reflection, (half skip) for the notch "A10". The notch is at the expected half skip depth (one times the combined wall thickness) $0.048 + 0.027$ or 0.075 inch. The peak to peak amplitude of this reflection is 165 counts or 64% full screen height.

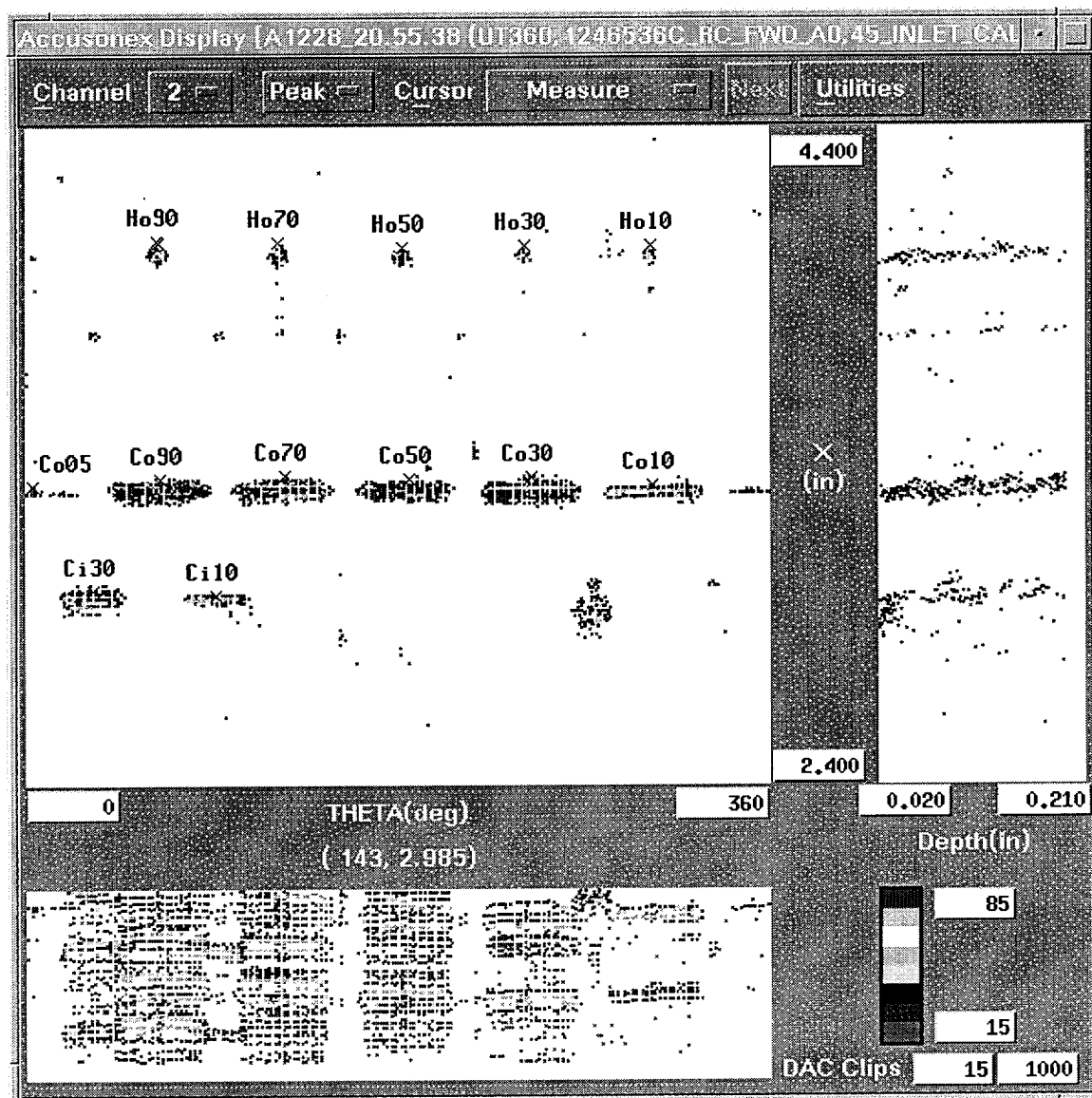


Figure R6-9. Calibration Standard 1246536C-1: Parent Tube Region Flaws
Circumferential Shear Wave Detection

The flaws labeled "Ci" are parent tube inner diameter circumferential EDM notches. The flaws labeled "Co" are parent tube outer diameter circumferential EDM notches. The flaws labeled with the first character "H" are EDM contoured bottom holes. Of interest is the detection of "Ci10", the 0.004 inch deep inner diameter notch.

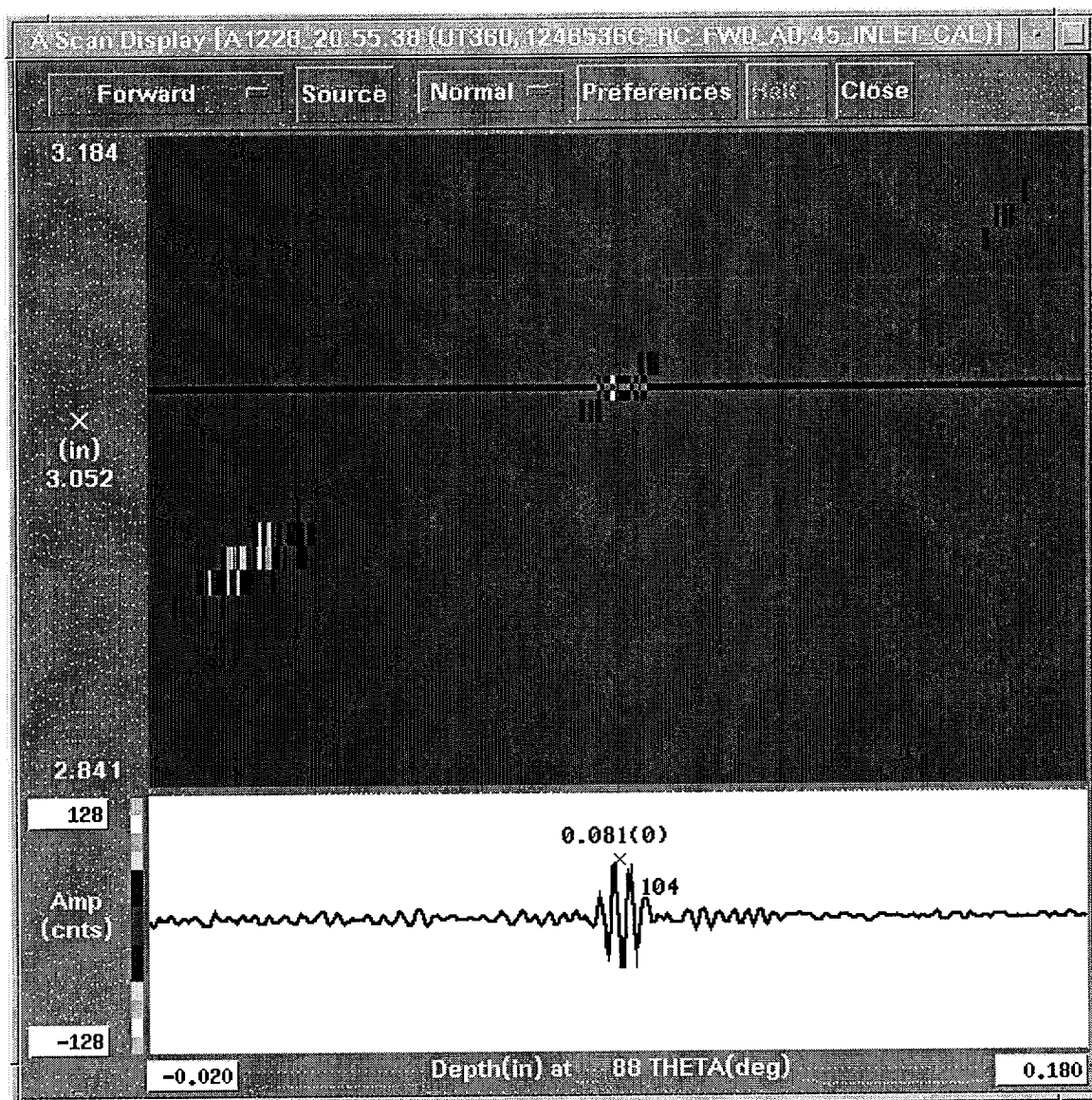


Figure R6-10. EDM Notch Ci10: Parent Tube Inner Diameter, 0.004" depth

This is the A-Scan plot showing the inner diameter corner reflection, (full skip) for the notch "Ci10". The notch is at the expected depth for the full skip, (~two times the wall thickness) 0.081 inch. The peak to peak amplitude of this reflection is 104 counts or 41% full screen height.

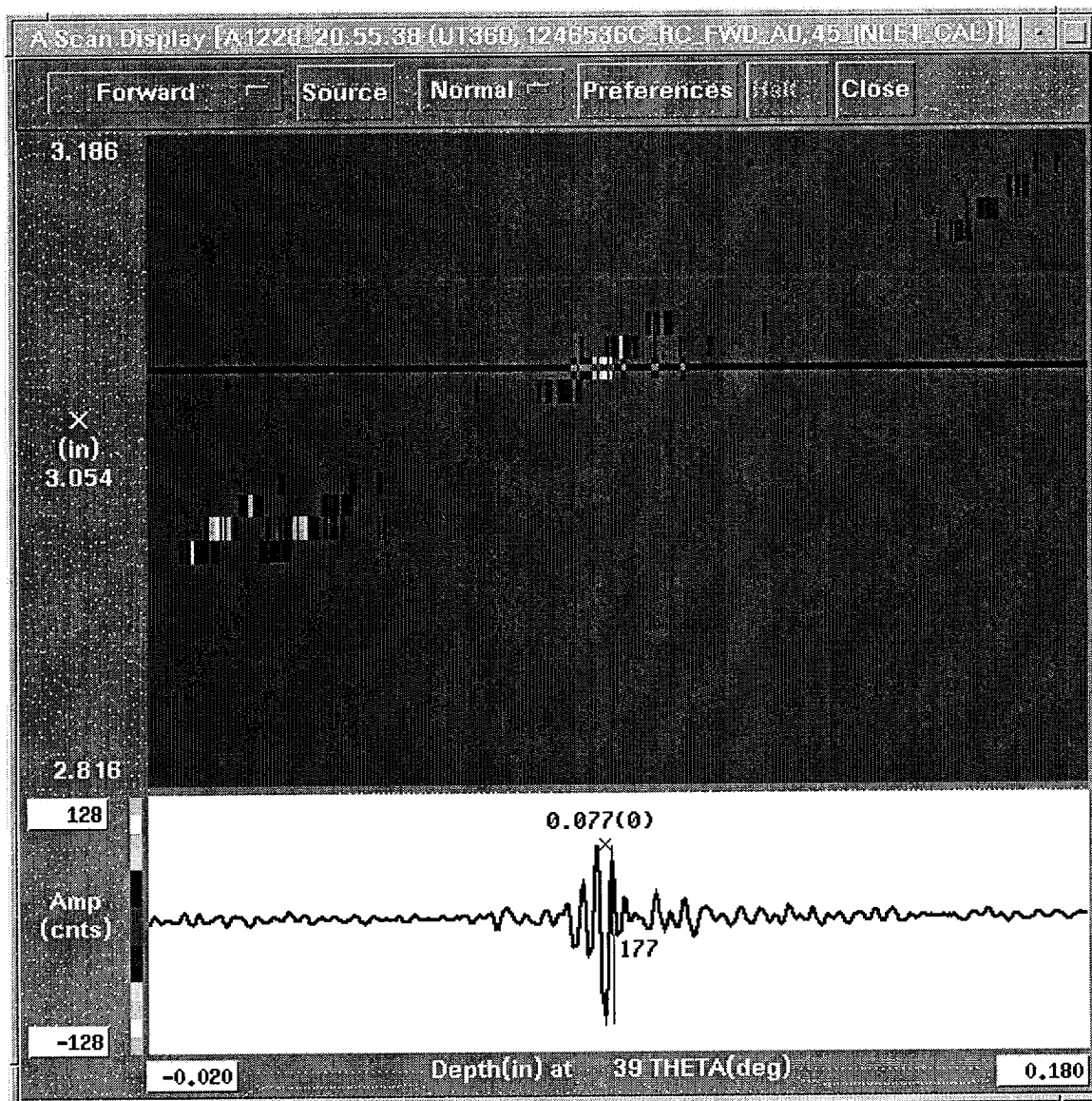


Figure R6-11. EDM Notch Ci30: Parent Tube Inner Diameter, 0.012" depth

This is the A-Scan plot showing the inner diameter corner reflection, (full skip) for the notch "Ci30". The peak to peak amplitude of this reflection is 177 counts or 69% full screen height.

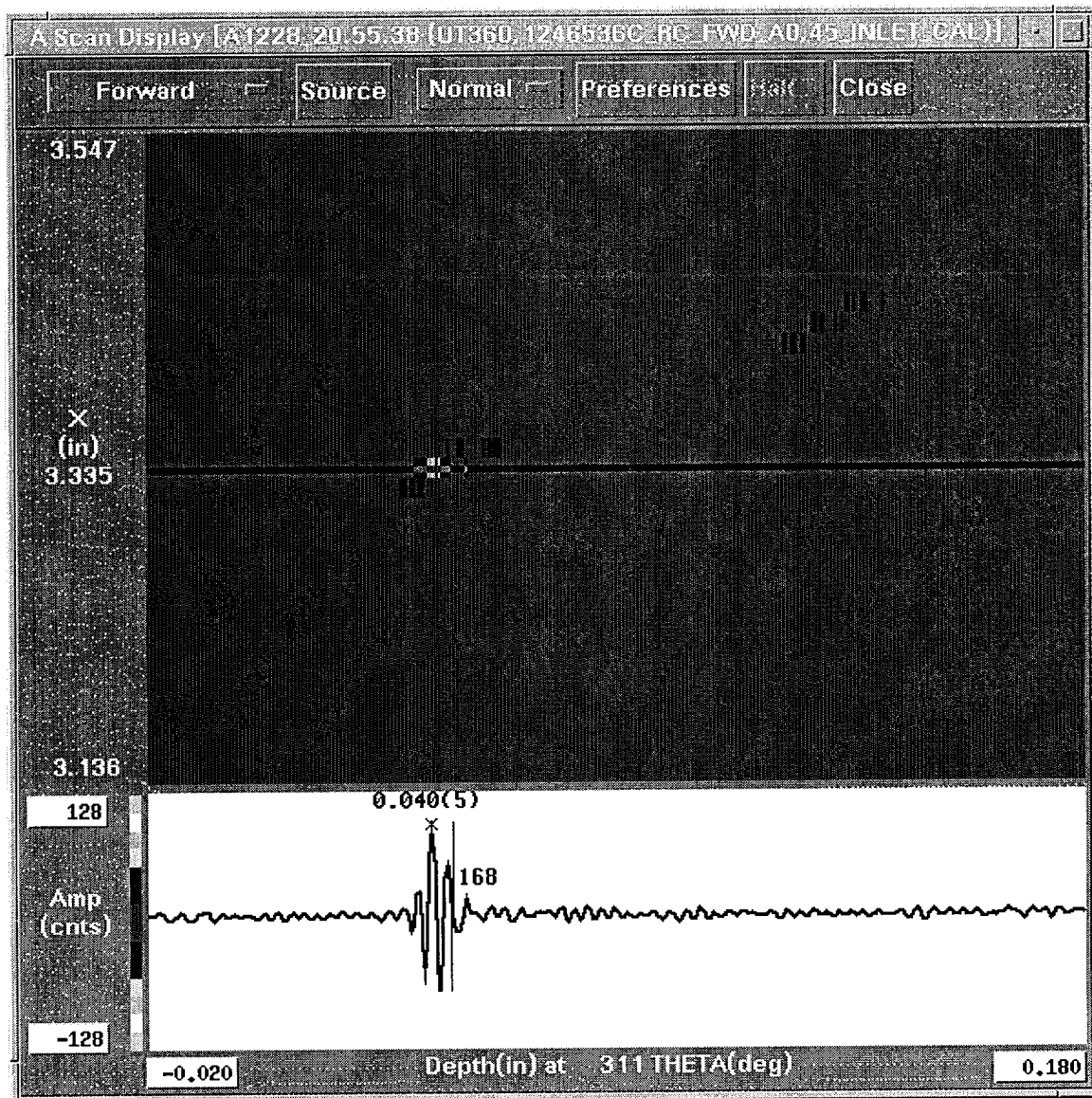


Figure R6-12. EDM Notch Co10: Parent Tube Outer Diameter, 0.003" depth

This is the circumferential EDM notch that is used to establish the sensitivity and time-of-flight to depth calibration. The amplitude of this reflection is 168 counts or $(168/256)$, 66%.

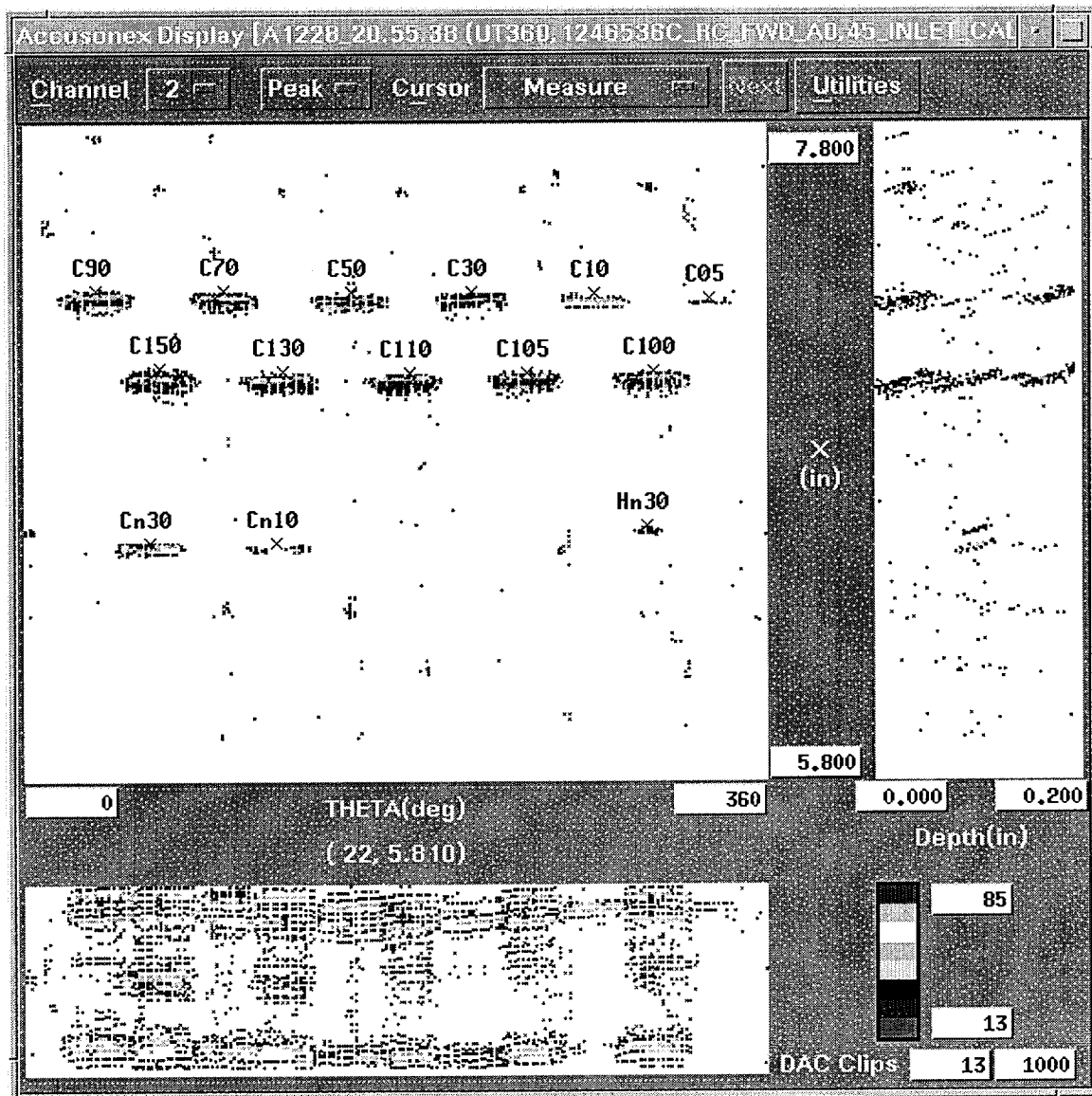


Figure R6-13. Calibration Standard 1246536C-1: Sleeve Flaws
Circumferential Shear Wave Detection

The flaws labeled "Cn" are sleeve inner diameter circumferential EDM notches. The flaws labeled "C" are combined wall outer diameter circumferential EDM notches. The flaws labeled with the first character "H" are outer diameter EDM contoured bottom holes. Of interest is the detection of "Cn10", the 0.004 inch deep inner diameter notch.

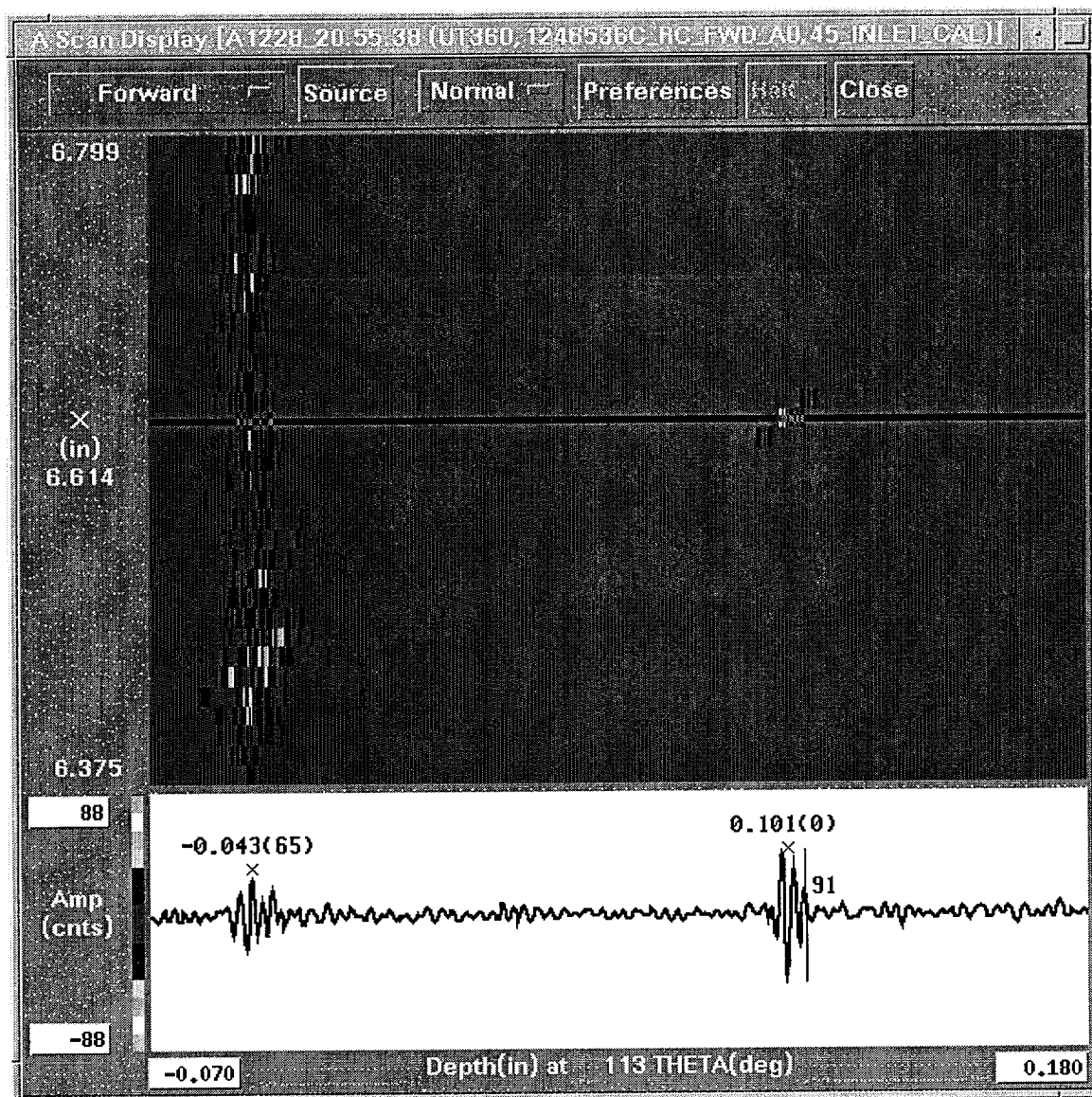


Figure R6-14. EDM Notch Cn10: Sleeve Inner Diameter, 0.005" depth

This is the A-Scan plot showing the inner diameter corner reflection, (full skip) for the notch "Cn10". The peak to peak amplitude of this reflection is 91 counts or 36% full screen height.

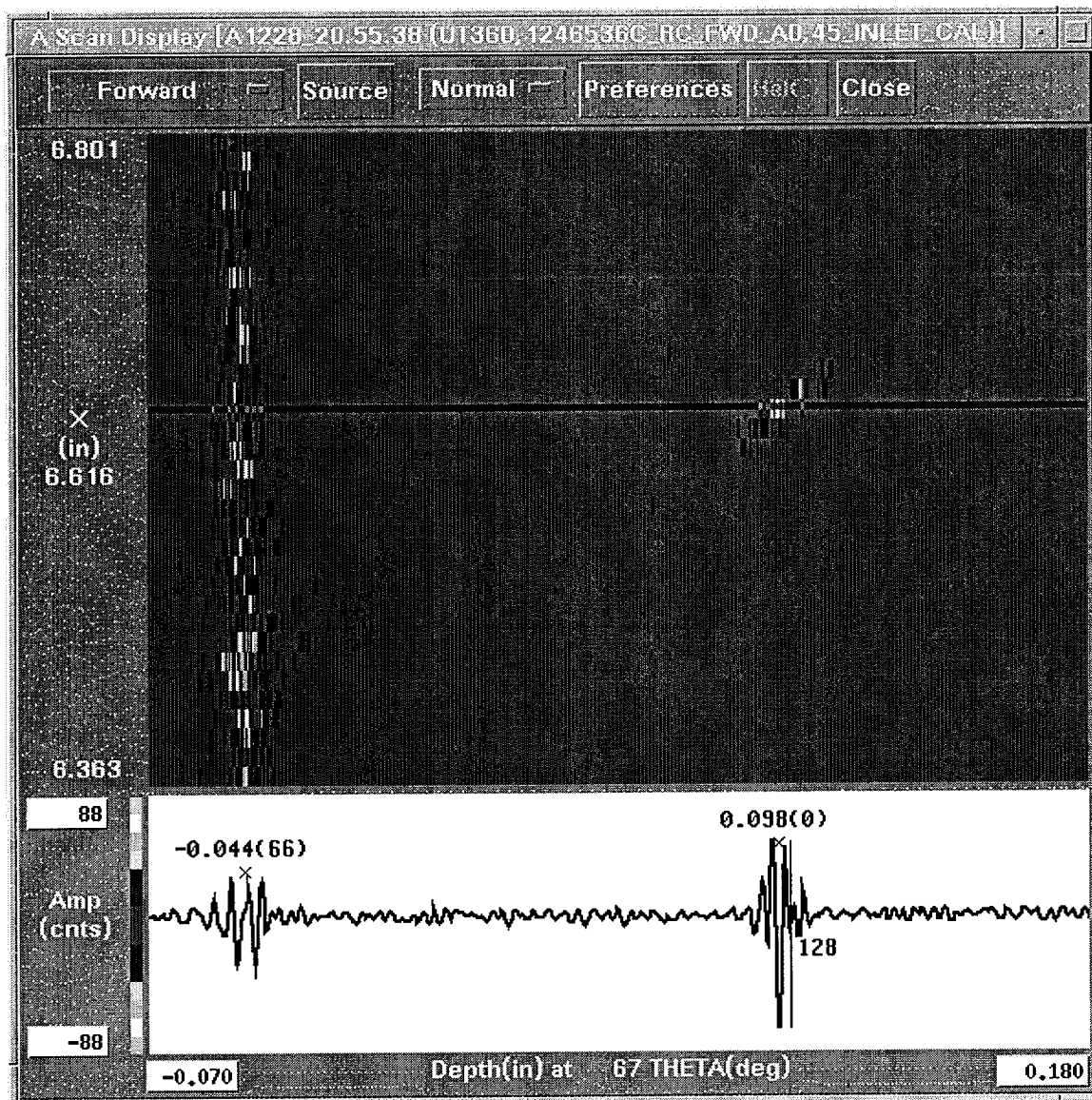


Figure R6-15. EDM Notch Cn30: Sleeve Inner Diameter, 0.012" design depth

This is the A-Scan plot showing the inner diameter corner reflection, (full skip) for the notch "Cn30". The peak to peak amplitude of this reflection is 128 counts or 50% full screen height.

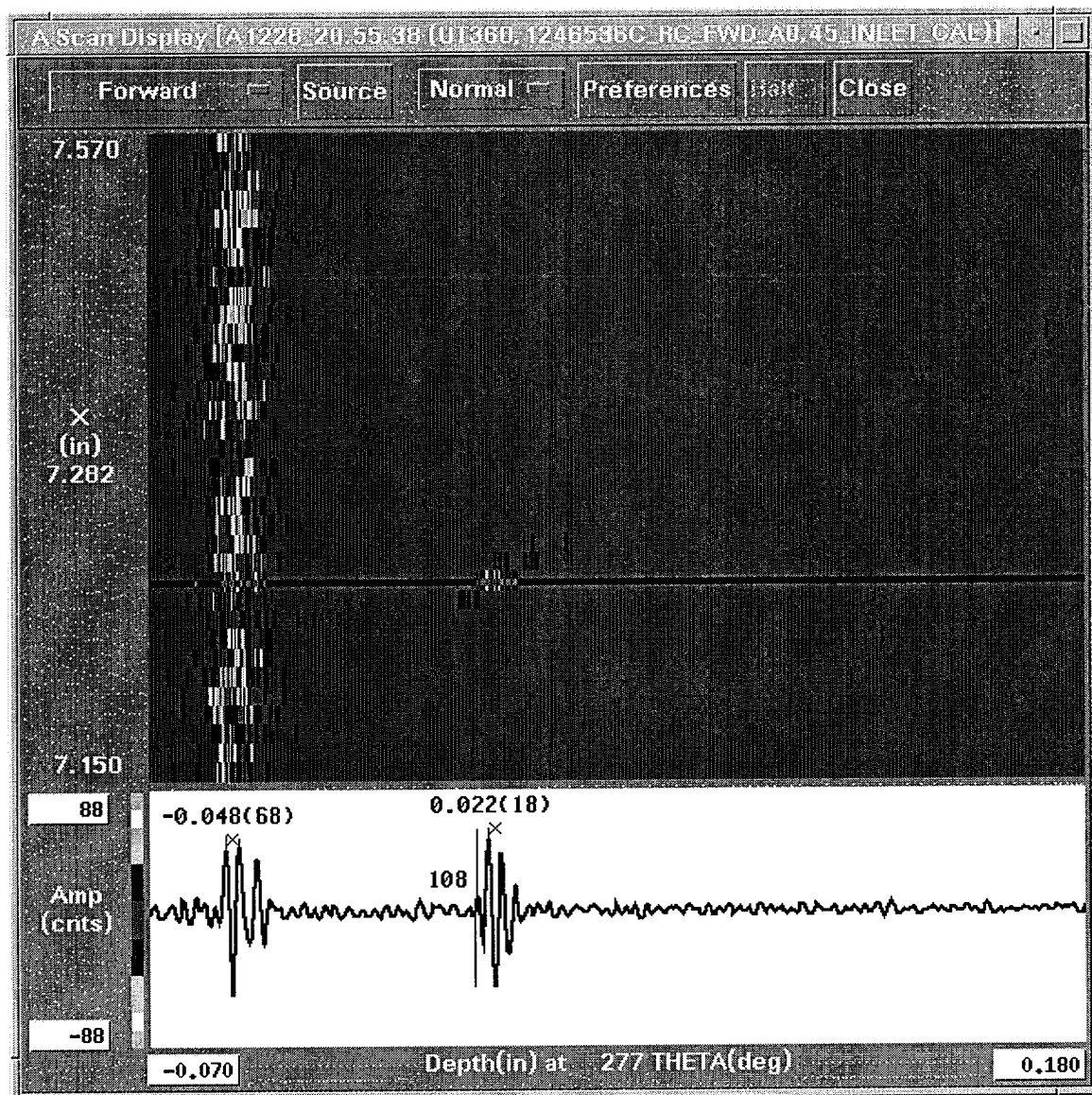


Figure R6-16. EDM Notch C10: Sleeved Region Outer Diameter, 0.004" depth

This is the A-Scan plot showing the combined wall outer diameter corner reflection, (half skip) for the notch "C10". The peak to peak amplitude of this reflection is 108 counts or 42% full screen height.

The second presentation will support the argument: if the system is sensitive to shallow outer diameter ODSCC, as evident by detection at the one and one half skip (three times the wall thickness) as well as detection at the half skip (one times the wall thickness), there would be a high confidence that the system would detect PWSCC of equivalent depth at the full skip (two times the wall thickness). This argument is supported in part by the definition of the depth sizing technique Full Skip Normalization (FSN) where in the ratio of the full skip amplitude to the average of the two outer diameter skip amplitudes (half skip and one & one half skip) is used to calculate the crack depth. The presentation consists of A-Scan plots for axial cracks A12 and A22, which are part of the ODSCC depth sizing qualification data set (Table 11.9.5, BAW-10219P-Rev.4). The post sleeve data will be presented. For both cracks, the one & one half skip reflection, in addition to the half skip reflection will be presented at several locations along the axial extent (length) of the crack. The following tables present the DE values at specific axial locations where DE crack depth measurements were made.

Table R6-1

crack A12		crack A22	
DE axial location (inch)	DE crack depth (inch)	DE axial location (inch)	DE crack depth (inch)
6.25	NDD	5.81	NDD
6.30	NDD	5.86	NDD
6.35	0.011	5.91	0.008
6.40	0.007	5.96	0.008
6.45	NDD	6.01	NDD
6.50	NDD	6.06	0.006
6.55	NDD	6.11	0.004
		6.16	NDD
		6.21	0.006
		6.26	0.011
		6.31	NDD
		6.36	NDD

For crack A12, the UT measured combined wall thickness is 0.073 inch at the 6.3 and 6.4 inch axial locations. For crack A22, the UT measured combined wall thickness is 0.077 inch at the 5.9 and 6.1 inch axial locations and 0.080 inch at the 6.25 inch axial location. Both cracks are in the expansion transitions of their respective tubes. The expansion transition geometry did not adversely affect the detection of these cracks.

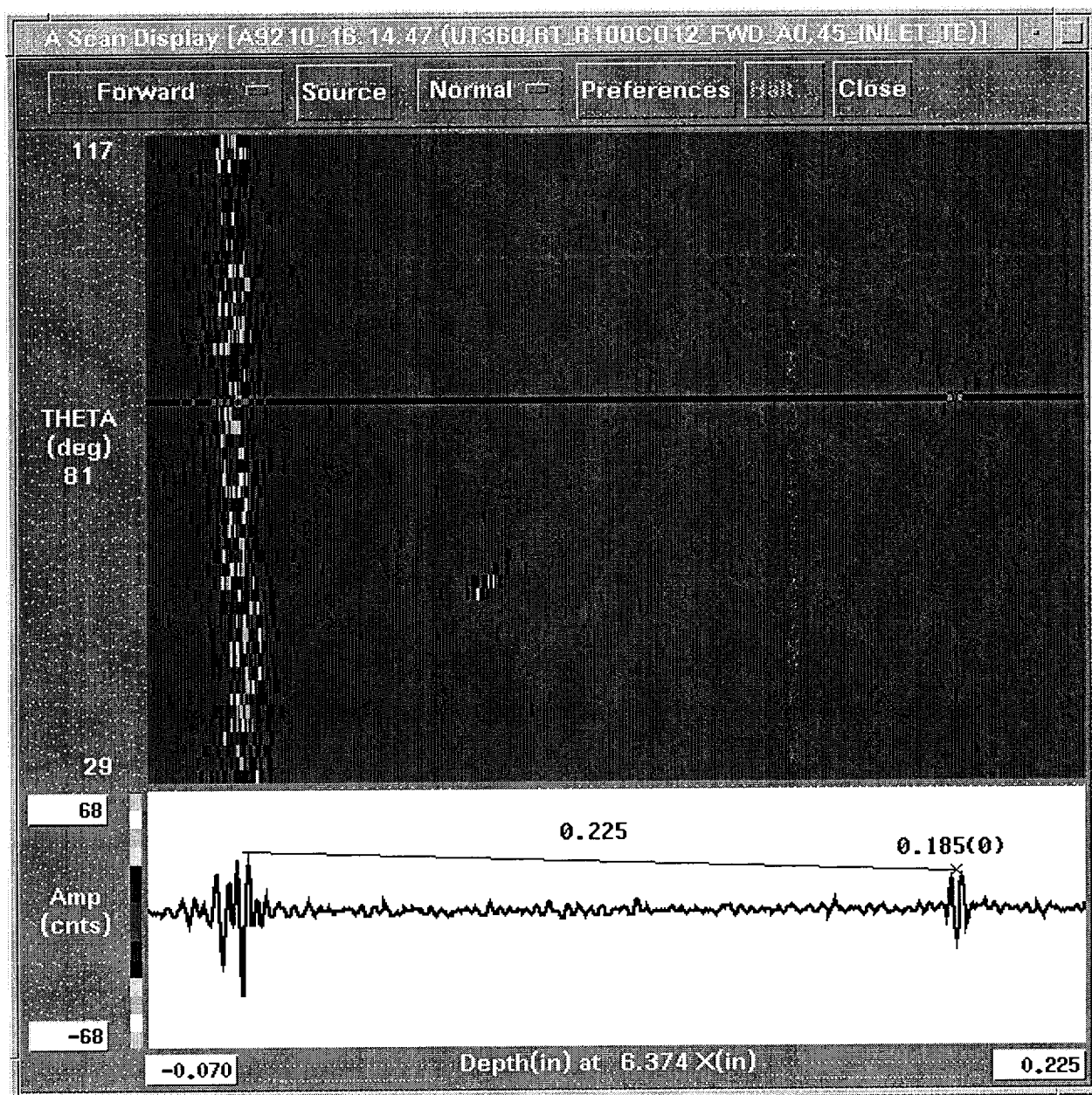


Figure R6-17. Crack A12: One and One Half Skip Reflection

This is the one and one half skip reflection for crack A12 at the 6.374 inch axial location. The 0.185 inch depth (time of flight) and the 81 degree circumferential location will be used to qualify this reflection with the half skip reflection. The reflection depth from the surface, 0.225 inch, is nearly equal to the expected depth (three times the combined wall thickness) or $(0.073 * 3) = 0.219$ inch.

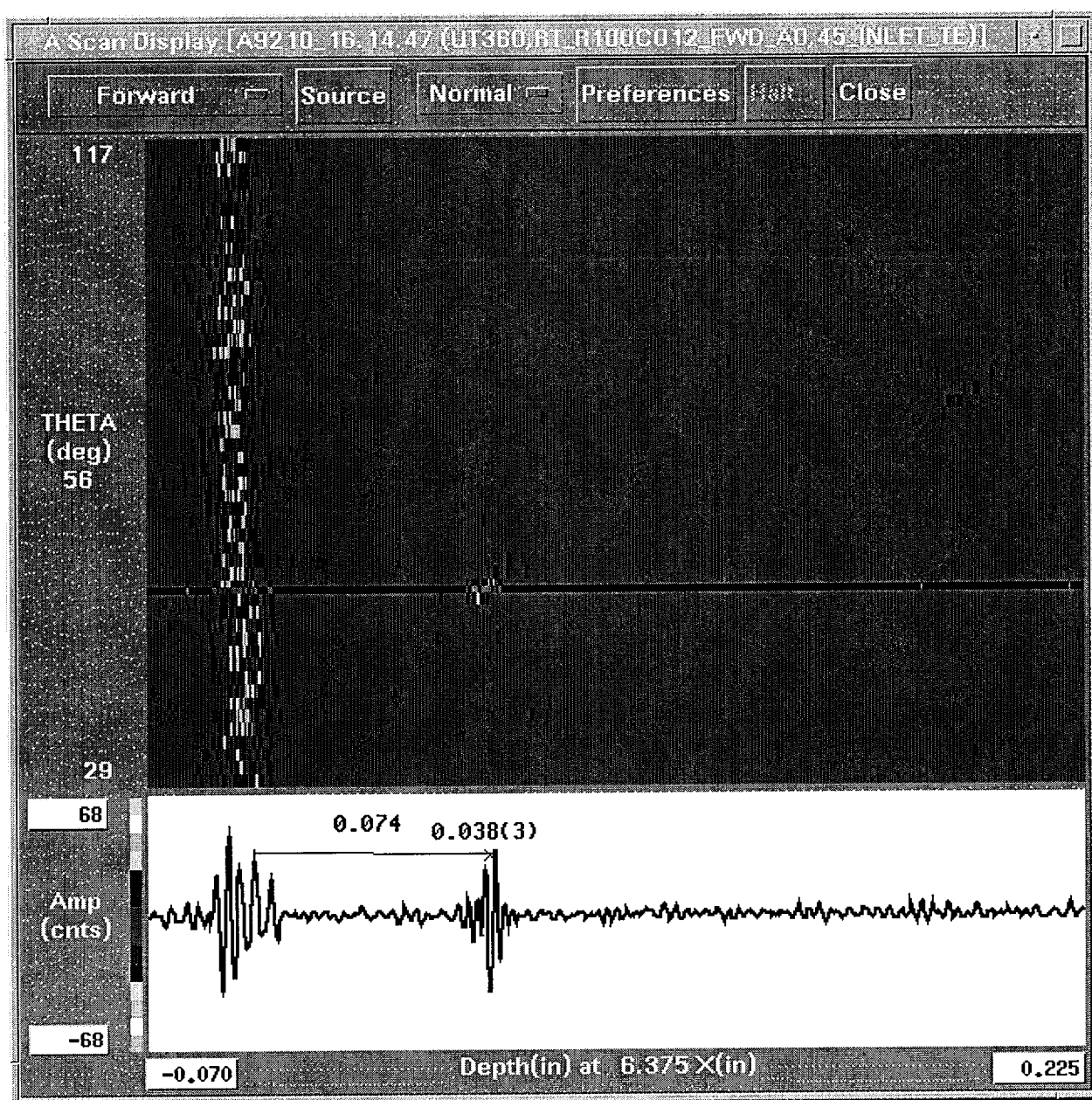


Figure R6-18. Crack A12: Half Skip Reflection

This is the half skip reflection for crack A12 at the 6.375 inch axial location. The 0.038 inch depth (time of flight) and the 56 degree circumferential location will be used to qualify this reflection with the one and one half skip reflection. The reflection depth from the surface, 0.074 inch, is nearly equal to the expected depth (one times the combined wall thickness) or 0.073 inch. In accordance with the depth sizing procedure, “the selected half skip reflection and the associated one and one-half skip reflection should have a depth versus displacement difference less than one pitch (0.015 inch)”. The delta depth is determined by subtracting the half skip depth, 0.038, from the one and one-half skip depth, 0.185, or $(0.185 - 0.038) = 0.147$ inch. The delta displacement is determined by subtracting the circumferential location for the half skip, 56 degrees, from the circumferential location for the one and one-half skip, 81 degrees, and converting the result to inches by multiplying the difference

by 0.006 (inch/degree). For these two reflections the displacement is $((81 - 56) * 0.006) = 0.150$ inch. Since these two results, (0.147 and 0.150), are within one pitch (0.015 inch), the half skip and the one and one-half skip have been correctly identified. The delta depth and delta displacement are also nearly equal to the expected value of two times the wall thickness because there is a full skip difference between them.

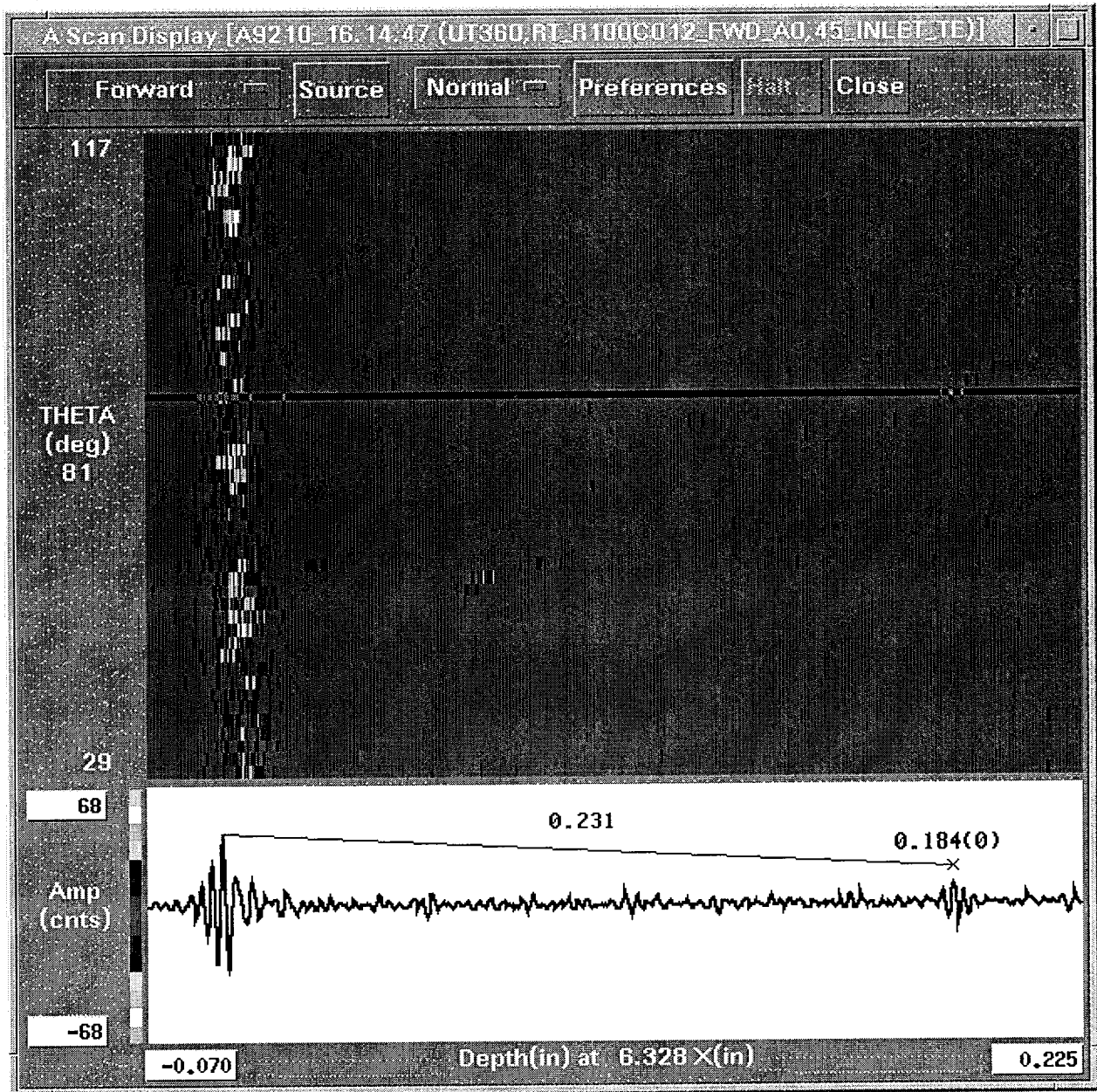


Figure R6-19. Crack A12: One and One Half Skip Reflection

This is the one and one half skip reflection for crack A12 at the 6.328 inch axial location.

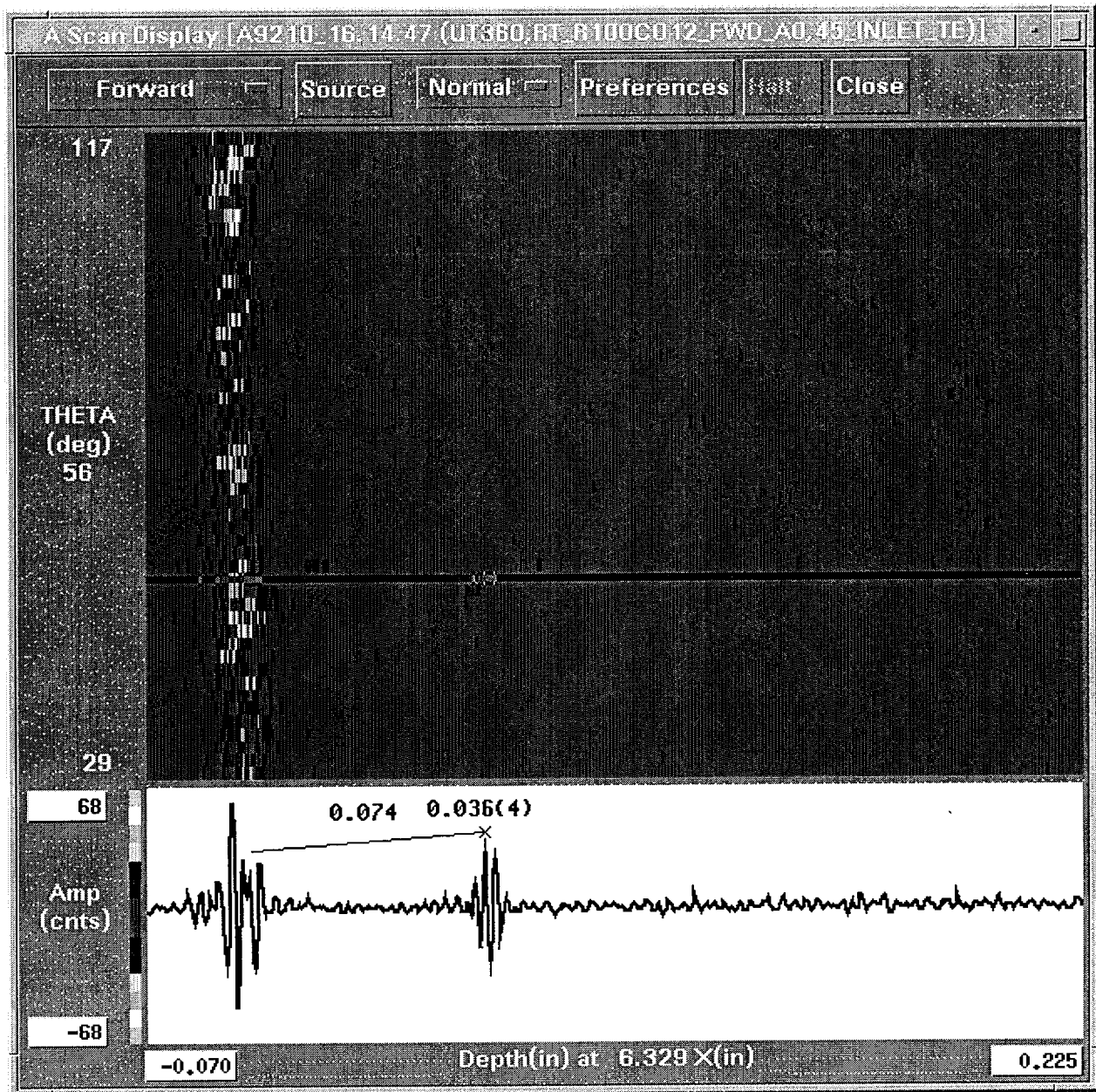


Figure R6-20. Crack A12: Half Skip Reflection

This is the half skip reflection for crack A12 at the 6.329 inch axial location. The delta depth is $(0.184 - 0.036) = 0.148$ inch. The delta displacement is $((81 - 56) * 0.006) = 0.150$ inch. Since these two results, (0.148 and 0.150), are within one pitch (0.015 inch), the half skip and the one and one-half skip have been correctly identified. The delta depth and delta displacement are also nearly equal to the expected value of two times the wall thickness.

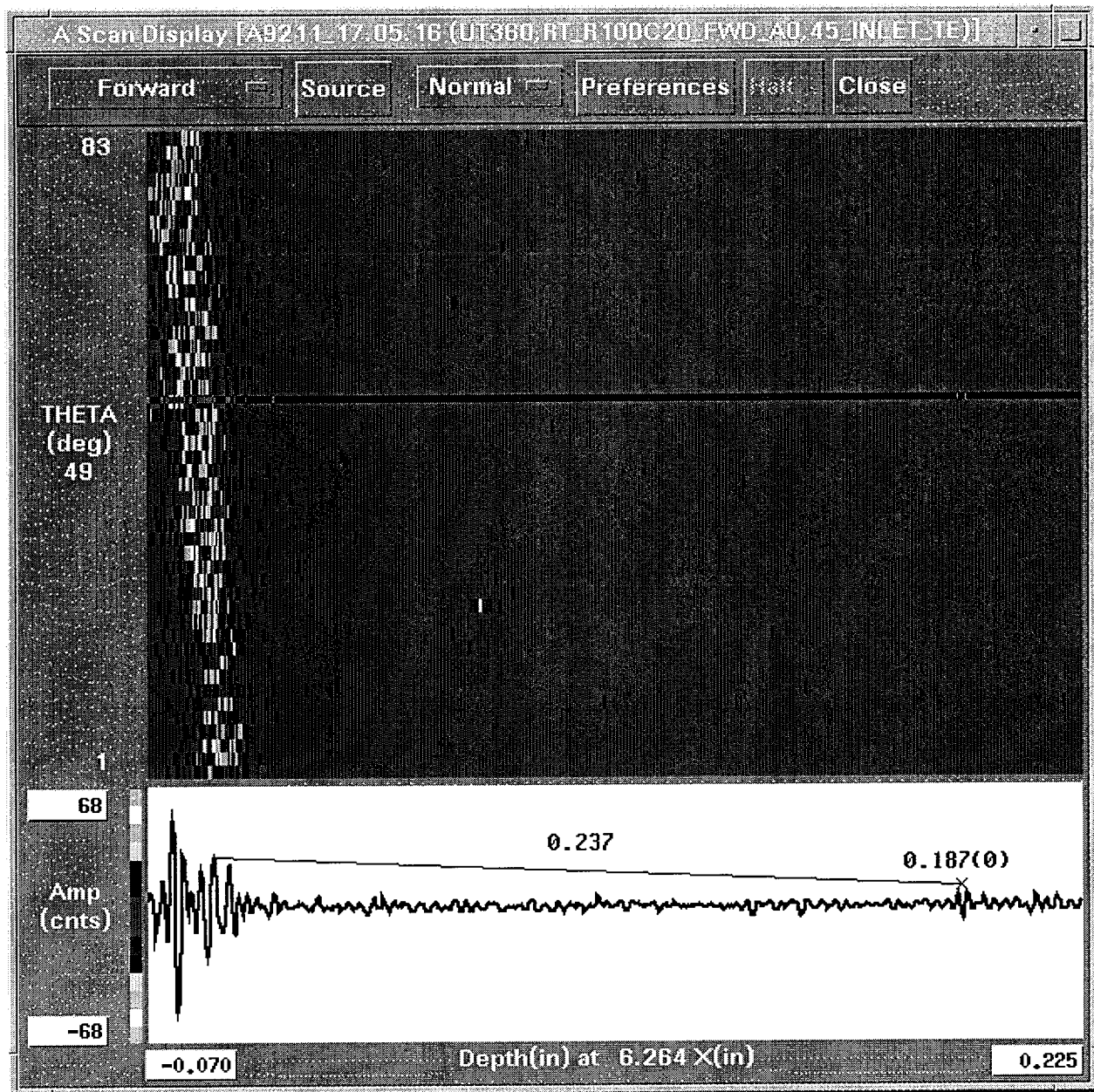


Figure R6-21. Crack A22: One and One Half Skip Reflection

This is the one and one half skip reflection for crack A22 at the 6.264 inch axial location. The 0.187 inch depth (time of flight) and the 49 degree circumferential location will be used to qualify this reflection with the half skip reflection.

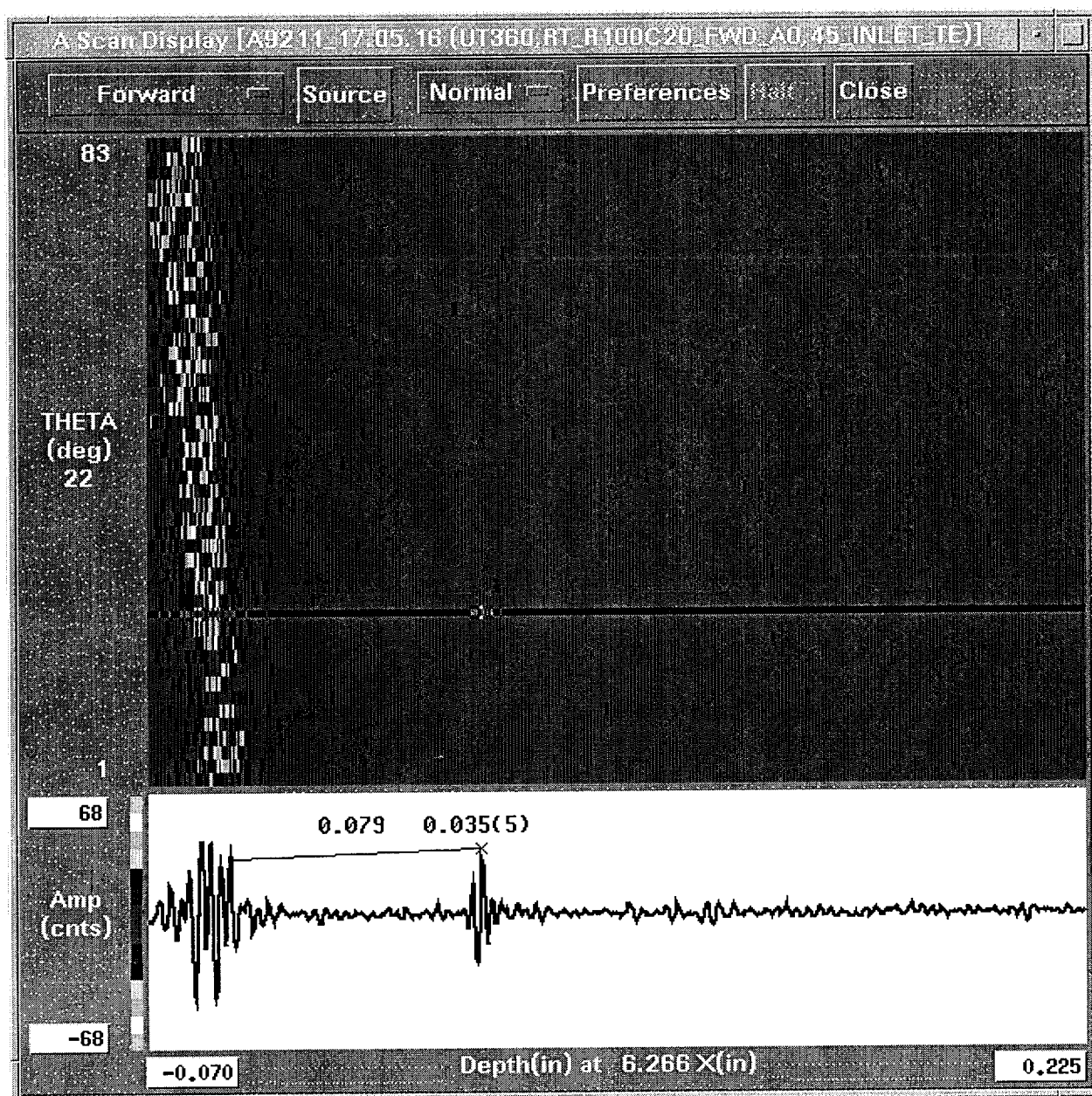


Figure R6-22. Crack A22: Half Skip Reflection

This is the half skip reflection for crack A22 at the 6.266 inch axial location. The delta depth is $(0.187 - 0.035) = 0.152$ inch. The delta displacement is $((49 - 22) * 0.006) = 0.162$ inch. Since these two results, (0.152 and 0.162), are within one pitch (0.015 inch), the half skip and the one and one-half skip have been correctly identified. The delta depth and delta displacement are also nearly equal to the expected value of two times the wall thickness.

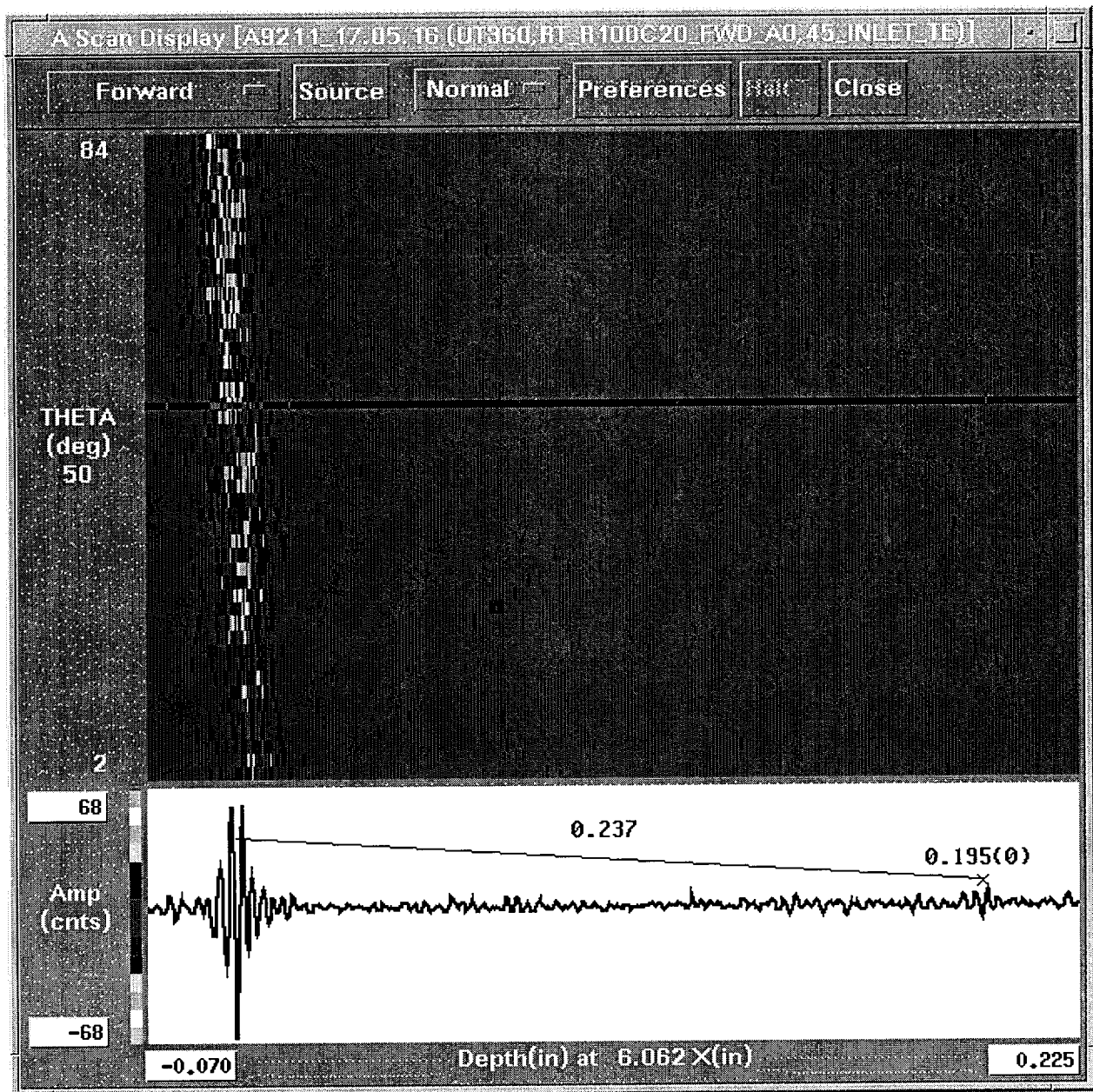


Figure R6-23. Crack A22: One and One Half Skip Reflection

This is the one and one half skip reflection for crack A22 at the 6.062 inch axial location. The 0.195 inch depth (time of flight) and the 50 degree circumferential location will be used to qualify this reflection with the half skip reflection.

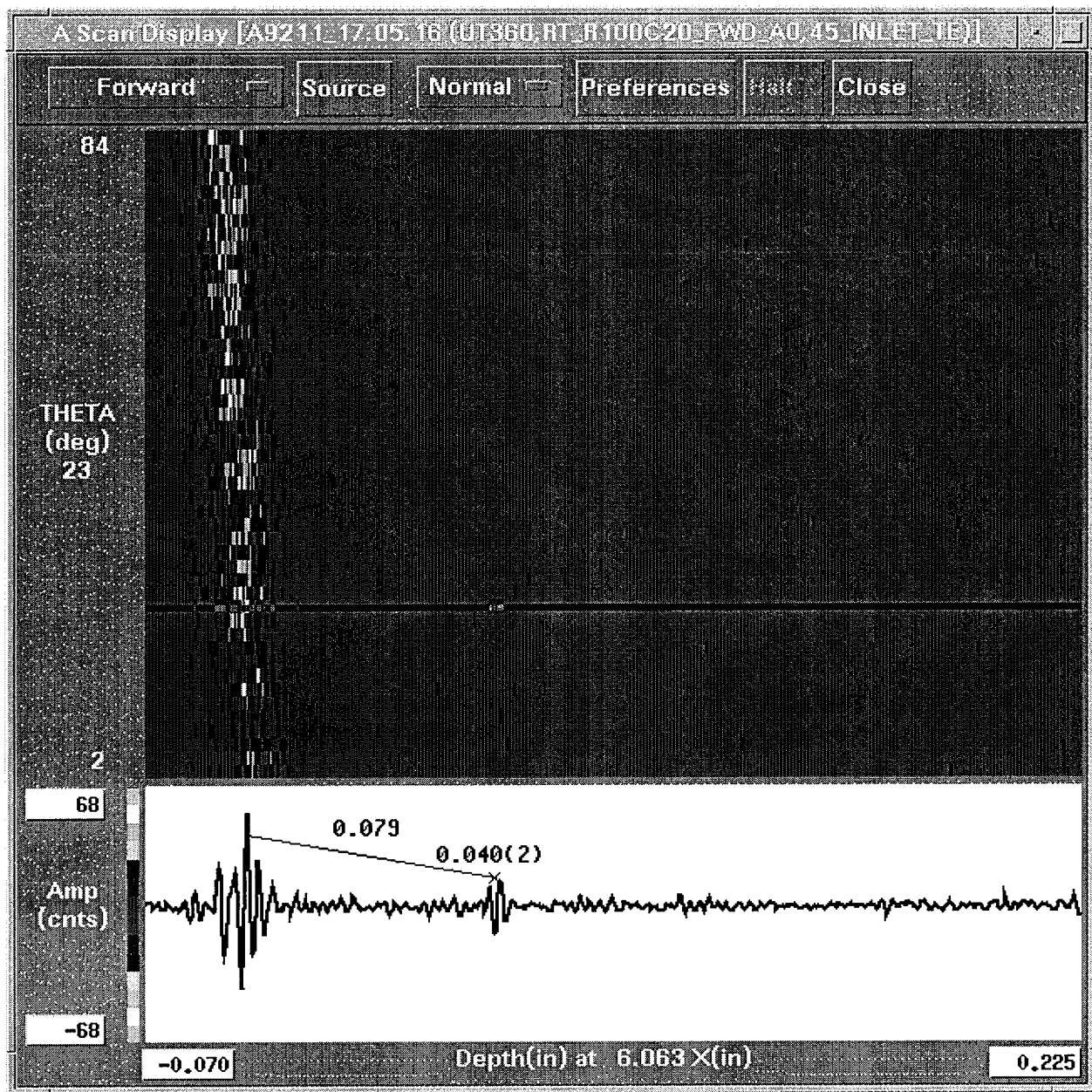


Figure R6-24. Crack A22: Half Skip Reflection

This is the half skip reflection for crack A22 at the 6.063 inch axial location. The delta depth is $(0.195 - 0.040) = 0.154$ inch. The delta displacement is $((50 - 23) * 0.006) = 0.162$ inch. Since these two results, (0.154 and 0.162), are within one pitch (0.015 inch), the half skip and the one and one-half skip have been correctly identified. The delta depth and delta displacement are also nearly equal to the expected value of two times the wall thickness.

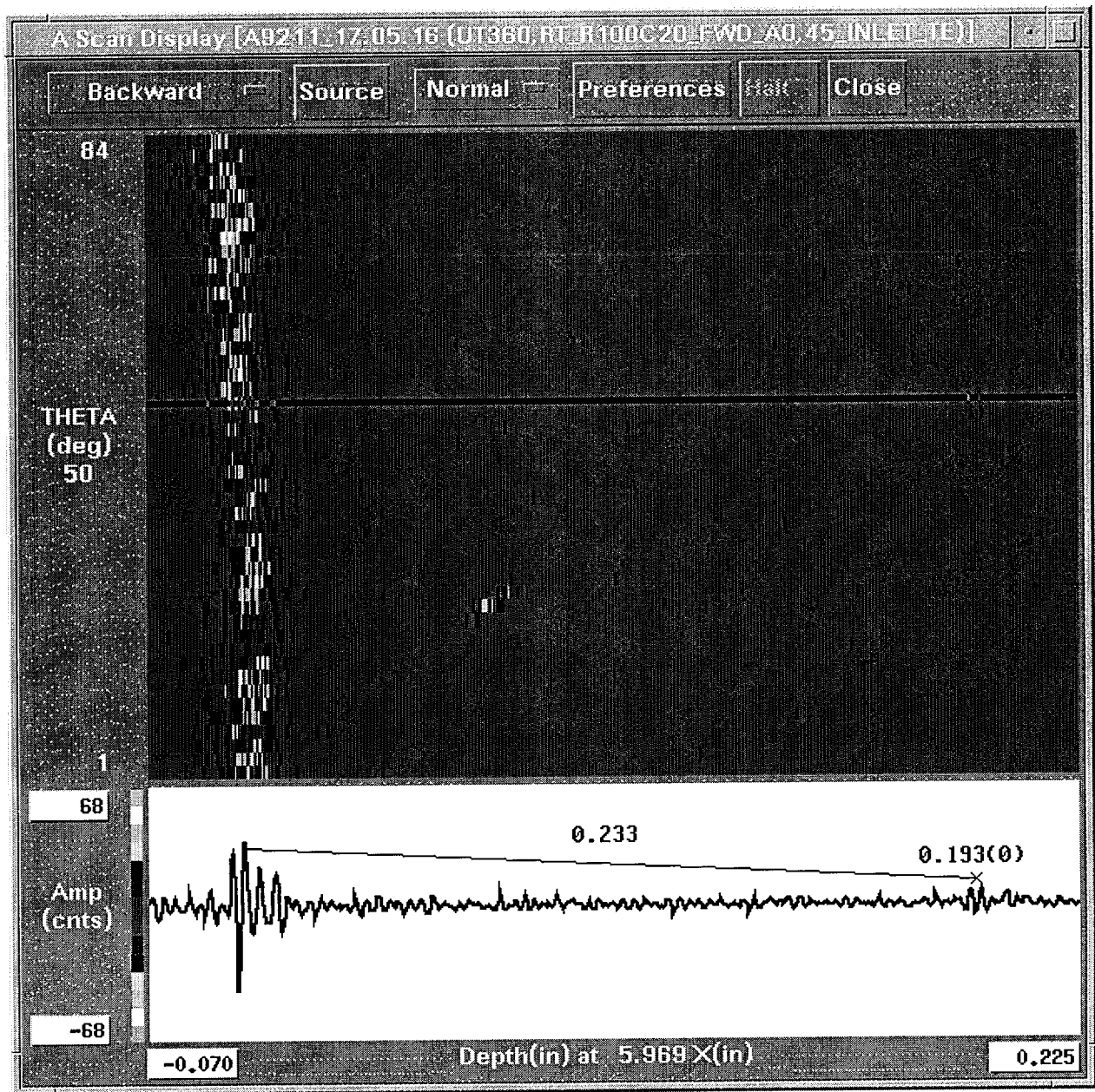


Figure R6-25. Crack A22: One and One Half Skip Reflection

This is the one and one half skip reflection for crack A22 at the 5.969 inch axial location. The 0.193 inch depth (time of flight) and the 50 degree circumferential location will be used to qualify this reflection with the half skip reflection.

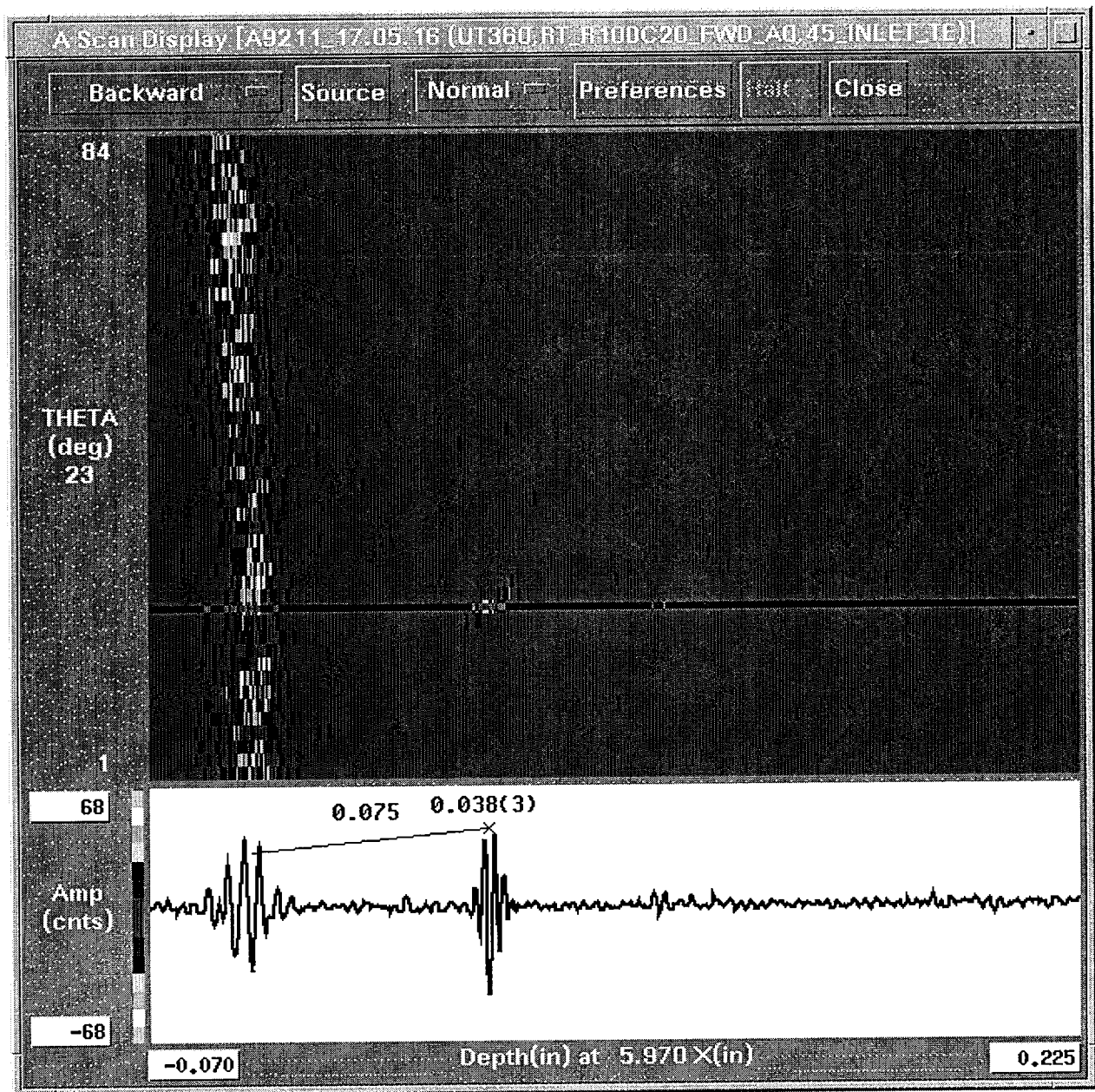


Figure R6-26. Crack A22: Half Skip Reflection

This is the half skip reflection for crack A22 at the 5.970 inch axial location. The delta depth is $(0.193 - 0.038) = 0.155$ inch. The delta displacement is $((50 - 23) * 0.006) = 0.162$ inch. Since these two results, (0.155 and 0.162), are within one pitch (0.015 inch), the half skip and the one and one-half skip have been correctly identified. The delta depth and delta displacement are also nearly equal to the expected value of two times the wall thickness.

The final presentation will support the argument that the system is capable of detecting PWSCC in the parent tube material. Tube TST4-076-1 (nominal 7/8" OD x 0.050" wall) was an additional sample that underwent fatigue cycling after the deposition of ~0.012 inch of sleeve thickness. During the pre-sleeve ultrasonic inspection, inner diameter circumferential cracks were identified in addition to the outer diameter circumferential crack (ODSCC). This presentation consists of C-Scan and A-Scan plots at three process steps; pre-sleeve, post sleeve and post fatigue. The A-Scan plots, at each process step will identify the inner diameter crack relative to the outer diameter crack.

From the DE, an inner diameter crack was found at the 156 degree location in addition to the expected outer diameter crack. These two circumferential cracks are axially separated by 0.034 inch. The outer diameter crack was reported at axial location 4.551 inches with a 0.035 inch depth. The inner diameter crack was reported at axial location 4.585 inches with a 0.012 inch depth. For the forward scan motion of the probe, the detection of the inner diameter crack would be expected to precede the detection of the outer diameter crack. In other words, the full skip target motion associated with the inner diameter crack should be detected at a higher axial location than the half skip target motion associated with the outer diameter crack.

After the deposition, the full skip target motion for the inner diameter crack disappears. This is expected since this crack no longer terminates at the inner diameter surface. It has become an inclusion.

During the fatigue cycling, fatigue cracks developed in the sleeve wall at the inner diameter crack site as well as at the outer diameter crack site. The post fatigue portion of this presentation will show the return of the full skip reflection at the inner diameter crack location as well as the increase in the FSN result for the outer diameter crack.

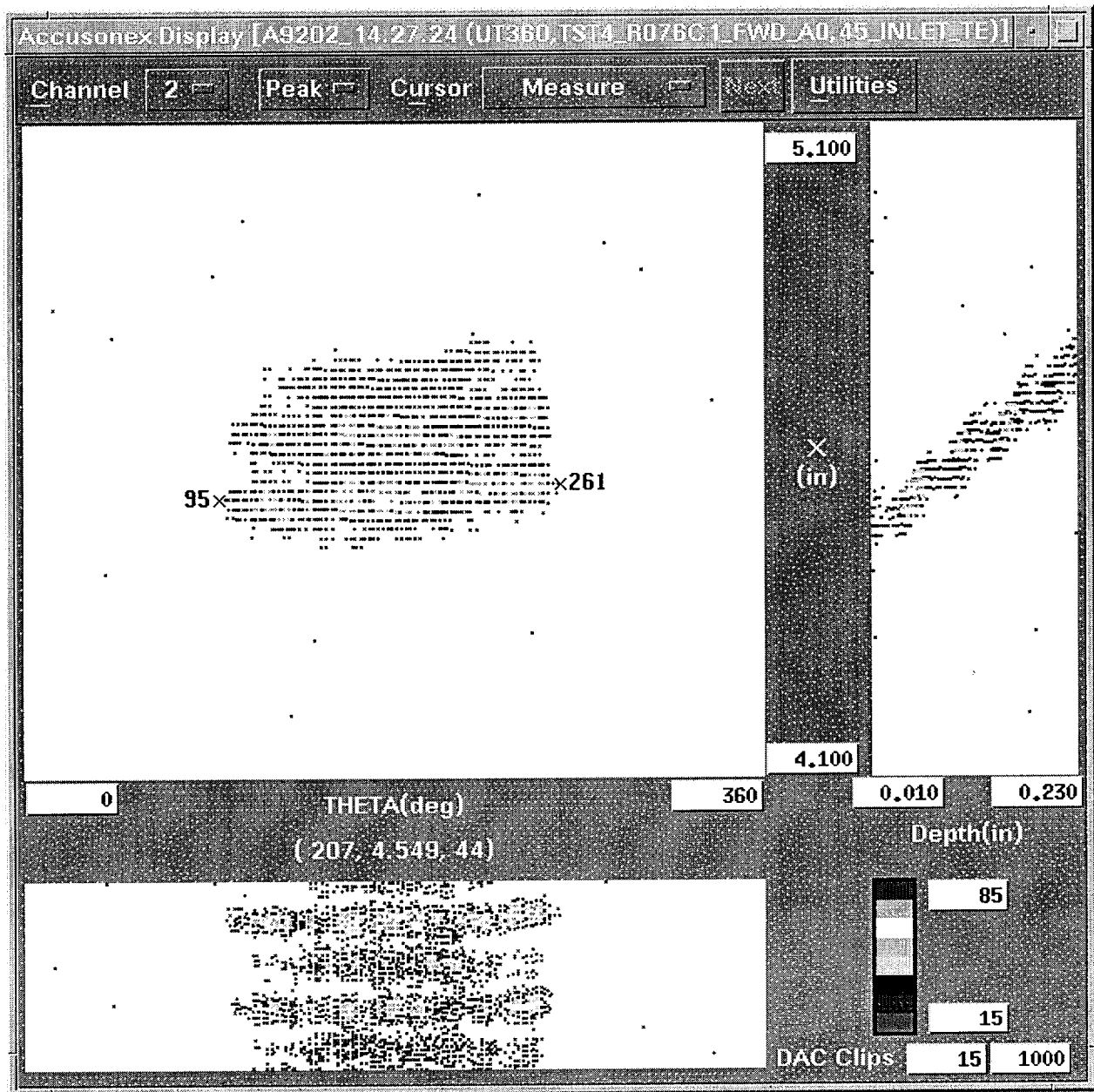


Figure R6-27

This is the pre-sleeve C-Scan plot of the ODSCC circumferential crack in tube TST4-076-1. The outer diameter crack extent (length) can be estimated from the C-Scan plot as $(261 - 95)$ or 166 degrees. The plot shows the presence of a half skip response, a one and one half skip response and a considerable amount of full skip and two skip reflections.

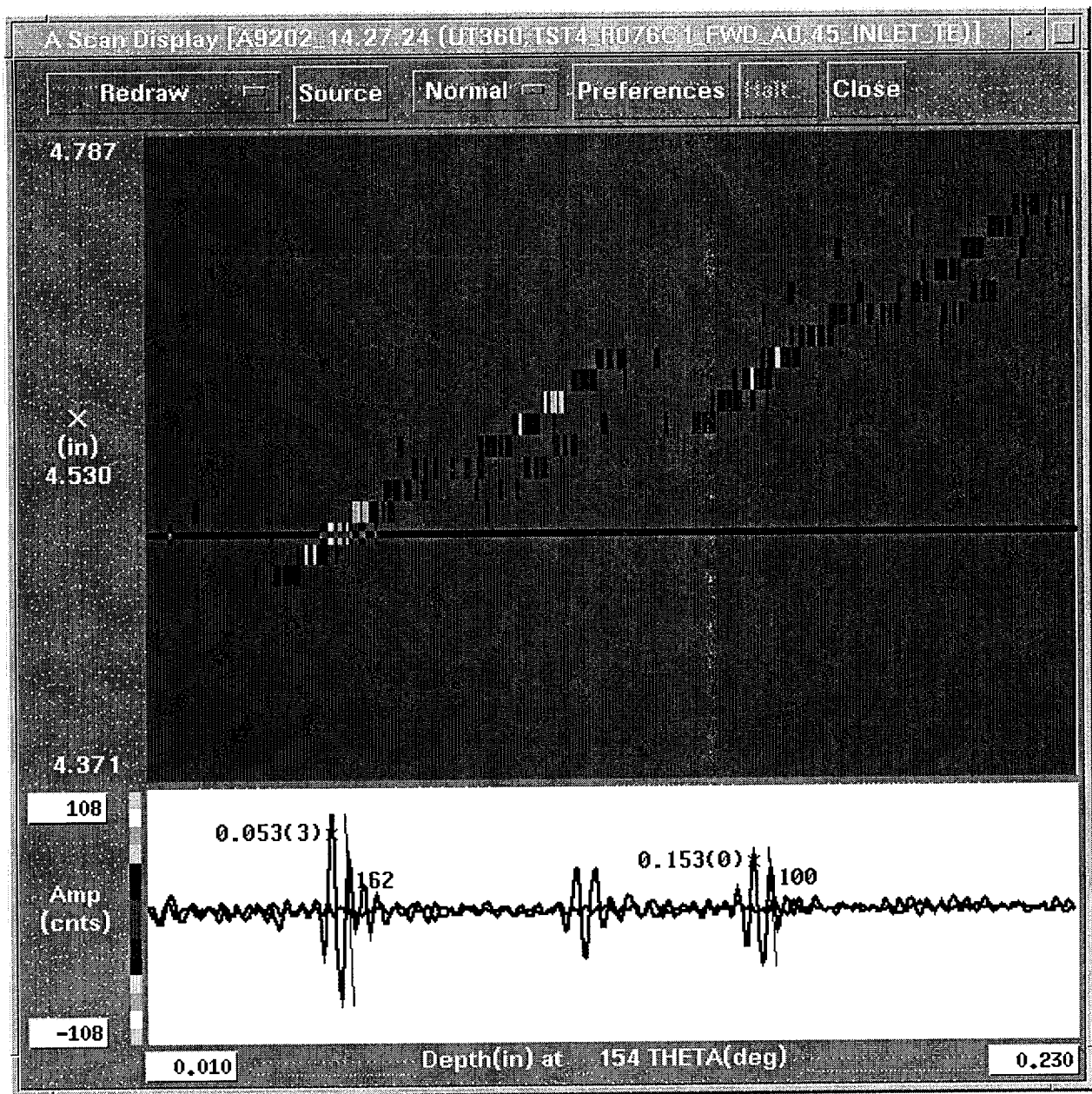


Figure R6-28

This is the A-Scan plot showing the half skip (0.053) and the one and one half skip (0.153) reflections associated with the outer diameter crack at the 154 degree location. Their amplitudes (162, 100), along with the full skip reflection amplitude (next plot), will be used to calculate a FSN result.

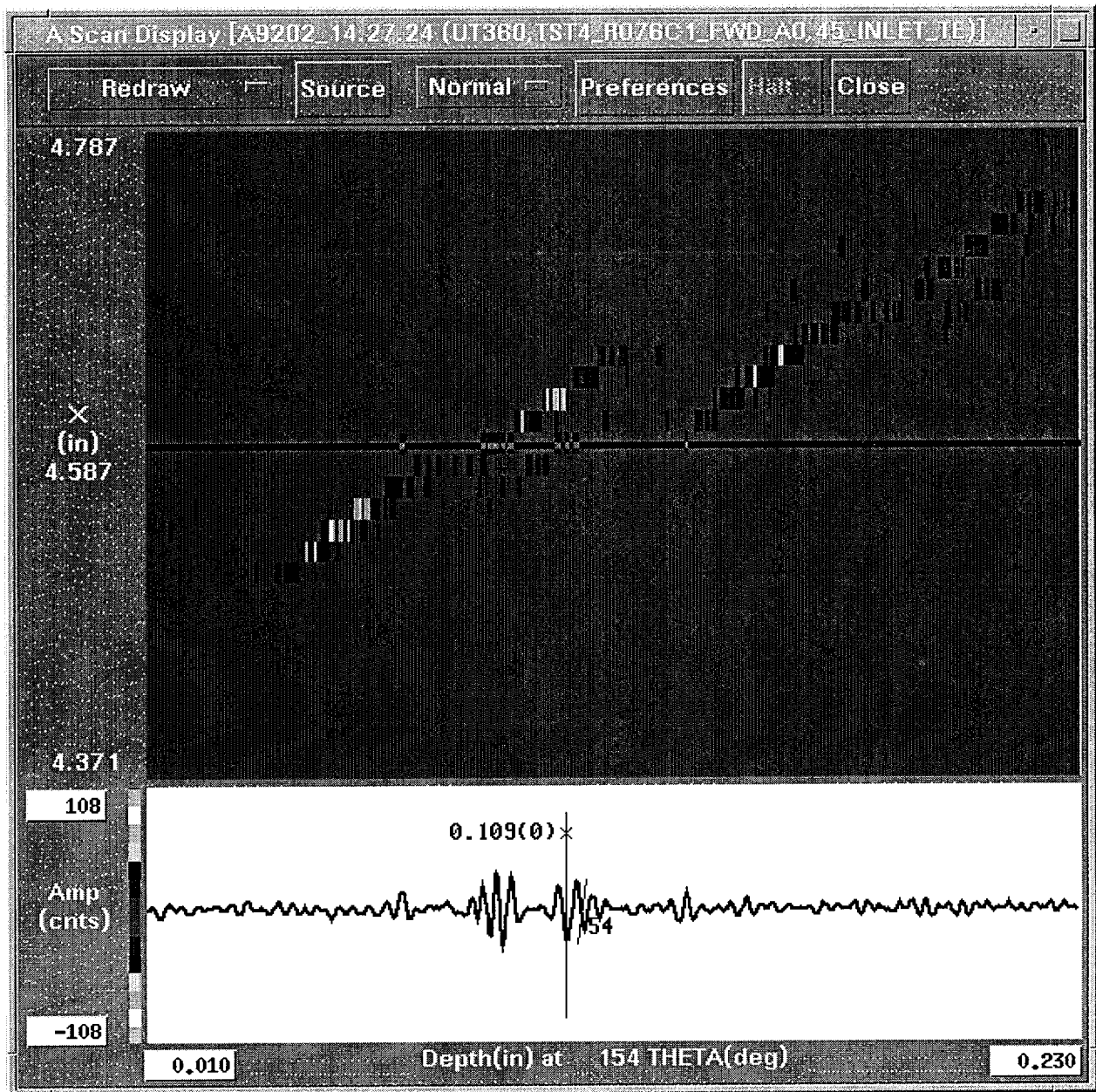


Figure R6-29

This is the A-Scan plot showing the full skip reflection associated with the outer diameter crack at the 154 degree location. The half skip (first outer diameter reflection) was the waveform 0.053 with a 162 count amplitude. The full skip (first inner diameter reflection) is the waveform 0.109 with a 54 count amplitude. The one and one half skip (second outer diameter reflection) was the waveform 0.153 with a 100 count amplitude. The calculated FSN value is $54 / ((162 + 100) * .5)$ or 0.41. The regression equation would be solved as $(0.050 - (0.031 - 0.031 * 0.41))$ or 0.032 inch..

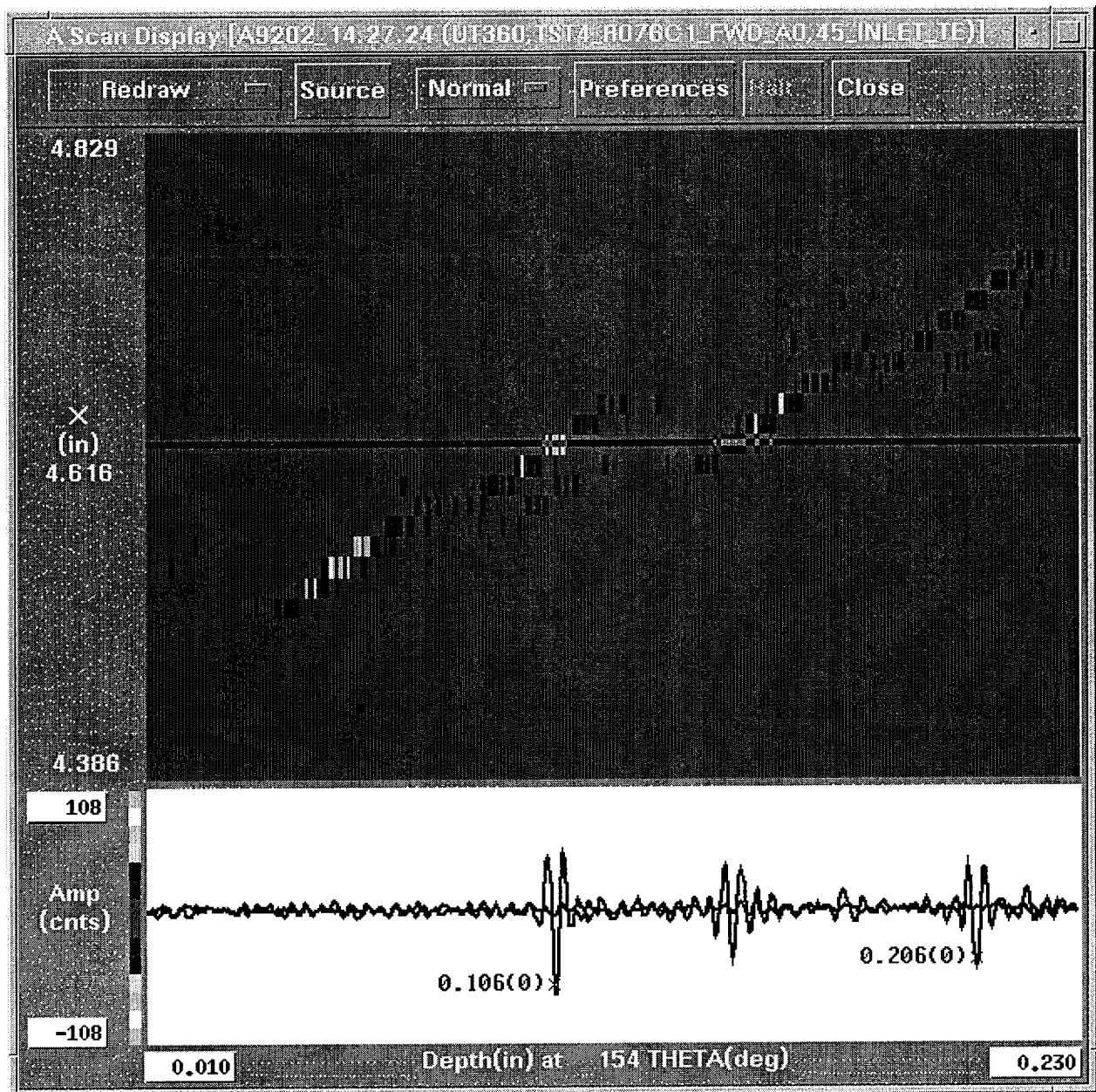


Figure R6-30

This is the A-Scan plot showing the full skip and the two skip reflections associated with the inner diameter crack at the 154 degree location. The full skip reflection occurs at the expected delta depth and delta displacement from the half skip. The delta depth is calculated as $(0.106 - 0.053)$ or 0.053 inch (~one wall thickness). The delta displacement is calculated as $((\text{full skip axial location} - \text{half skip axial location}) - (\text{one wall thickness}))$ or $((4.616 - 4.530) - 0.050) = 0.036$ inch. This value (0.036) is within one pitch of the DE reported crack separation 0.034 inch. This is sufficient to confirm that these are the reflections associated with the inner diameter crack identified during the DE.

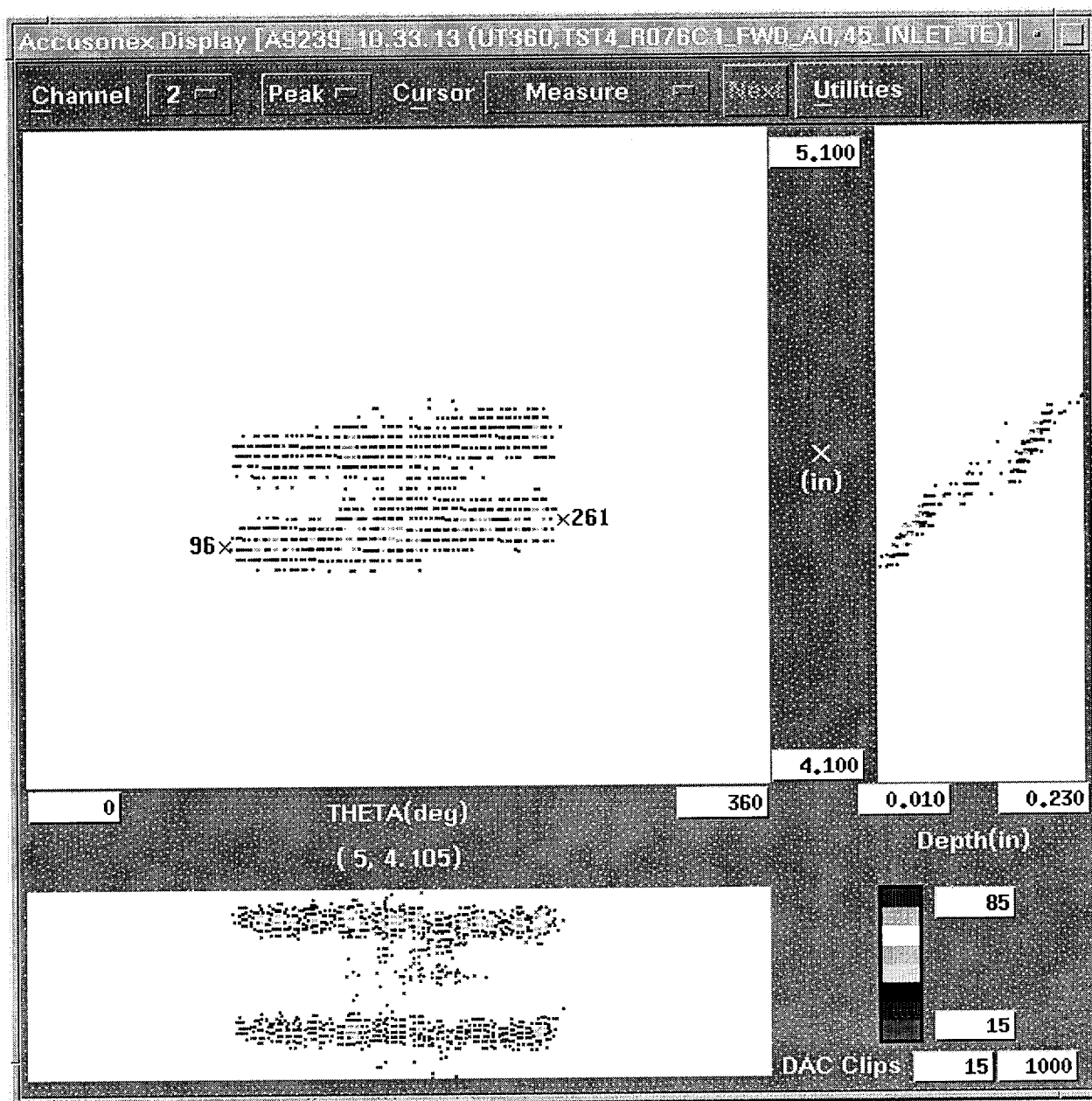


Figure R6-31

This is the post sleeve (pre-fatigue) C-Scan plot of the ODSCC circumferential crack in tube TST4-076-1. The outer diameter crack extent (length) can be estimated from the C-Scan plot as (261– 96) or 165 degrees. The plot shows the presence of a half skip response, a one and one half skip response and some full skip reflections between the 170 degree and 220 degree locations.

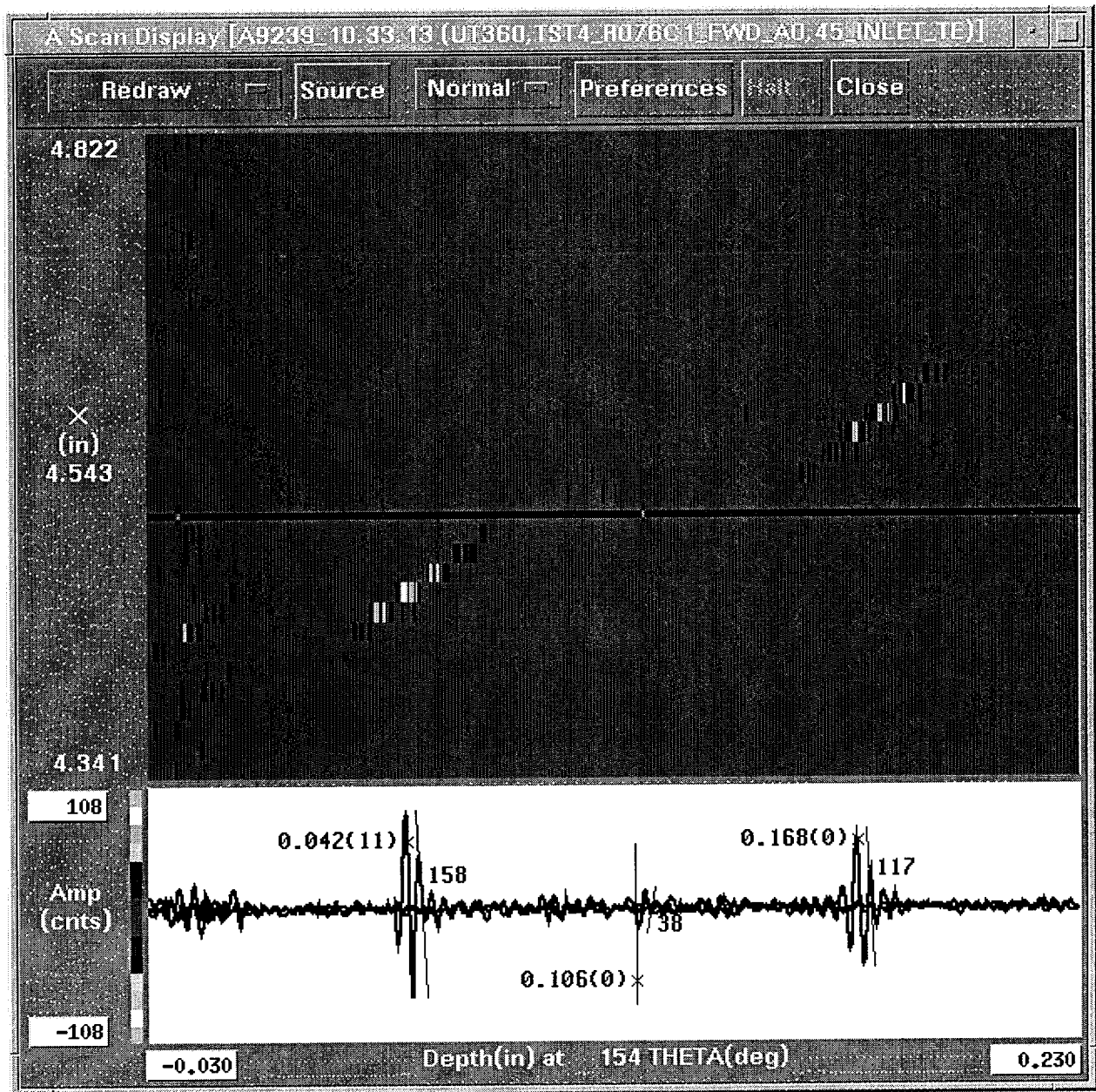


Figure R6-32

This is the A-Scan plot showing the skip reflections associated with the outer diameter crack at the 154 degree location. This plot is essentially the same as the pre-fatigue plot for this circumferential location. The DE did not report fatigue crack propagation coincident with the outer diameter crack at this circumferential location. The half skip (first outer diameter reflection) is the waveform 0.042 with a 158 count amplitude. The full skip (first inner diameter reflection) is the waveform 0.106 with a 38 count amplitude. The one and one half skip (second outer diameter reflection) is the waveform 0.168 with a 117 count amplitude. The calculated FSN value is $38 / ((158 + 117) * .5)$ or 0.28. The regression equation would be solved as $(0.062 - (0.031 - 0.031 * 0.28))$ or 0.040 inch.

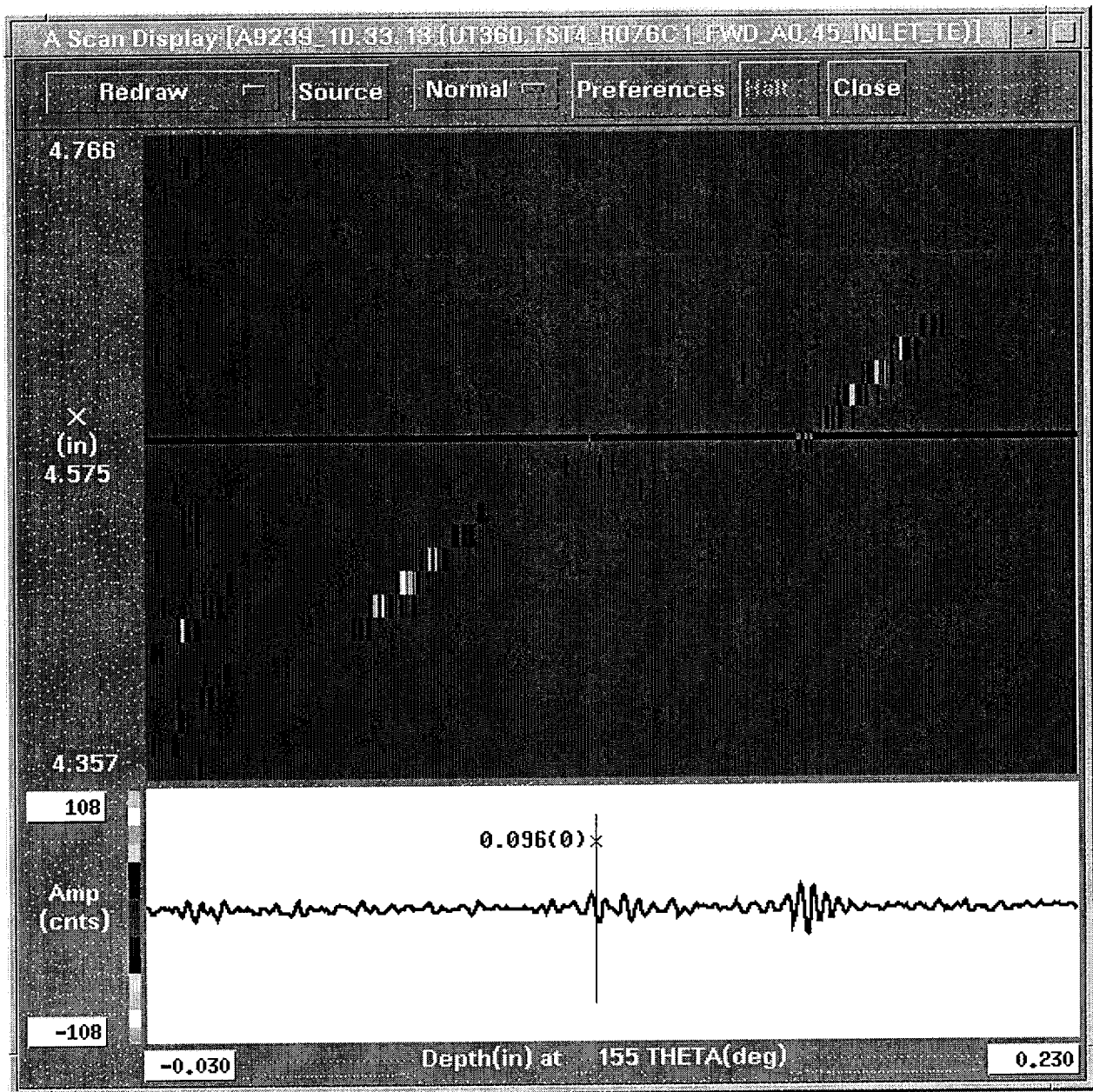


Figure R6-33

This A-Scan plot shows the reduced amplitude reflections from the inner diameter crack that has been plated over.

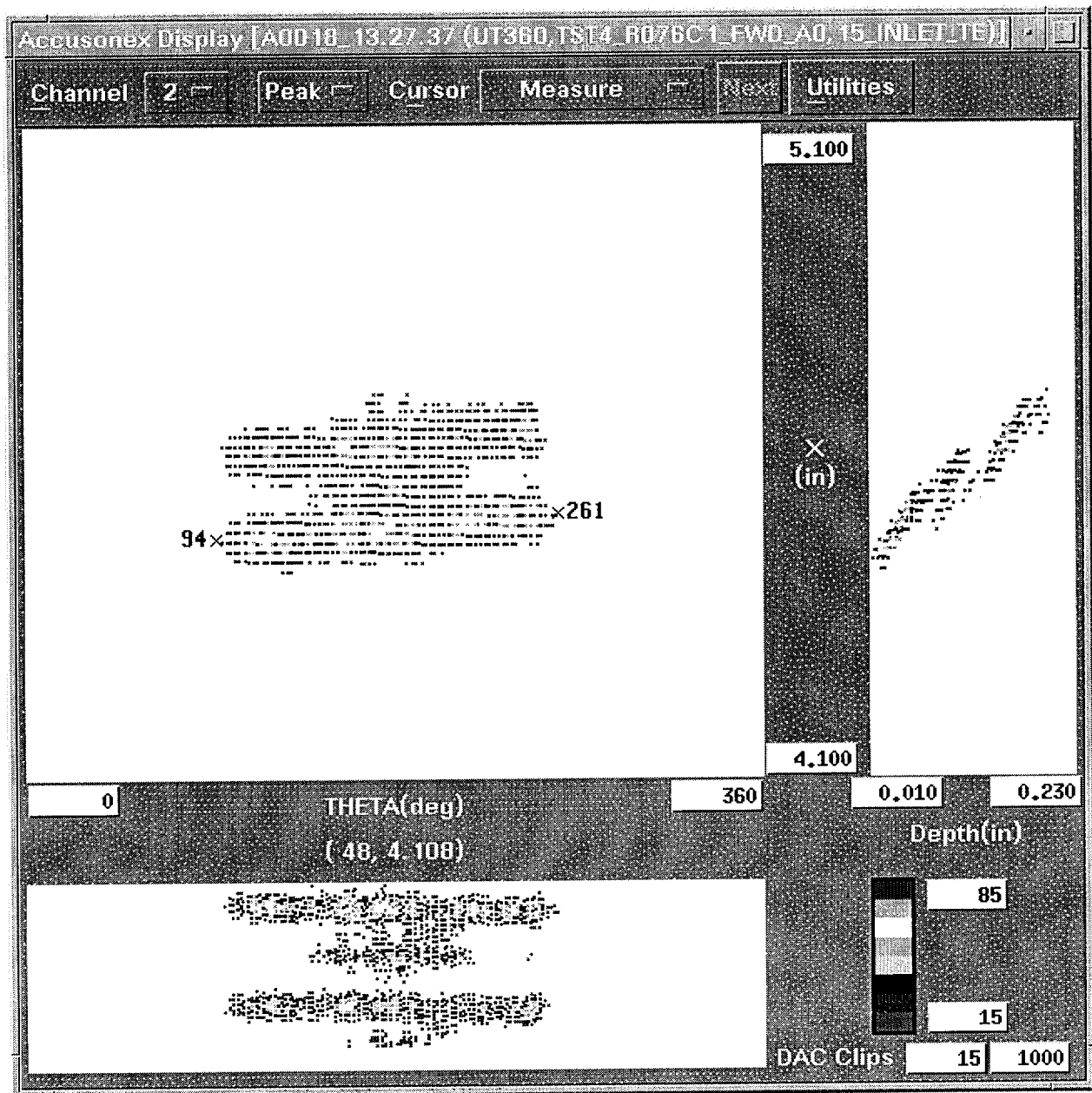


Figure R6-34

This is the post fatigue crack C-Scan plot of the ODSCC circumferential crack in tube TST4-076-1. The crack extent (length) can be estimated from the C-Scan plot as $(261 - 94)$ or 167 degrees. The plot shows the presence of a half skip response, a one and one half skip response and the return of the full skip reflections.

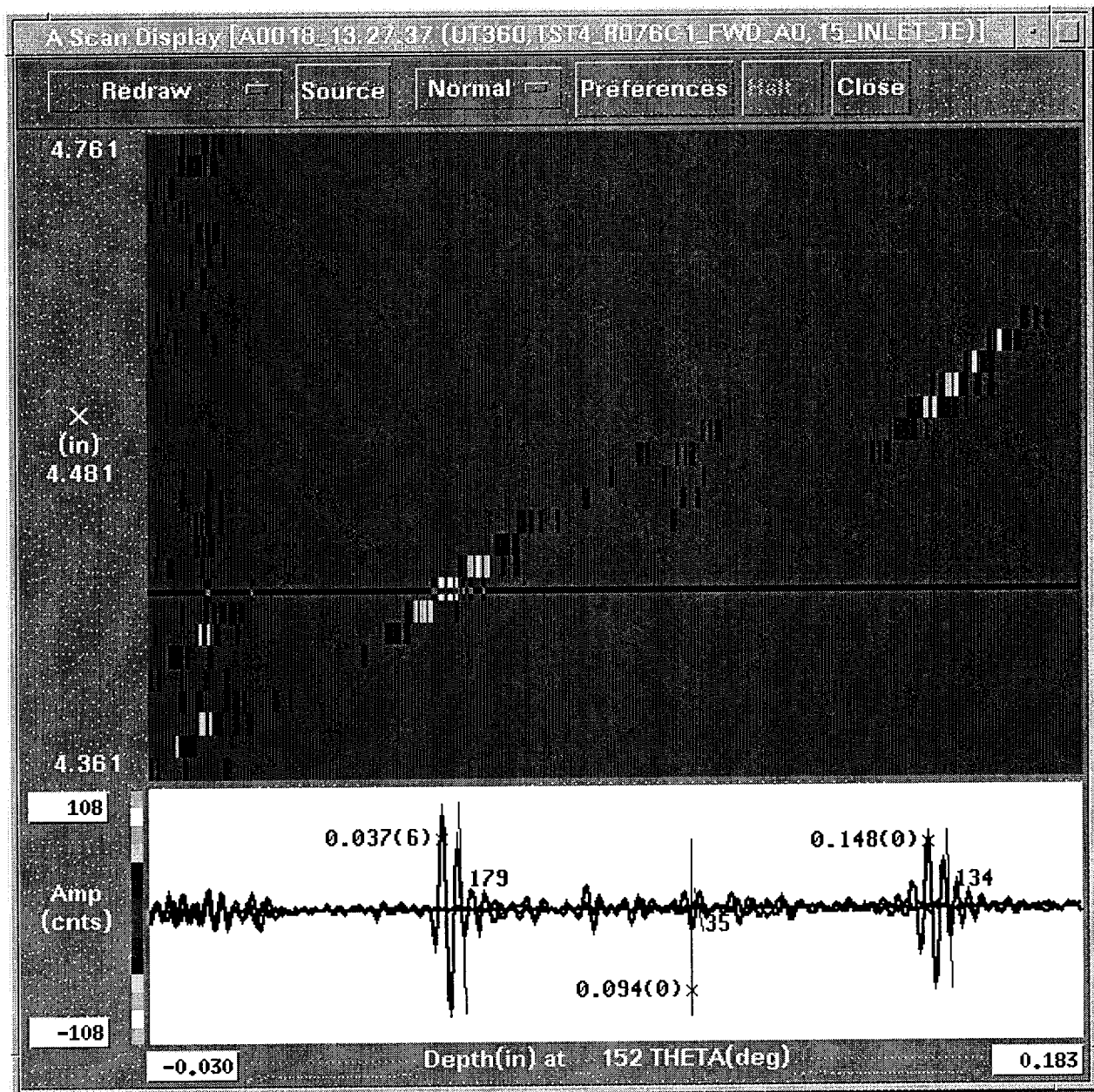


Figure R6-35

This is the A-Scan plot showing the skip reflections associated with the outer diameter crack at the 152 degree location. This plot is essentially the same as the pre-fatigue plot for this circumferential location. The DE did not report fatigue crack propagation coincident with the outer diameter crack at this circumferential location. The half skip (first outer diameter reflection) is the waveform 0.037 with a 179 count amplitude. The full skip (first inner diameter reflection) is the waveform 0.094 with a 35 count amplitude. The one and one half skip (second outer diameter reflection) is the waveform 0.148 with a 134 count amplitude. The calculated FSN value is $35 / ((179 + 134) * .5)$ or 0.22. The regression equation would be solved as $(0.062 - (0.031 - 0.031 * 0.22))$ or 0.038 inch.

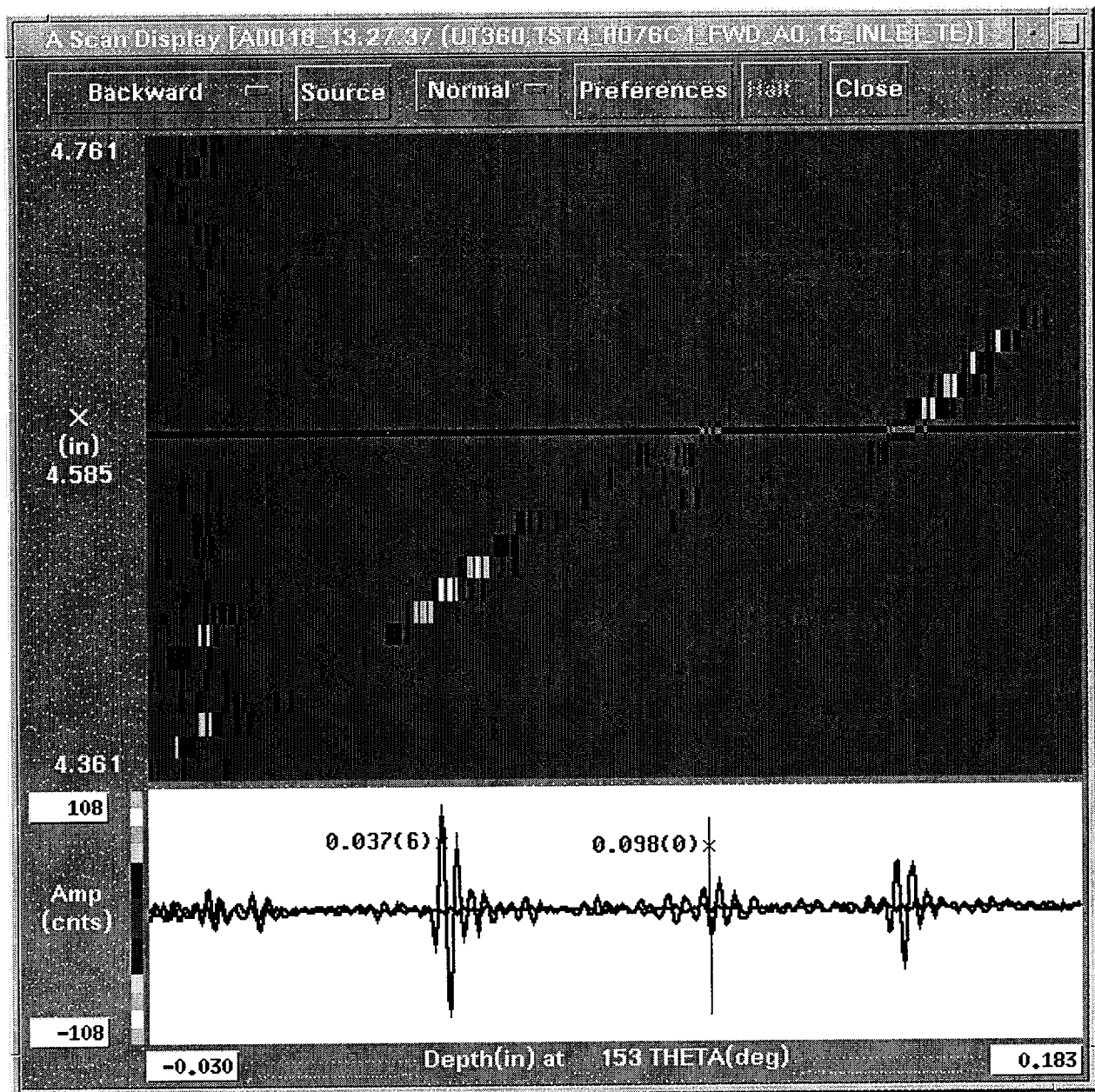


Figure R6-36

This is the A-Scan plot showing the half skip reflection associated with the outer diameter crack, and the full skip reflection associated with the inner diameter fatigue crack coincident with the parent tube inner diameter SCC crack at the 153 degree location. The full skip reflection occurs at the expected delta depth and delta displacement from the half skip. The delta depth is calculated as $(0.098 - 0.037)$ or 0.061 inch (one combined wall thickness). The delta displacement is calculated as $((\text{full skip axial location} - \text{half skip axial location}) - (\text{one combined wall thickness}))$ or $((4.585 - 4.481) - 0.062) = 0.042$ inch. This value (0.042) is within one pitch of the DE reported crack separation 0.034 inch. This is sufficient to confirm the propagation of a fatigue crack at the inner diameter crack axial location.

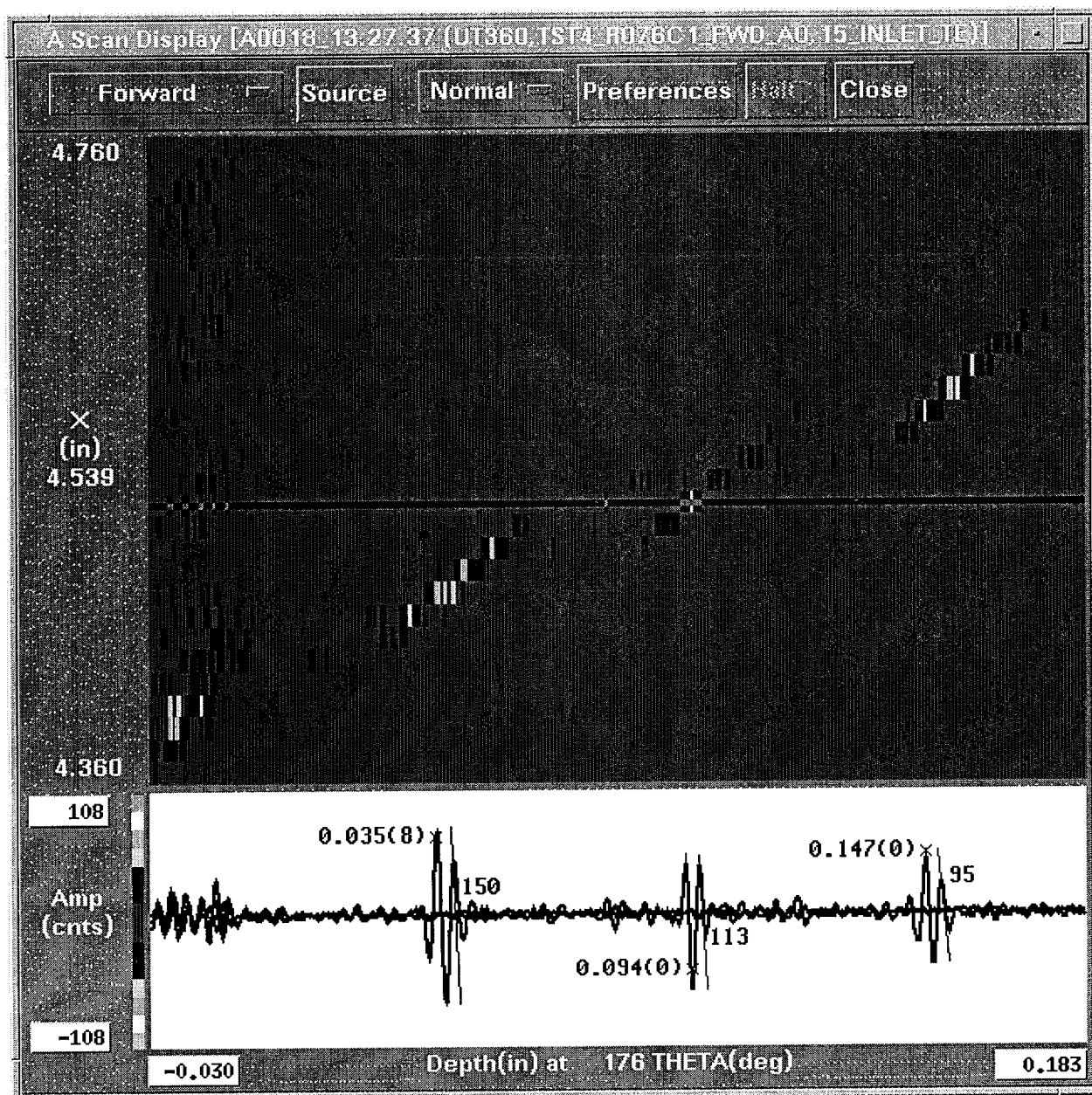


Figure R6-37

This is an A-Scan plot that presents the three waveforms that would be used for a FSN calculation at the 176 degree location. The DE reported fatigue crack propagation coincident with the outer diameter crack at this circumferential location. The half skip (first outer diameter reflection) is the waveform 0.035 with a 150 count amplitude. The full skip (first inner diameter reflection) is the waveform 0.094 with a 113 count amplitude. The one and one half skip (second outer diameter reflection) is the waveform 0.147 with a 95 count amplitude. The calculated FSN value is $113 / ((150 + 95) * .5)$ or 0.92. The regression equation would be solved as $(0.062 - (0.031 - 0.031 * 0.92))$ or 0.060 inch.

By the use of C-Scan and A-Scan plots, the presentations have demonstrated:

1. The ultrasonic method acquires sufficient time-of-flight to detect outer diameter flaws at the half skip and at the one and one-half skip as well as detect inner diameter flaws at the full skip.
2. After deposition of a structural sleeve, the ultrasonic method has sufficient sensitivity to detect shallow depth ODSCC at the one and one-half skip as well as at the half skip. Detection of ODSCC at depths as shallow as 0.006 inch were illustrated in the presentation. The amplitude of the full skip reflection would be expected to be equal to the average of the amplitudes of the outer diameter skips presented. Therefore, sensitivity to inner diameter sleeve flaws of similar depth would be expected at the full skip. These flaws are much more shallow than the structural limit for sleeve ID cracks, which is > 0.020 inch based on limits determined for OD cracks in Table 12.4.3 of the topical report.
3. The ultrasonic method acquired data at sufficient sensitivity to detect inner and outer diameter cracks in the parent tube material prior to plating. The system acquired sufficient data to detect the presence of a fatigue flaw propagating from the original inner diameter crack as well as the propagation of the ODSCC flaw, as fatigue, through the sleeve material.

RAI # 7. In the 6/7/01 meeting, UE stated that they only need to detect, not size, ID flaws in the Electrosleeve, because the tubes would be plugged upon detection of ID flaws in the Electrosleeve. This provision is not currently included in the Callaway Technical Specifications. Include in the Technical Specification a requirement that tubes with sleeve ID flaws will be taken out of service. (Question from the 6/7/01 meeting held with UE, FTI, and the NRC staff)

Response:

The current wording in the Technical Specification was intended to require that all sleeve ID flaws at Callaway be plugged. If an ID flaw is detected, there is a high probability the flaw will be an ID pit produced during the installation. Page 11-45, BAW-10219P-Rev.4, states that "ID pits are conservatively assumed to be 100% through the sleeve material." Therefore, if an ID pit is detected in a sleeve installed in Callaway, the depth of the ID pit is assumed to be 100% of the sleeve wall (by definition). Since 100% is greater than the 20% plugging criteria applicable to Callaway, the sleeve/tube would be removed from service. Thus, the wording in the Technical Specification results in a "plug on detection" requirement for ID pits.

For all other (non-pit) sleeve ID indications, no qualified sizing technique exists. Therefore the 20% TW plugging criteria contained in the Technical Specification results in a "plug-on-detection" requirement for all sleeve ID indications.

AmerenUE will revise the wording in the Technical Specification to clarify that all tubes with ID indications in the Electrosleeve will be plugged.

RAI # 8. The topical report does not discuss the detectability of PWSCC in the original tube once the tube defect has been sleeved. During the meeting on 6/7/01, the licensee indicated that this is because shallow PWSCC flaws are not detectable once the sleeve was installed, and additionally, further degradation of these flaws are not expected. In response to a staff question at this meeting, the licensee stated that if the PWSCC flaw did, unexpectedly, continue to degrade, it would be expected to grow towards the OD of the parent tube and not towards the sleeve. As the PWSCC flaw approached the parent tube OD, it would be detectable, and the UT depth sizing technique would be utilized to monitor the flaw. (Question from the 6/7/01 meeting held with UE, FTI, and the NRC staff)

A. Explain the basis and level of confidence for why the tube PWSCC flaw would grow towards the tube OD, versus into the sleeve.

B. During the license amendment review for the safety evaluation report approving electrosleeving for Callaway in May 1999, the staff noted that the largest depth sizing NDE uncertainties (undersizing) were associated with through-wall PWSCC flaws that were electrosleeved. The topical report for the current proposed amendment does not include flaws of this type. Therefore, given the potential situation proposed above (i.e., parent tube PWSCC flaws that continue to degrade after sleeving) the staff believes no information has been provided in the topical report to support the licensee's stated actions (i.e., depth size the flaw using the ODSCC technique). Explain why it would be acceptable to take this action given the previous experience and the lack of supporting data in the current topical report. Otherwise, provide supporting data for this action.

Response:

A parent tube PWSCC crack is not expected to grow in any direction after it has been covered by installation of an Electrosleeve, since the crack has been isolated from the primary side environment necessary to cause the crack to propagate. This is supported by results from the initial in-service examination of installed Electrosleeves at Callaway (see response to Question # 25). Comparison of the UT examination results immediately after installation with the results of the inspection after the first cycle of operation confirmed that the parent tube indications had not grown in length or depth, within the accuracy of the UT technique. Many of these flaws were initiated from the ID of the tube.

As stated previously in the response to Question #6, nanophase Electrosleeve material is highly resistant to corrosion and SCC in PWR primary and secondary water environments. This is supported by test results discussed in BAW-10219P-Rev.4 on pages 9-21, 9-33, and 9-51, as well as statements made by D.R. Dierecks of Argonne National Laboratory. This is further supported by operational history of electrosleeves installed in Doel-2, summarized on page 3-3 of BAW-10219P-Rev.4. In that study, two tubes with through-wall cracks were pulled from Doel-2 after nine months and two years of service, respectively. Destructive examination of these tubes verified that the parent tube cracking did not propagate into the nickel sleeve.

Alloy 600 tube material, by comparison, is known to be susceptible to cracking. If the crack did unexpectedly continue to grow after installation of the sleeve, it is reasonable to expect that the crack would propagate in the susceptible material at a much higher rate than it would propagate through the Electrosleeve. The crack would therefore break through the tube OD surface before it would reach a depth in the Electrosleeve where it could challenge the integrity of the sleeve. Note that the structural limit of a sleeve crack in the Electrosleeve is []^{b,c,e} TW (BAW-10219P-Rev. 4, Table 12.4.4). Given the relative susceptibility of the two materials, it is virtually certain that a crack would break through the tube OD surface long before it could propagate through the Electrosleeve to this depth.

Stated another way, the tube will already have demonstrated the potential of PWSCC, otherwise the need for repair would not exist. The PWSCC will be identified by an ET technique to define the tube as needing repair or sleeve installation. The sleeve will remove the environment, PW of the PWSCC. The additional thickness of the sleeve will reduce the stress in the tube, thus the S of SCC is reduced. The remaining CC (corrosion cracking) has been evaluated and the sleeve material is more resistant than the alloy 600, therefore, if the flaw were to grow, the flaw would logically grow in the alloy 600 (parent tube).

It is also noted that the PWSCC flaws referred to in the question were used as ODSKC flaws in the qualification process, since the flaws were 100% TW (tube leaked). It was called PWSCC simply because it was grown from the tube ID in the laboratory. Previous versions of the topical did not present depth sizing information for PWSCC, nor does the current version.

ODSCC

RAI # 9. Rev. 3 of BAW-10219P contained typical full skip normalization (FSN) values that were obtained by using various EDM notch depths. Were any actual crack data used to develop the regression equation mentioned in Rev. 4 that would be used to correlate the FSN value to a crack depth, rather than just the EDM notch data as in Rev. 3? Is the regression equation based on the data from Table 11.7.1 in Rev. 3 (page 11-34 of Rev. 3)? (Page 11-30, BAW-10219P, Rev. 4)

Response:

The regression equation was derived from data acquired on EDM notches. The data population consisted of acquisitions using three different transducer types (variation in beam diameter and focal point), three separate gain settings (variation in signal reflection amplitude), and three separate axial pitches (variation in probe motion). From this development, it was determined that the FSN ratio was independent of axial pitch for axial pitch between 0.010 inch and 0.020 inch and independent of reflected signal amplitude over a range of 6dB. This implied that the technique would perform as well for actual flaws that would be expected to produce reflected signal amplitudes less than a typical EDM notch.

The FSN regression is a simple first order equation used to calculate the remaining wall:

$$\text{Remaining Wall} = 0.031 - (\text{FSN ratio} * 0.031)$$

The crack depth is determined by subtracting the remaining wall from the measured wall thickness.

$$\text{Depth} = (\text{measured wall thickness}) - (0.031 - (\text{FSN ratio} * 0.031))$$

The regression was used to depth size flaws within the extent sizing set that produced full skip reflections in addition to the two outer diameter reflections (half skip and the one and one half skip). This trial set indicated that the regression performed as well for actual cracks as for the EDM notches and no adjustments were made to the regression coefficients.

The regression equation was used to depth size the flaws, in the crack depth sizing data set, that presented full skip reflections in addition to the outer diameter skip reflections. The overall accuracy of the crack depth sizing procedure is a function of the accuracy of the three individual techniques and their procedural combinations. Since the overall accuracy is acceptable for this (the sleeve inspection) application, the FSN regression accuracy is acceptable and within the bounds of the overall accuracy for the depth sizing procedure.

RAI # 10. The report discusses an 0.8 inch ODSCC length in the parent tube that was established for repair using a minimal Electrosleeve thickness. What is this thickness? Does this also assume a 100% throughwall depth through the parent tube? Is there a structural integrity graph of ODSCC length in parent tube versus minimum Electrosleeve thickness? Please discuss the statement "axial cracks of extent 0.8 to 1.5 inches are of interest to the structural Electrosleeve for certain adverse plant operational conditions," especially covering the significance of the crack length range of 0.8 to 1.5 inches. (Page 11-58, BAW-10219P, Rev. 4)

Response:

The 0.8-inch length is significant to show that flaws less than 3/4-inch in length can be detected and extent (length) sized. The 3/4-inch length represents a normal breakpoint in the structural limits as shown in Table 8.5.3 and can be derived from Figure 8.5.1. Axial cracks greater than 3/4-inch are also of importance since the structural percent through wall limit changes as shown in Table 8.5.3.

The 0.8-inch length and reference to minimal Electrosleeve™ thickness refers to a separate Framatome ANP research and development program for repairing specific tube defects within drilled TSPs (~0.8-inch length). A tube flaw of 0.8 inch length, 100% TW parent tube can be sleeved with a minimum Electrosleeve thickness and satisfy Reg. Guide 1.121 pressure differentials requirements.

ODSCC detection and extent (length) sizing can be demonstrated using Electrosleeve™ samples with a nickel thickness of approximately 0.012 to 0.015-inch, which is less than the installed structural thickness as shown in Table 8.1.1. For the circumferential flaws, the minimal thickness samples (quantity 10) were used along with structural Electrosleeve™ samples (quantity 8) in the qualification. The qualification thus shows that detection and extent (length) sizing can be accomplished over a wide range of sleeve thickness.

RAI # 11. The report states that “three analysts performed the analysis of the data.” Yet, in Tables 11.9.1 through 11.9.8, data is only provided for 2 of the 3 analysts. Please provide the data in Tables 11.9.1 through 11.9.8 for all three analysts. (Pages 11-59 to 11-63, 11-64 to 11-69, BAW-10219P, Rev. 4)

Response:

In those cases where BAW-10219P, Rev. 4 states that multiple analysts were used, it should not be assumed that all analysts examined all of the data. Typically, one analyst was used to examine a mix of the total data set such as (**forward scan, pre-sleeve**) and (**reverse scan, post sleeve**) while a second analyst was used to examine the (**reverse scan, pre-sleeve**) and the (**forward scan, post sleeve**). The third analyst was typically tasked to perform the (**forward scan, pre-sleeve**) and the (**forward scan, post sleeve**) since these two combinations were used for the Appendix J qualification. For example, analyst one and analyst three performed the pre-sleeve extent sizing analysis for Table 11.9.1 while analyst two and analyst three performed the post sleeve extent sizing analysis for Table 11.9.2.

This analyst mix provided a more rigorous test of the analysis procedures as opposed to the typical single analyst (**expert**) approach used in a typical EPRI Appendix H or Appendix J qualification. This approach of including analyst variability in the statistical determination of the RMSE and the confidence level eliminated the need for a separate performance demonstration to determine analyst variability. Any analyst, attempting to qualify to these (Framatome ANP) procedures, must complete the qualification test to within the accuracy for the given technique stated in Table 11.10.2 of the topical report.

Since all error determinations were computed using DE results, no single analyst was treated as the expert. Analysts qualifying to this procedure would meet the average error and standard deviation results presented in Table 11.10.2. Consequently, the NDE uncertainty used in chapter 12 includes the system (technique and analyst) variability.

RAI # 12. The report states that the accuracy to which UT can measure crack depth determines the ability of the technique to determine if the crack has propagated into the sleeve material. The goal of the qualification was to demonstrate that the combination of the three depth sizing techniques (tip sizing, shear wave Mode Converted Signal, and Full Skip Normalization) could accurately determine the crack depth of penetration to 0.011 inch. Please discuss how the stated crack depth accuracy for ODSCC depth sizing of 0.011 inch was determined. (Page 11-64, BAW-10219P, Rev. 4)

Response:

The "crack depth accuracy for ODSCC depth sizing of 0.011 inch" was defined as the objective of the UT qualification. The value of 0.011 inch is based on previous topical submittals and review of the NRC SER (May 21, 1999, pg.16) which "identified concern with the depth sizing capability of the shear wave examination when sizing stress corrosion cracks." Specifically, the RMSE UT crack depth sizing error and the "Allowed Structural Degradation", reported in BAW-10219P-Revision 3, provided a basis for defining the minimum repair limit.

Table 12.4.4, BAW-10219P-Rev.4 defines 0.008 inch or 8 mils as the UT 95% LCL for crack depth sizing. This table provides the process for definition of the crack specific "Repair Limit" which includes Structural evaluation, UT system variability and postulated crack growth. A value of 1.5 mils was assumed for uniform thinning and pitting growth based on the corrosion data discussed in Section 9.3.4. Crack growth in the sleeve was assumed to be []^{b,c,e} of the nominal sleeve thickness based on the fracture analysis discussed in Section 8.5. These values are considered in the calculation of the sleeve repair limits defined in Tables 12.4.3 and 12.4.4.

The statistical "UT crack depth accuracy for ODSCC" performance, Table 11.10.2, typically overcalls the depth by 0.004 inch. The consistency of this performance (standard deviation of the error) is 0.007 inch. Thus in a worst case scenario, there is a 5% chance the flaw could be undersized by 0.008 inch ($0.004 - 1.645 * .007$). When this value is incorporated into Table 12.4.4 the minimum repair limit for 11/16" tubing is 37%TW. Thus the topical recommends a 30% TW Electrosleeve plugging limit, Section 12.4.

OD Pits

RAI # 13. Please provide the data from analysts 1 and 2 in their pit sizing for the pits listed in Table 11.8.1, as well as the destructive analysis results. You have provided the summary information in Table 11.8.2, but not the actual analyst data or destructive analysis results. (Page 11-33, BAW-10219P, Rev. 4)

Response:

As stated on page 11-32, BAW-10219P-Rev.4, "the reported actual depths were determined using a pin micrometer to a measurement uncertainty of +/- 0.002 inch." The seven tubes in this sample set were provided by EPRI and no destructive examination was performed. The seven tubes have been returned to EPRI where they continue to be used to evaluate NDE techniques. Table 11.8.1 presents the results of the pin micrometer measurements of the pits used for the qualification. The pin micrometer measurements were used as 'truth' for comparisons with the ultrasonic analysis.

The data set consisted of three acquisitions at axial pitch values of 0.010, 0.015 and 0.020 inch. This was performed to determine if depth sizing accuracy was a function of acquisition pitch. Two analysts were used to depth size each pit for each acquisition pitch. This resulted in (2 analysts * 3 pitches * 31 pits) 186 depth values. The three pages that follow contain the results for each acquisition pitch. The MIN, AVE, and STDEV values, (**BOLD** type) were reported in Table 11.8.2.

Table R13-1. Analysis Results for OD Pit Depth Sizing, Acquisition Pitch = 0.010"

Sample	Ind.	Actual Measured Pit Depth (inch)	FTI1 Measured Pit Depth (inch)	FTI2 Measured Pit Depth (inch)	Delta FTI1 vs. Actual Depth (inch)	Delta FTI2 vs. Actual Depth (inch)	Delta FTI1 vs. FTI2 Depth (inch)
P6	A	0.012	0.014	0.015	0.002	0.003	0.001
	B	0.015	0.016	0.015	0.001	0.000	0.001
	C	0.010	0.012	0.012	0.002	0.002	0.000
	D	0.011	0.012	0.015	0.001	0.004	0.003
	E	0.009	0.006	0.006	-0.003	-0.003	0.000
	F	0.008	0.008	0.008	0.000	0.000	0.000
P35	A	0.017	0.018	0.020	0.001	0.003	0.002
	B	0.016	0.014	0.013	-0.002	-0.003	0.001
	C	0.016	0.019	0.021	0.003	0.005	0.002
	D	0.021	0.022	0.021	0.001	0.000	0.001
	E	0.025	0.025	0.026	0.000	0.001	0.001
	F	0.009	0.010	0.011	0.001	0.002	0.001
P38	A	0.018	0.018	0.021	0.000	0.003	0.003
	B	0.015	0.018	0.020	0.003	0.005	0.002
	C	0.008	0.006	0.007	-0.002	-0.001	0.001
P39	B	0.019	0.018	0.018	-0.001	-0.001	0.000
	C	0.020	0.020	0.021	0.000	0.001	0.001
	E	0.023	0.020	0.021	-0.003	-0.002	0.001
	G	0.012	0.007	0.007	-0.005	-0.005	0.000
P44	A	0.018	0.019	0.020	0.001	0.002	0.001
	B	0.013	0.008	0.013	-0.005	0.000	0.005
P48	A	0.016	0.022	0.022	0.006	0.006	0.000
	B	0.010	0.014	0.014	0.004	0.004	0.000
	C	0.020	0.021	0.023	0.001	0.003	0.002
	D	0.020	0.016	0.017	-0.004	-0.003	0.001
	E	0.013	0.015	0.015	0.002	0.002	0.000
P51	A	0.016	0.019	0.019	0.003	0.003	0.000
	B	0.020	0.027	0.019	0.007	-0.001	0.008
	C	0.023	0.021	0.021	-0.002	-0.002	0.000
	D	0.031	0.026	0.026	-0.005	-0.005	0.000
	E	0.018	0.017	0.021	-0.001	0.003	0.004
max:					0.007	0.006	0.008
min:					-0.005	-0.005	0.000
ave:					0.000	0.001	0.001
stdev:					0.003	0.003	0.002

Table R13-2. Analysis Results for OD Pit Depth Sizing, Acquisition Pitch = 0.015"

Sample	Ind.	Actual Measured Pit Depth (inch)	FTI1 Measured Pit Depth (inch)	FTI2 Measured Pit Depth (inch)	Delta FTI1 vs. Actual Depth (inch)	Delta FTI2 vs. Actual Depth (inch)	Delta FTI1 vs. FTI2 Depth (inch)
P6	A	0.012	0.013	0.012	0.001	0.000	0.001
	B	0.015	0.015	0.015	0.000	0.000	0.000
	C	0.010	0.012	0.013	0.002	0.003	0.001
	D	0.011	0.013	0.014	0.002	0.003	0.001
	E	0.009	0.006	0.007	-0.003	-0.002	0.001
	F	0.008	0.007	0.007	-0.001	-0.001	0.000
P35	A	0.017	0.017	0.020	0.000	0.003	0.003
	B	0.016	0.014	0.015	-0.002	-0.001	0.001
	C	0.016	0.019	0.020	0.003	0.004	0.001
	D	0.021	0.022	0.022	0.001	0.001	0.000
	E	0.025	0.023	0.025	-0.002	0.000	0.002
	F	0.009	0.011	0.010	0.002	0.001	0.001
P38	A	0.018	0.013	0.015	-0.005	-0.003	0.002
	B	0.015	0.019	0.019	0.004	0.004	0.000
	C	0.008	0.006	0.007	-0.002	-0.001	0.001
P39	B	0.019	0.020	0.020	0.001	0.001	0.000
	C	0.020	0.020	0.021	0.000	0.001	0.001
	E	0.023	0.021	0.022	-0.002	-0.001	0.001
	G	0.012	0.005	0.006	-0.007	-0.006	0.001
P44	A	0.018	0.020	0.020	0.002	0.002	0.000
	B	0.013	0.012	0.013	-0.001	0.000	0.001
P48	A	0.016	0.021	0.021	0.005	0.005	0.000
	B	0.010	0.013	0.012	0.003	0.002	0.001
	C	0.020	0.021	0.021	0.001	0.001	0.000
	D	0.020	0.017	0.015	-0.003	-0.005	0.002
	E	0.013	0.013	0.015	0.000	0.002	0.002
P51	A	0.016	0.019	0.018	0.003	0.002	0.001
	B	0.020	0.018	0.018	-0.002	-0.002	0.000
	C	0.023	0.019	0.021	-0.004	-0.002	0.002
	D	0.031	0.026	0.025	-0.005	-0.006	0.001
	E	0.018	0.019	0.018	0.001	0.000	0.001
max:					0.005	0.005	0.003
min:					-0.007	-0.006	0.000
ave:					0.000	0.000	0.001
stdev:					0.003	0.003	0.001

Table R13-3. Analysis Results for OD Pit Depth Sizing, Acquisition Pitch = 0.020"

Sample	Ind.	Actual Measured Pit Depth (inch)	FTI1 Measured Pit Depth (inch)	FTI2 Measured Pit Depth (inch)	Delta FTI1 vs. Actual Depth (inch)	Delta FTI2 vs. Actual Depth (inch)	Delta FTI1 vs. FTI2 Depth (inch)
P6	A	0.012	0.012	0.014	0.000	0.002	0.002
	B	0.015	0.016	0.014	0.001	-0.001	0.002
	C	0.010	0.009	0.011	-0.001	0.001	0.002
	D	0.011	0.012	0.013	0.001	0.002	0.001
	E	0.009	0.007	0.006	-0.002	-0.003	0.001
	F	0.008	0.007	0.007	-0.001	-0.001	0.000
P35	A	0.017	0.017	0.019	0.000	0.002	0.002
	B	0.016	0.014	0.015	-0.002	-0.001	0.001
	C	0.016	0.019	0.019	0.003	0.003	0.000
	D	0.021	0.021	0.020	0.000	-0.001	0.001
	E	0.025	0.023	0.026	-0.002	0.001	0.003
	F	0.009	0.008	0.009	-0.001	0.000	0.001
P38	A	0.018	0.017	0.017	-0.001	-0.001	0.000
	B	0.015	0.015	0.018	0.000	0.003	0.003
	C	0.008	0.006	0.006	-0.002	-0.002	0.000
P39	B	0.019	0.016	0.015	-0.003	-0.004	0.001
	C	0.020	0.020	0.021	0.000	0.001	0.001
	E	0.023	0.022	0.022	-0.001	-0.001	0.000
	G	0.012	0.005	0.006	-0.007	-0.006	0.001
P44	A	0.018	0.019	0.020	0.001	0.002	0.001
	B	0.013	0.011	0.008	-0.002	-0.005	0.003
P48	A	0.016	0.019	0.021	0.003	0.005	0.002
	B	0.010	0.013	0.014	0.003	0.004	0.001
	C	0.020	0.021	0.021	0.001	0.001	0.000
	D	0.020	0.016	0.014	-0.004	-0.006	0.002
	E	0.013	0.014	0.014	0.001	0.001	0.000
P51	A	0.016	0.020	0.019	0.004	0.003	0.001
	B	0.020	0.020	0.017	0.000	-0.003	0.003
	C	0.023	0.020	0.020	-0.003	-0.003	0.000
	D	0.031	0.027	0.026	-0.004	-0.005	0.001
	E	0.018	0.019	0.019	0.001	0.001	0.000
max:					0.004	0.005	0.003
min:					-0.007	-0.006	0.000
ave:					-0.001	0.000	0.001
stdev:					0.002	0.003	0.001

Since there was no significant difference between the results, it was determined that the accuracy of the depth measurement was independent of the axial pitch for axial pitch between 0.010 and 0.020 inch. The results of the combined analyst population for the 0.015 axial pitch were reported in Table 11.10.2.

Table R13-4. Combined Analysis vs. DE Depth Differences, OD Pit Depth Sizing
Acquisition Pitch = 0.015"

0.001	0.000
0.000	0.000
0.002	0.003
0.002	0.003
-0.003	-0.002
-0.001	-0.001
0.000	0.003
-0.002	-0.001
0.003	0.004
0.001	0.001
-0.002	0.000
0.002	0.001
-0.005	-0.003
0.004	0.004
-0.002	-0.001
0.001	0.001
0.000	0.001
-0.002	-0.001
-0.007	-0.006
0.002	0.002
-0.001	0.000
0.005	0.005
0.003	0.002
0.001	0.001
-0.003	-0.005
0.000	0.002
0.003	0.002
-0.002	-0.002
-0.004	-0.002
-0.005	-0.006
0.001	0.000
max:	0.005
min:	-0.007
ave:	0.000
stdev:	0.003

The maximum delta between analysts is not significant because neither analyst is considered the “expert”, as is the current practice for most Appendix H and Appendix J qualifications. The analyst variation with respect to “truth” was used for this qualification. Therefore, the system uncertainty (technique and analyst) is included in the confidence level. Any analyst wishing to qualify to this procedure must meet the average error and standard deviation as presented in Table 11.10.2.

It was decided that the additional axial pitch acquisitions would not be necessary of the sleeve OD pit qualification. An axial pitch of 0.015 inch was used for the sleeve OD pit qualification in addition to the two tube diameters and their associated nominal sleeve wall thickness values.

RAI # 14. Confirm that there is a typographical error on page 11-36, first paragraph. The last sentence reads, "Although dip pits...", and we assume that it should read, "Although deep pits ..." (Page 11-36, BAW-10219P, Rev. 4)

Response:

Correct, this statement should read "deep pits". This is a typographical error and is not considered to be significant enough to require revision of the topical.

RAI # 15. The report states that “when the signals merge, the UT analyst makes a call that indicates that the pit is deep but an accurate measurement of the pit depth is beyond the capability of the system.” When the signals merge, does the analyst detect the signals saturating or does the data provide erroneous depth values (or some other phenomena)? (Page 11-36, BAW-10219P, Rev. 4)

Response:

There is no saturation or other phenomenon. The resulting ultrasonic waveform consists of an inner diameter surface reflection and no outer diameter (back wall) reflections. The actual remaining wall thickness would be less than one-half wavelength or 0.012 inch for a typical 10MHz transducer. The analyst could assign any value to the remaining wall thickness between 0.000 inch and 0.012 inch with no certainty of accuracy. If the value of 0.006 inch were chosen, there would be equal probability that the actual value would be within +/- 0.006 inch and therefore the accuracy would be no worse than 0.006 inch. Applying this bound is not relevant or necessary in that a remaining wall of 0.012 inch or less is well beyond the repair criteria of 40% for the parent tube material or 30% (20% for Callaway) for the sleeve material.

A typical pit of 0.100 inch diameter would have a minimum of (0.100/0.015) or 6 detection waveforms for an axial pitch of 0.015 inch and a minimum of (0.100/0.014) or 7 detection waveforms for a circumferential pitch of 2 degrees (0.007 inch per degree resolution). From this population of nearly 42 waveforms, the contour of the pit depth is measured until the maximum depth (minimum remaining wall thickness) is determined or remaining wall resolution is reached. During this profiling of the pit depth, many of the resulting depth determinations will exceed the repair criteria values (40% for the parent tube and 30% (20% for Callaway) for the sleeve. Once the repair criterion has been exceeded, any additional depth determinations are academic. For Callaway, the remaining wall resolution for the parent tube wall outside the sleeve region would be $((0.040 - 0.012)/0.040)$ or 70% through wall. For Callaway, the remaining wall resolution for the sleeve wall would be $((0.028 - 0.012)/0.028)$ or 57% through wall for a minimum sleeve thickness of 0.028 inch.

RAI # 16. In Table 11.8.3, would subtracting the “UT Parent Tube Thickness” from the “UT Combined Thickness at Pit Center Line” give the thickness of the Electrosleeve at each pit location? (Page 11-37, BAW-10219P, Rev. 4)

Response:

Yes. Subtracting the “UT Parent Tube (Wall) Thickness” from the “UT Combined (Wall) Thickness at (the) Pit Center Line” yields the non-degraded sleeve material thickness at each pit location. With this result, the depth of the pit into the sleeve material can be determined as well as the percent through wall. The response to RAI #32 provides the results of the DE comparison that supports this method of determining the sleeve thickness at each pit location.

RAI # 17. The staff notes that the data from two tubes were removed from Table 11.8.3 (samples 081897-02M and 082597-08S) in revising report BAW-10219P from Rev. 3 to Rev. 4. However, the staff noticed that Tables 11.8.4 and 11.8.5 that summarized the sleeve OD pit sizing analysis results for the data set as presented in Table 11.8.3 were identical from Rev. 3 to Rev. 4, even after deleting data from the two tubes. The staff does not understand how deleting data from an analysis would result in the same numerical results as including the same data. Please discuss this apparent discrepancy. (Pages 11-37, 11-38, 11-39, BAW-10219P, Rev. 4)

Response:

During the pit fabrication and procedure development portion of the qualification, the ultrasonic data was acquired using a single transducer articulating zero degree probe. This data was analyzed by two individuals for comparison with the DFO results since the DFO technique and the ultrasonic technique have similar uncertainties. Since the two tubes "081897-02M and 082597-08S", six OD sleeve pits, were destroyed, they were not available for acquisition using the three channel probe that formed the basis for the Appendix J qualification. The results for the analysis of the three channel probe data were reported in Tables 11.8.4 and Table 11.8.5, BAW-10219P-Rev.3 and BAW-10219P-Rev.4. **The two tubes (6 pits) were not used for the statistics in either revision**, thus the numerical results were identical.

RAI # 18. Please provide the UT data for the depth sizing for each pit listed in Table 11.8.3, and any destructive examination data, if performed. Since the remaining wall resolution of the UT system restricts the measurement of pits with 0.012 inch or less of remaining wall, the staff assumes that measurements for pit depths over 0.026" for a nominal sleeve thickness of 0.038" for a 7/8" tube or measurements for pit depths over 0.022" for a nominal sleeve thickness of 0.034" for a 3/4" tube could not be measured. This would potentially affect pit C in tube 041897-06 and pit C in tube 082297-01S for the 7/8" tubes as well as pit C in tube 081897-04M, pits A and C in tube 081897-07M, and pit B in tube 082597-02M for the 3/4" tubes. Please confirm if the previously mentioned tubes were those excluded from Tables 11.8.4 and 11.8.5. (Pages 11-37, 11-38, BAW-10219P, Rev. 4)

Response:

The term "could not be measured", should be "can not be measured to the same accuracy as a pit that presents a back wall reflection". For the 7/8 inch tube size, the 0.026 inch OD sleeve pit depth in the 0.038 inch sleeve would represent a 68% through wall depth, which clearly exceeds the repair limit. For the 3/4 inch tube size, the 0.022 inch OD sleeve pit depth in the 0.034 inch sleeve would represent a 64% through wall depth, which clearly exceeds the repair limit. Once the measured OD sleeve pit depth exceeds the repair limit the sleeved tube would be removed from service.

The analyst makes the determination as to whether a back wall reflection is present. If it is not, the analyst makes a "remaining wall resolution" determination, which indicates that the pit is too deep to be measured in accordance with the procedure. For pits **081897-04M-C** and **082297-01S-C**, both analysts made depth determinations there by indicating that a back wall reflection was present. Subtracting the DFO 'Measured Pit Depth' from the 'UT Combined Thickness at Pit Center Line' produces the expected remaining wall thickness at the pit site. For pit **081897-04M-C**, the expected remaining wall thickness would be (0.092 – 0.072) or 0.020 inch, which is sufficient thickness to produce back wall reflections. For pit **082297-01S-C**, the expected remaining wall thickness would be (0.089 – 0.074) or 0.015 inch, which is sufficient thickness to produce back wall reflections. The analysts should not, (and did not), make remaining wall resolution determinations for these two pits.

Analyst 1 did not make a depth determination for 091197-002-C, 081897-07M-A, 081897-07M-C, 082597-02M-B, 041897-06-C, and 042297-03-A.

Analyst 2 did not make a depth determination for 091197-002-C, 081897-07M-A, 081897-07M-C, 082597-02M-B, 041897-06-C, 042297-03-A, and 042297-03-B.

The following table presents the calculated remaining wall thickness for the samples where one or both analysts made a remaining wall resolution determination.

Table R18-1

Pit	Combined Thickness	Measured Depth	Expected Remaining Thickness
091197-002-C	0.082	0.074	0.008
081897-07M-A	0.079	0.074	0.005
081897-07M-C	0.083	0.075	0.008
082597-02M-B	0.083	0.075	0.008
041897-06-C	0.090	0.078	0.012
042297-03-A	0.085	0.077	0.008
042297-03-B	0.097	0.077	0.020

A remaining wall resolution determination would naturally result in the removal of the sleeve from service in that the depth has exceeded the 30% (20% for Callaway) depth of penetration. Analyst 2 made a remaining wall resolution determination for pit **042297-03-B**. The actual depth of penetration is calculated as $(0.077 - 0.052)$ or 0.025 inch (0.052 is the UT measured parent tube thickness for this sample as shown in Table 11.8.3). This depth of penetration is $(0.025 / (0.097 - 0.052))$ or 56% through wall, which is well in excess of the 30% (20% for Callaway) repair criteria.

The two pages that follow contain the results for each tube size. The MIN, AVE, and STDEV values, (**BOLD** type) were reported in Table 11.8.4 for the 3/4 tube diameter and Table 11.8.5 for the 7/8 tube diameter.

Table R18-2. Pit Depth Results for ¾" Tube OD Samples

Sample	Ind.	Actual Measured Pit Depth (inch)	FTI1 Measured Pit Depth (inch)	FTI2 Measured Pit Depth (inch)	Delta FTI1 vs. Actual Depth (inch)	Delta FTI2 vs. Actual Depth (inch)	Delta FTI1 vs. FTI2 Depth (inch)
081897-03M 3/4	A	0.068	0.066	0.067	-0.002	-0.001	0.001
	B	0.055	0.052	0.052	-0.003	-0.003	0.000
	C	0.065	0.064	0.063	-0.001	-0.002	0.001
081897-04M 3/4	A	0.056	0.052	0.051	-0.004	-0.005	0.001
	B	0.047	0.046	0.047	-0.001	0.000	0.001
	C	0.072	0.071	0.072	-0.001	0.000	0.001
081897-05M 3/4	A	0.060	0.058	0.057	-0.002	-0.003	0.001
	B	0.069	0.069	0.067	0.000	-0.002	0.002
	C	0.066	0.067	0.068	0.001	0.002	0.001
081897-07M 3/4	A	0.074					
	B	0.065	0.065	0.068	0.000	0.003	0.003
	C	0.075					
082597-02M 3/4	A	0.065	0.062	0.064	-0.003	-0.001	0.002
	B	0.075					
	C	0.042	0.041	0.042	-0.001	0.000	0.001
091197-002 3/4	A	0.065	0.063	0.064	-0.002	-0.001	0.001
	B	0.059	0.061	0.059	0.002	0.000	0.002
	C	0.074					

max: 0.002 0.003 0.003
 min: **-0.004** **-0.005** 0.000
 ave: **-0.001** **-0.001** 0.001
 stdev: **0.002** **0.002** 0.001

Table R18-3. Pit Depth Results for 7/8" Tube OD Samples

Sample	Ind.	Actual Measured Pit Depth (inch)	FTI1 Measured Pit Depth (inch)	FTI2 Measured Pit Depth (inch)	Delta FTI1 vs. Actual Depth (inch)	Delta FTI2 vs. Actual Depth (inch)	Delta FTI1 vs. FTI2 Depth (inch)
041897-06 7/8	A	0.056	0.056	0.056	0.000	0.000	0.000
	B	0.068	0.070	0.069	0.002	0.001	0.001
	C	0.078					
042297-01 7/8	A	0.056	0.054	0.056	-0.002	0.000	0.002
	B	0.066	0.066	0.067	0.000	0.001	0.001
	C	0.074	0.073	0.071	-0.001	-0.003	0.002
042297-03 7/8	A	0.077					
	B	0.077	0.071		-0.006		
	C	0.070	0.066	0.068	-0.004	-0.002	0.002
042297-08 7/8	A	0.058	0.053	0.054	-0.005	-0.004	0.001
	B	0.068	0.068	0.071	0.000	0.003	0.003
	C	0.069	0.067	0.066	-0.002	-0.003	0.001
082297-01S 7/8	A	0.058	0.057	0.057	-0.001	-0.001	0.000
	B	0.070	0.076	0.080	0.006	0.010	0.004
	C	0.074	0.077	0.069	0.003	-0.005	0.008
max:					0.006	0.010	0.008
min:					-0.006	-0.005	0.000
ave:					-0.001	0.000	0.002
stdev:					0.003	0.004	0.002

Since there was no significant difference between the results, it was determined that the accuracy of the depth measurement was independent of the tube diameter and sleeve thickness. The result of the combined analyst population was reported in Table 11.10.2.

Table R18-4. Combined Pit Depth Analysis vs. Actual Deltas
Acquisition Pitch = 0.015"

-0.002	-0.001
-0.003	-0.003
-0.001	-0.002
-0.004	-0.005
-0.001	0.000
-0.001	0.000
-0.002	-0.003
0.000	-0.002
0.001	0.002
0.000	0.003
-0.003	-0.001
-0.001	0.000
-0.002	-0.001
0.002	0.000
0.000	0.000
0.002	0.001
-0.002	0.000
0.000	0.001
-0.001	-0.003
-0.006	-0.002
-0.004	-0.004
-0.005	0.003
0.000	-0.003
-0.002	-0.001
-0.001	0.010
0.006	-0.005
0.003	
max:	0.010
min:	-0.006
ave:	-0.001
stdev:	0.003

The actual (not rounded) average error is -0.000811 and the actual (not rounded) standard deviation is 0.002767. These values yield the -0.005 inch value for the 95%LCL reported in Table 11.10.2.

ID Pits

RAI # 19. The report states that UT is required to detect ID pits with diameters in excess of 0.050 inch - why a threshold of 0.050 inch? The staff noted that the technique cannot detect a pit sized at 0.016 inch actual pit diameter (see Table 11.8.11, page 11-49). Why is it not significant that the technique cannot detect ID pits in service that are 0.016 inch in diameter or greater, especially since they cannot be depth sized on the ID. (Page 11-45, BAW-10219P, Rev. 4)

Response:

The 0.050 inch diameter pit was selected as significant because the leak rate through this pit if coincident with at 100% TW parent tube corrosion crack of an assumed 0.003 inch width, 0.050 inch length, produces less than 0.1 gpm leak rate.

The term "could not be depth sized", should be "can not be accurately depth sized on the ID". The statement "can not detect a pit sized at 0.016 inch" should read "did not detect a pit sized at 0.016 inch".

During the physical measurement of the pit diameters, those pits that would allow access for a pin gauge were also measured for depth. The depths, for the ID pits with pin gauge depth measurements, range from 0.007 inch to 0.035 inch with an average population depth of 0.025 inch. The depths of the pits that could not be measured by the pin gauge were measured using replicant. The replicant depth for pit **112396-02-1** was recorded as 0.000 inch but since the pit is visible to the naked eye, the depth is expected to be at least 0.001 inch. With a depth less than 0.006 inch, this pit (**112396-02-1**) would not be detected by the ultrasonic technique. The pit **111396-02-7** has a pin gauge depth of 0.007 inch which is at the threshold for detection of two distinct surface reflections.

Detection is a function of pit depth, not pit diameter as evident by the detection of three pits of diameters 0.008, 0.009 and 0.010. These pits had depths in excess of the 0.006 inch required for the identification of two distinct surface reflections.

RAI # 20. The report states that because ID pits are conservatively assumed to be 100% through the sleeve, no depth sizing is required. However, the report states that UT can detect the ID pits. The report states that "ID pits with a depth greater than one wavelength" which is approximately 0.006 inches for a 10MHz transducer and a 0.058 inch/ μ s speed of sound in water can be detected because there should be at least two distinct surface reflections. Please provide UT data to support your ability to detect ID pits. (Page 11-45, BAW-10219P, Rev. 4)

Response:

The following seven pages present the RF waveforms (A-Scan plots) for tube 120196-03, which has seven pits of diameters ranging from 0.008 to 0.042 inch. This tube was selected for the variety of pit diameters present in the inner diameter surface. The tube identification and the pit number, as listed in Table 11.8.10 of the topical identify each plot.

Each RF waveform shows the two surface reflections along with the UT estimated pit depth. Since the zero degree UT transducer is calibrated for thickness, the reported displacement between the two surface reflections must be corrected for time-of-flight in water versus time-of-flight in the tube wall. This is accomplished by multiplying the displacement by the ratio of the velocities (0.058/0.233).

For those pits that could be measured with a pin gauge (micrometer), depth has been reported in inches. For those pits where the pin gauge measurement was not possible due to the restricted diameter, (typically less than 0.015 inch), the depth measurement was determined using replicant. Four of the seven pits have both pin gauge and replicant results.

Repeated measurements were performed with the pin gauge to determine the uncertainty associated with getting the pin to reach the "bottom" of the pit. From the repeatability testing, it was decided that the pin gauge accuracy was no better than +/- 0.002 inch.

The quality control inspector performing the replicant measurements indicated that the values for depth were accurate to +/- 0.002 inch.

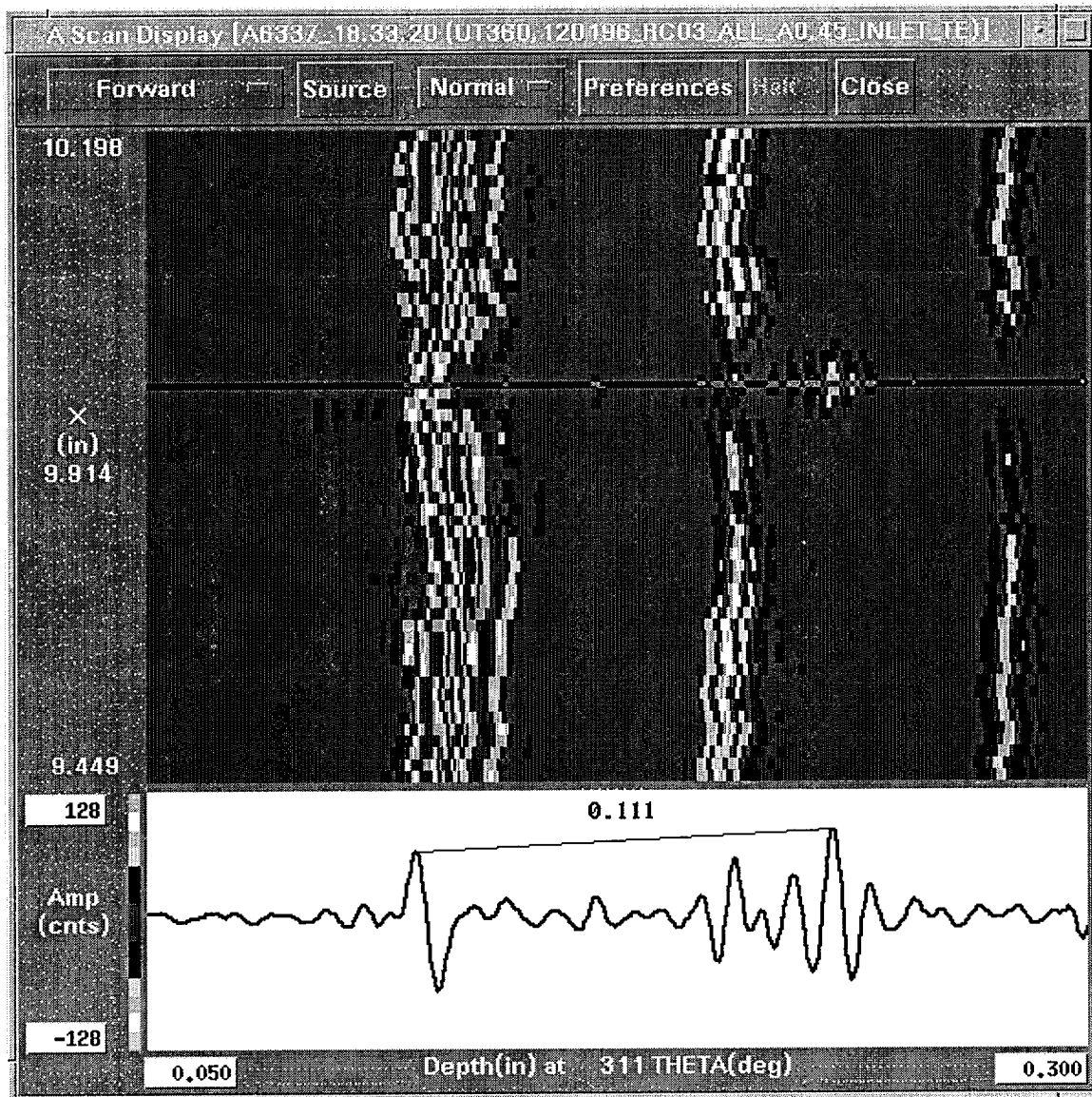


Figure R20-1, Sample: 120196-03
ID pit: 1

Actual pit diameter: 0.042
Pit depth (pin gauge): 0.022
Pit depth (replicant): 0.018

UT estimated depth: $(0.111 * 0.058 / 0.233) = 0.028$

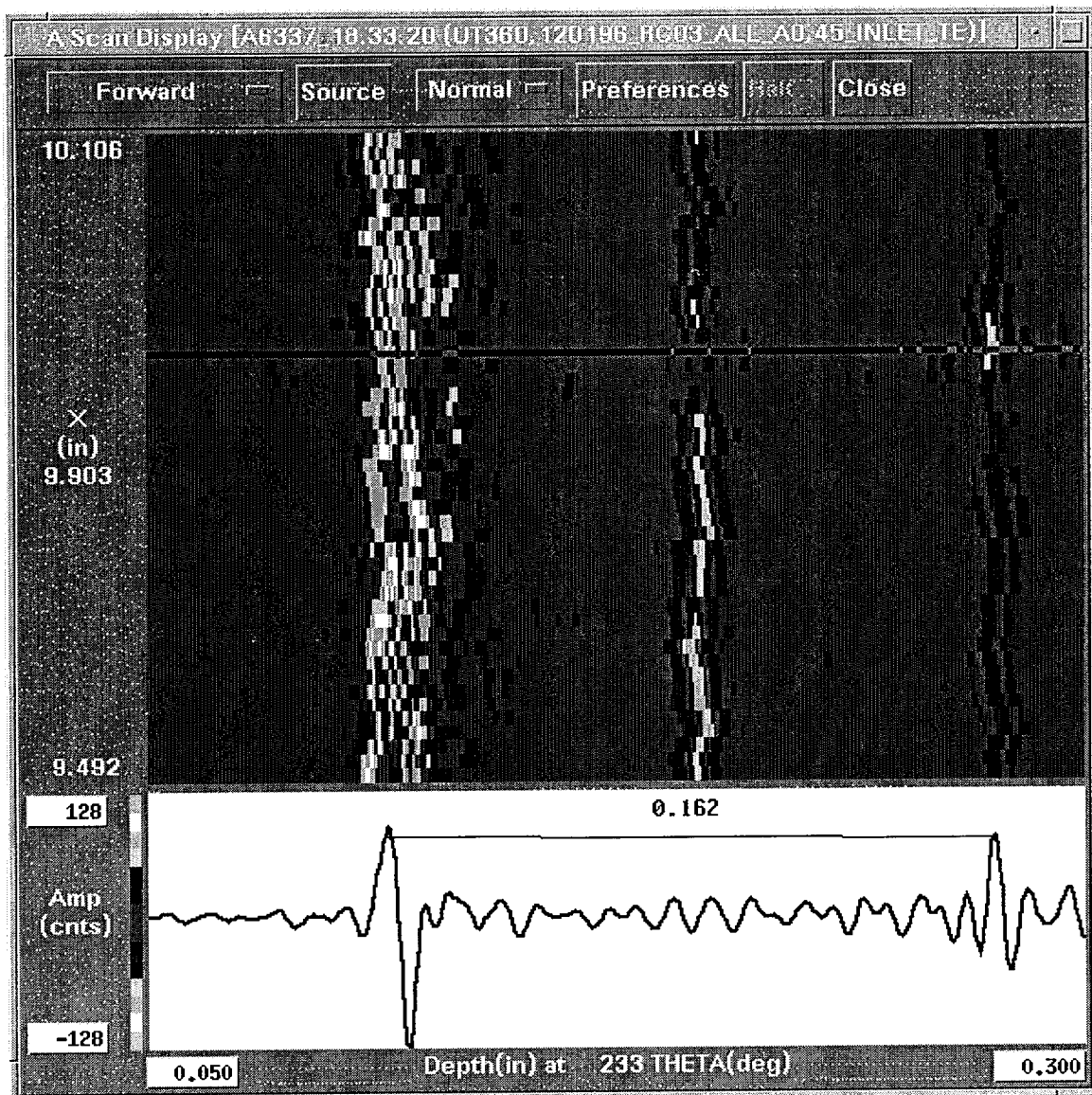


Figure R20-2, Sample: 120196-03
ID pit: 2

Actual pit diameter: 0.020
Pit depth (pin gauge): 0.017

UT estimated depth: $(0.162 * 0.058 / 0.233) = 0.040$

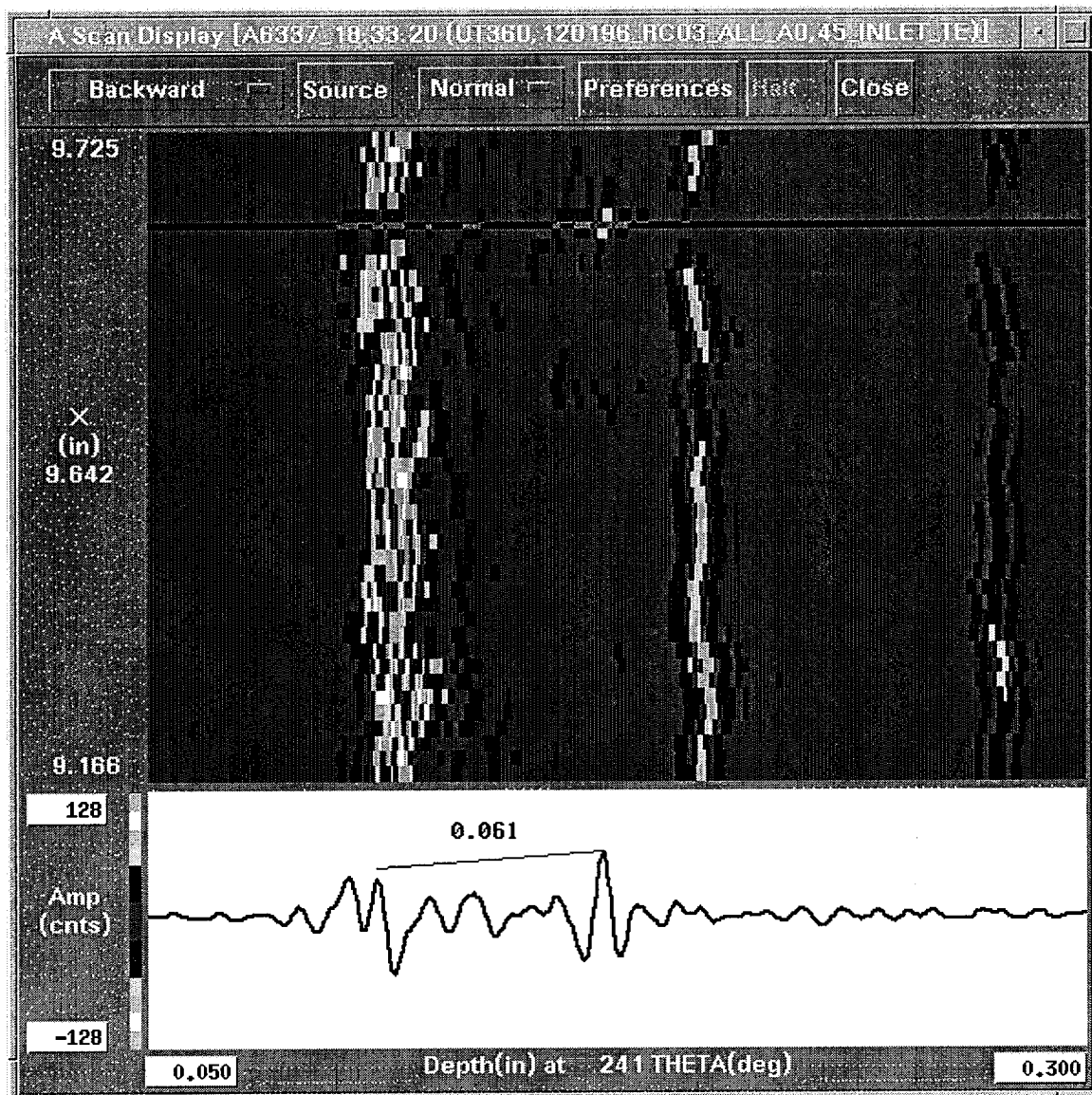


Figure R20-3, Sample: 120196-03
ID pit: 3

Actual pit diameter: 0.025
Pit depth (pin gauge): 0.025

UT estimated depth: $(0.061 * 0.058 / 0.233) = 0.015$

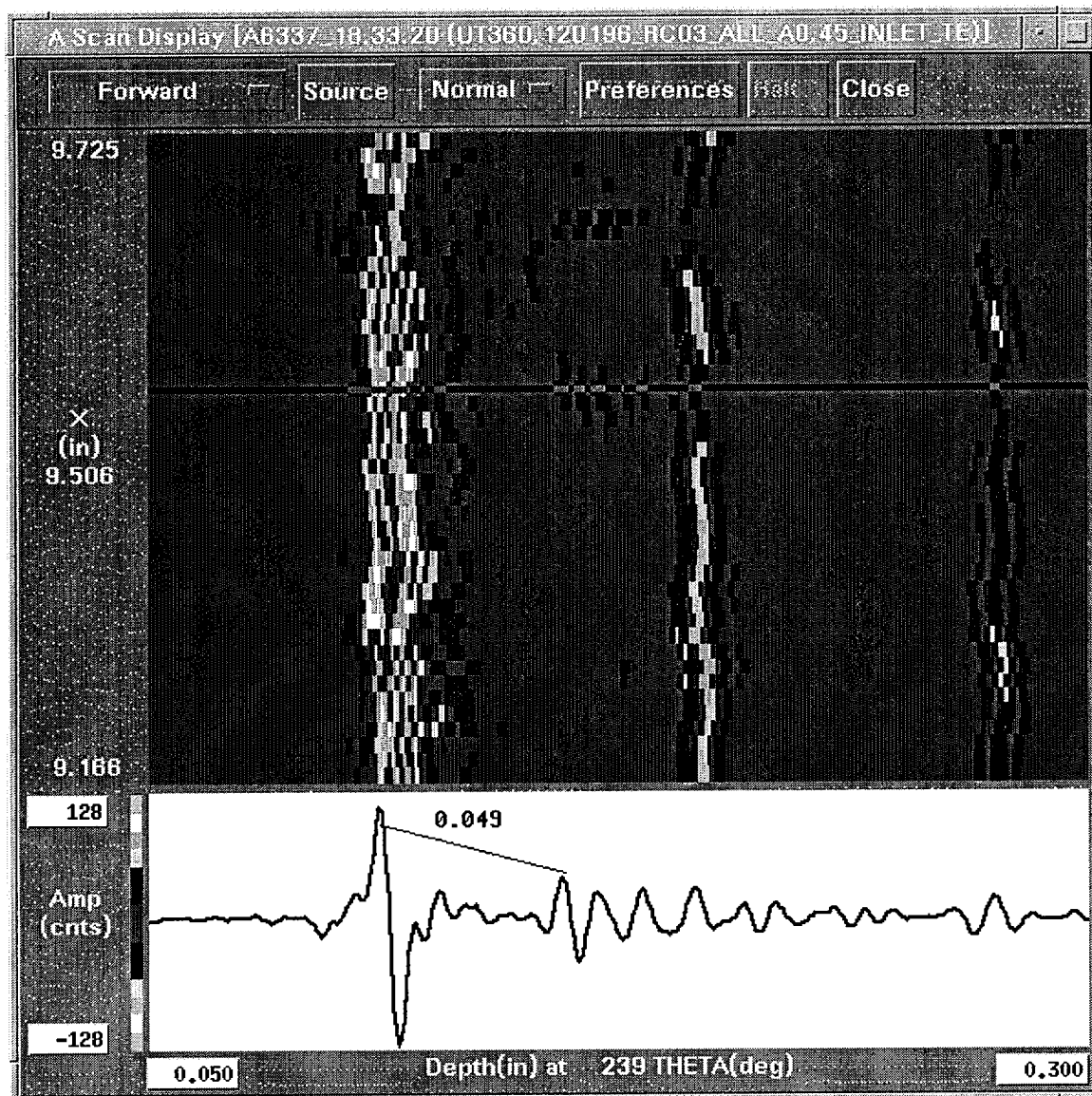


Figure R20-4, Sample: 120196-03
ID pit: 4

Actual pit diameter: 0.008
Pit depth (replicant): 0.019

UT estimated depth: $(0.049 * 0.058 / 0.233) = 0.012$

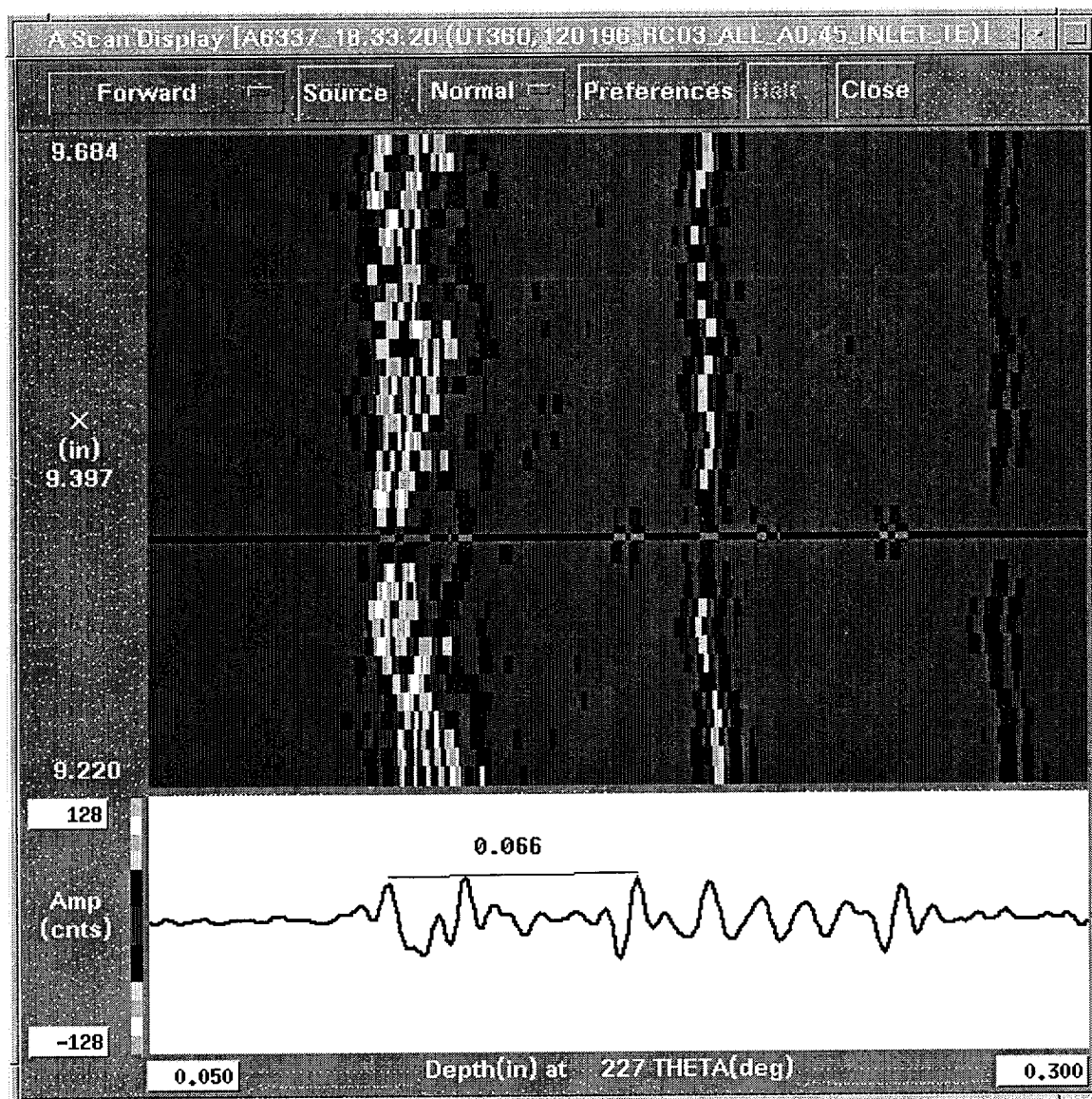


Figure R20-5, Sample: 120196-03
ID pit: 5

Actual pit diameter: 0.010
Pit depth (pin gauge): 0.012

UT estimated depth: $(0.066 * 0.058 / 0.233) = 0.016$

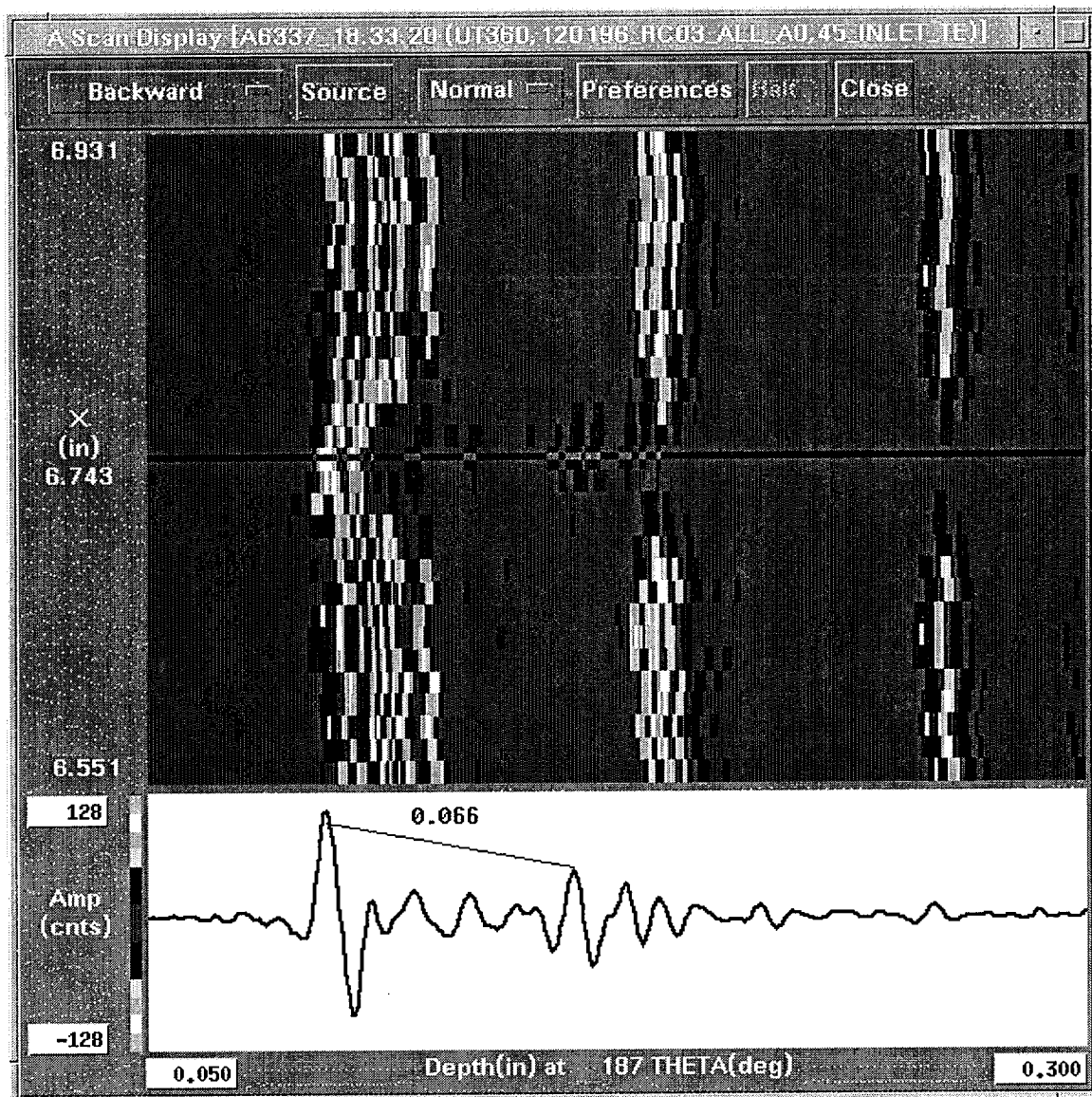


Figure R20-6, Sample: 120196-03
ID pit: 6

Actual pit diameter: 0.042
Pit depth (pin gauge): 0.028
Pit depth (replicant): 0.023

UT estimated depth: $(0.066 * 0.058 / 0.233) = 0.016$

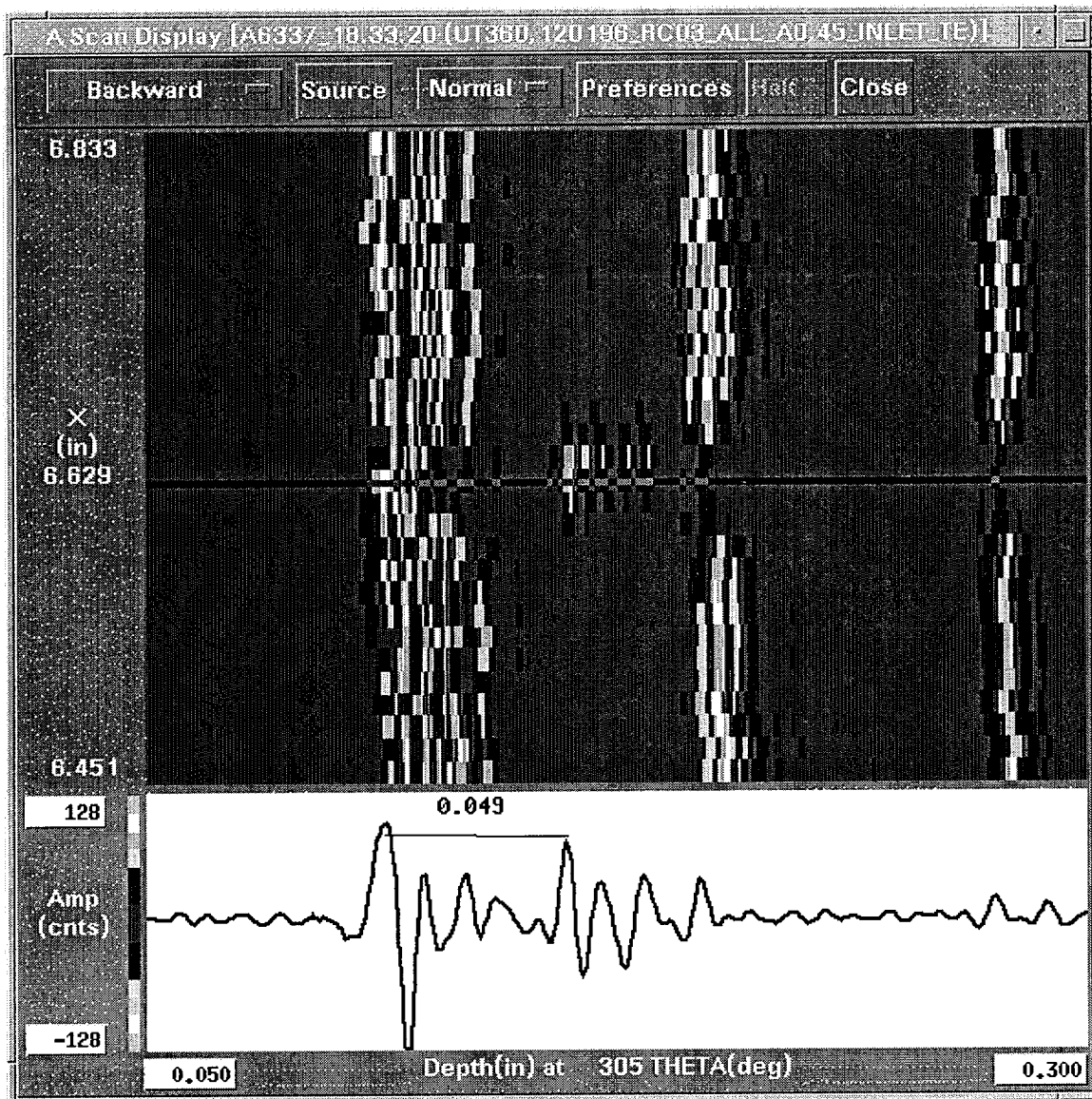


Figure R20-7, Sample: 120196-03
ID pit: 7

Actual pit diameter: 0.027
Pit depth (pin gauge): 0.024
Pit depth (replicant): 0.029

UT estimated depth: $(0.049 * 0.058 / 0.233) = 0.012$

RAI # 21. The report states that the set of tubes with ID pits was selected from the process pre-qualification and training runs. What size pits are normally left in service as a result of the field deposition process (diameter and depth)? (Page 11-46, BAW-10219P, Rev. 4)

Response:

The electro-deposition process variables are controlled to produce a good ID surface as discussed in Section 10.4, pages 10-6 and 10-7. ID pit formation is related to process parameters as described on page. 10-7. Witness tubes are evaluated using UT and visual examination to evaluate the process prior to sleeve installation in steam generator tubing. The only pits left in service would be those that are not detected by UT, which are less than 0.006 inch depth (see response to Question #19). Pits of this depth are not structurally significant, and are less than the administrative plugging limit of 30%TW (20%TW for Callaway).

The goals of the process pre-qualification were to determine the range of essential process variables. Electro-deposition with process variables outside acceptable limits can produce ID pitting as well as disbond. The field implementation is controlled such that formation of ID pits is not expected.

Response Callaway Specific:

Callaway Tech Spec requires that all detected pits (in Regions B and C) be removed from service. (One sleeved tube was removed from service in RF-10 due to an "ID pit indication.")

Disbond

RAI # 22. Please provide the UT data for analysts 1 and 2 that is summarized in Tables 11.8.8 and 11.8.9. (Pages 11-43, 44, BAW-10219P, Rev. 4)

Response:

The acquisition of the disbond samples with three axial pitch values (0.010, 0.015 and 0.020 inch), and the subsequent analysis by two analysts to determine the axial and circumferential extent of each disbond resulted in the values reported in Tables 11.8.8 and 11.8.9. The six pages that follow present the analysis results by pitch, by tube diameter, and by analyst. From these tables, the MIN, AVE and STDEV results (**BOLD** type) are consistent with the results in Tables 11.8.8 and Table 11.8.9. Since the circumferential “edge” determinations were in degrees, the conversion to inch resulted in values that had to be expressed to the nearest thousandth of an inch for presentation in the tables that follow. This resulted in some instances of a 0.001 inch difference versus the average value as reported in the Table 11.8.8. Had the rounding not been performed, the values for the individual analyst deltas and the delta between analysts would not have been the algebraic difference between the reported measured values. This is only true for the circumferential extent since the “edge” determinations for the axial extent were in inches. This is not significant in that the entire population for the 0.015 inch pitch (2 analysts, 18 disbond flaws) was used for the 95%LCL determination for Table 11.10.2.

Table R22-1. Analysis Results for Disbond Circumferential Extent Sizing, 0.010" Pitch

Sample	Ind.	Actual Measured Circ. Extent (inch)	FTI1 Measured Circ. Extent (inch)	FTI2 Measured Circ. Extent (inch)	Delta FTI1 vs. Actual Extent (inch)	Delta FTI2 vs. Actual Extent (inch)	Delta FTI1 vs. FTI2 Extent (inch)
081897-03M 3/4	A	0.101	0.103	0.091	0.002	-0.010	0.012
	B	0.073	0.074	0.068	0.001	-0.005	0.006
	C	0.126	0.125	0.120	-0.001	-0.006	0.005
081897-05M 3/4	A	0.293	0.296	0.296	0.003	0.003	0.000
	B	0.331	0.325	0.319	-0.006	-0.012	0.006
	C	0.373	0.376	0.371	0.003	-0.003	0.006
091197-002 3/4	A	0.167	0.165	0.171	-0.002	0.004	0.006
	B	0.206	0.200	0.217	-0.006	0.011	0.017
	C	0.251	0.239	0.245	-0.012	-0.006	0.006

max: 0.003 0.011 0.017
 min: **-0.012** **-0.012** 0.000
 ave: **-0.002** **-0.003** 0.007
 stdev: **0.005** **0.007** 0.005

041897-06 7/8	A	0.102	0.107	0.114	0.005	0.012	0.007
	B	0.072	0.094	0.094	0.022	0.022	0.000
	C	0.127	0.121	0.147	-0.006	0.020	0.026
042297-01 7/8	A	0.294	0.295	0.308	0.001	0.014	0.013
	B	0.330	0.322	0.335	-0.008	0.005	0.013
	C	0.371	0.362	0.355	-0.009	-0.016	0.007
042297-08 7/8	A	0.166	0.161	0.174	-0.005	0.008	0.013
	B	0.207	0.214	0.208	0.007	0.001	0.006
	C	0.251	0.255	0.255	0.004	0.004	0.000

max: 0.022 0.022 0.026
 min: **-0.009** **-0.016** 0.000
 ave: **0.001** **0.008** 0.009
 stdev: **0.010** **0.011** 0.008

The values in **bold** were reported in summary Table 11.8.8.

Table R22-2. Analysis Results for Disbond Axial Extent Sizing, 0.010" Pitch

Sample	Ind.	Actual Measured Axial Extent (inch)	FTI1 Measured Axial Extent (inch)	FTI2 Measured Axial Extent (inch)	Delta FTI1 vs. Actual Extent (inch)	Delta FTI2 vs. Actual Extent (inch)	Delta FTI1 vs. FTI2 Extent (inch)
081897-03M 3/4	A	0.101	0.108	0.110	0.007	0.009	0.002
	B	0.073	0.086	0.080	0.013	0.007	0.006
	C	0.126	0.130	0.110	0.004	-0.016	0.020
081897-05M 3/4	A	0.293	0.297	0.300	0.004	0.007	0.003
	B	0.331	0.331	0.340	0.000	0.009	0.009
	C	0.373	0.383	0.360	0.010	-0.013	0.023
091197-002 3/4	A	0.167	0.175	0.180	0.008	0.013	0.005
	B	0.206	0.219	0.220	0.013	0.014	0.001
	C	0.251	0.261	0.270	0.010	0.019	0.009

max: 0.013 0.019 0.023
min: **0.000** **-0.016** 0.001
ave: **0.008** **0.005** 0.009
stdev: **0.004** **0.012** 0.008

041897-06 7/8	A	0.102	0.098	0.110	-0.004	0.008	0.012
	B	0.072	0.064	0.060	-0.008	-0.012	0.004
	C	0.127	0.142	0.140	0.015	0.013	0.002
042297-01 7/8	A	0.294	0.304	0.303	0.010	0.009	0.001
	B	0.330	0.338	0.320	0.008	-0.010	0.018
	C	0.371	0.385	0.380	0.014	0.009	0.005
042297-08 7/8	A	0.166	0.174	0.180	0.008	0.014	0.006
	B	0.207	0.219	0.200	0.012	-0.007	0.019
	C	0.251	0.259	0.250	0.008	-0.001	0.009

max: 0.015 0.014 0.019
min: **-0.008** **-0.012** 0.001
ave: **0.007** **0.003** 0.008
stdev: **0.008** **0.010** 0.007

The values in **bold** were reported in summary Table 11.8.9.

Table R22-3. Analysis Results for Disbond Circumferential Extent Sizing, 0.015" Pitch

Sample	Ind.	Actual Measured Circ. Extent (inch)	FTI1 Measured Circ. Extent (inch)	FTI2 Measured Circ. Extent (inch)	Delta FTI1 vs. Actual Extent (inch)	Delta FTI2 vs. Actual Extent (inch)	Delta FTI1 vs. FTI2 Extent (inch)
081897-03M 3/4	A	0.101	0.114	0.097	0.013	-0.004	0.017
	B	0.073	0.068	0.068	-0.005	-0.005	0.000
	C	0.126	0.148	0.120	0.022	-0.006	0.028
081897-05M 3/4	A	0.293	0.296	0.302	0.003	0.009	0.006
	B	0.331	0.331	0.331	0.000	0.000	0.000
	C	0.373	0.359	0.376	-0.014	0.003	0.017
091197-002 3/4	A	0.167	0.165	0.165	-0.002	-0.002	0.000
	B	0.206	0.205	0.211	-0.001	0.005	0.006
	C	0.251	0.239	0.257	-0.012	0.006	0.018
max:					0.022	0.009	0.028
min:					-0.014	-0.006	0.000
ave:					0.000	0.001	0.010
stdev:					0.011	0.005	0.010
041897-06 7/8	A	0.102	0.114	0.107	0.012	0.005	0.007
	B	0.072	0.080	0.067	0.008	-0.005	0.013
	C	0.127	0.141	0.127	0.014	0.000	0.014
042297-01 7/8	A	0.294	0.295	0.295	0.001	0.001	0.000
	B	0.330	0.322	0.315	-0.008	-0.015	0.007
	C	0.371	0.369	0.355	-0.003	-0.016	0.013
042297-08 7/8	A	0.166	0.174	0.154	0.008	-0.012	0.020
	B	0.207	0.208	0.188	0.001	-0.019	0.020
	C	0.251	0.255	0.235	0.004	-0.017	0.021
max:					0.014	0.005	0.021
min:					-0.008	-0.019	0.000
ave:					0.004	-0.009	0.013
stdev:					0.007	0.009	0.007

The values in **bold** were reported in summary Table 11.8.8.

Table R22-4. Analysis Results for Disbond Axial Extent Sizing, 0.015" Pitch

Sample	Ind.	Actual Measured Axial Extent (inch)	FTI1 Measured Axial Extent (inch)	FTI2 Measured Axial Extent (inch)	Delta FTI1 vs. Actual Extent (inch)	Delta FTI2 vs. Actual Extent (inch)	Delta FTI1 vs. FTI2 Extent (inch)
081897-03M 3/4	A	0.101	0.110	0.090	0.009	-0.011	0.020
	B	0.073	0.095	0.060	0.022	-0.013	0.035
	C	0.126	0.142	0.110	0.016	-0.016	0.032
081897-05M 3/4	A	0.293	0.306	0.310	0.013	0.017	0.004
	B	0.331	0.334	0.330	0.003	-0.001	0.004
	C	0.373	0.367	0.370	-0.006	-0.003	0.003
091197-002 3/4	A	0.167	0.172	0.160	0.005	-0.007	0.012
	B	0.206	0.204	0.200	-0.002	-0.006	0.004
	C	0.251	0.266	0.250	0.015	-0.001	0.016

max: 0.022 0.017 0.035
 min: **-0.006** **-0.016** 0.003
 ave: **0.008** **-0.005** 0.014
 stdev: **0.009** **0.010** 0.012

041897-06 7/8	A	0.102	0.089	0.090	-0.013	-0.012	0.001
	B	0.072	0.060	0.060	-0.012	-0.012	0.000
	C	0.127	0.120	0.130	-0.007	0.003	0.010
042297-01 7/8	A	0.294	0.302	0.300	0.008	0.006	0.002
	B	0.330	0.335	0.320	0.005	-0.010	0.015
	C	0.371	0.380	0.360	0.009	-0.011	0.020
042297-08 7/8	A	0.166	0.180	0.170	0.014	0.004	0.010
	B	0.207	0.210	0.200	0.003	-0.007	0.010
	C	0.251	0.255	0.240	0.004	-0.011	0.015

max: 0.014 0.006 0.020
 min: **-0.013** **-0.012** 0.000
 ave: **0.001** **-0.006** 0.009
 stdev: **0.010** **0.008** 0.007

The values in **bold** were reported in summary Table 11.8.9.

Table R22-5. Analysis Results for Disbond Circumferential Extent Sizing, 0.020" Pitch

Sample	Ind.	Actual Measured Circ. Extent (inch)	FTI1 Measured Circ. Extent (inch)	FTI2 Measured Circ. Extent (inch)	Delta FTI1 vs. Actual Extent (inch)	Delta FTI2 vs. Actual Extent (inch)	Delta FTI1 vs. FTI2 Extent (inch)
081897-03M 3/4	A	0.101	0.108	0.103	0.007	0.002	0.005
	B	0.073	0.080	0.086	0.007	0.013	0.006
	C	0.126	0.125	0.131	-0.001	0.005	0.006
081897-05M 3/4	A	0.293	0.296	0.302	0.003	0.009	0.006
	B	0.331	0.336	0.336	0.005	0.005	0.000
	C	0.373	0.376	0.371	0.003	-0.003	0.006
091197-002 3/4	A	0.167	0.177	0.182	0.010	0.015	0.005
	B	0.206	0.200	0.211	-0.006	0.005	0.011
	C	0.251	0.245	0.245	-0.006	-0.006	0.000
max:					0.010	0.015	0.011
min:					-0.006	-0.006	0.000
ave:					0.002	0.005	0.005
stdev:					0.006	0.007	0.003
041897-06 7/8	A	0.102	0.121	0.121	0.019	0.019	0.000
	B	0.072	0.074	0.080	0.002	0.008	0.006
	C	0.127	0.134	0.127	0.007	0.000	0.007
042297-01 7/8	A	0.294	0.288	0.288	-0.006	-0.006	0.000
	B	0.330	0.315	0.328	-0.015	-0.002	0.013
	C	0.371	0.355	0.369	-0.016	-0.003	0.013
042297-08 7/8	A	0.166	0.168	0.168	0.002	0.002	0.000
	B	0.207	0.201	0.214	-0.006	0.007	0.013
	C	0.251	0.255	0.248	0.004	-0.003	0.007
max:					0.019	0.019	0.013
min:					-0.016	-0.006	0.000
ave:					-0.001	0.002	0.007
stdev:					0.011	0.008	0.006

The values in **bold** were reported in summary Table 11.8.8.

Table R22-6. Analysis Results for Disbond Axial Extent Sizing, 0.020" Pitch

Sample	Ind.	Actual Measured Axial Extent (inch)	FTI1 Measured Axial Extent (inch)	FTI2 Measured Axial Extent (inch)	Delta FTI1 vs. Actual Extent (inch)	Delta FTI2 vs. Actual Extent (inch)	Delta FTI1 vs. FTI2 Extent (inch)
081897-03M 3/4	A	0.101	0.104	0.120	0.003	0.019	0.016
	B	0.073	0.104	0.090	0.031	0.017	0.014
	C	0.126	0.125	0.120	-0.001	-0.006	0.005
081897-05M 3/4	A	0.293	0.312	0.310	0.019	0.017	0.002
	B	0.331	0.353	0.350	0.022	0.019	0.003
	C	0.373	0.373	0.370	0.000	-0.003	0.003
091197-002 3/4	A	0.167	0.185	0.190	0.018	0.023	0.005
	B	0.206	0.204	0.200	-0.002	-0.006	0.004
	C	0.251	0.264	0.250	0.013	-0.001	0.014
max:					0.031	0.023	0.016
min:					-0.002	-0.006	0.002
ave:					0.011	0.009	0.007
stdev:					0.012	0.012	0.006
041897-06 7/8	A	0.102	0.101	0.100	-0.001	-0.002	0.001
	B	0.072	0.060	0.060	-0.012	-0.012	0.000
	C	0.127	0.140	0.140	0.013	0.013	0.000
042297-01 7/8	A	0.294	0.286	0.310	-0.008	0.016	0.024
	B	0.330	0.327	0.330	-0.003	0.000	0.003
	C	0.371	0.390	0.390	0.019	0.019	0.000
042297-08 7/8	A	0.166	0.162	0.180	-0.004	0.014	0.018
	B	0.207	0.222	0.200	0.015	-0.007	0.022
	C	0.251	0.263	0.260	0.012	0.009	0.003
max:					0.019	0.019	0.024
min:					-0.012	-0.012	0.000
ave:					0.003	0.006	0.008
stdev:					0.011	0.011	0.010

The values in **bold** were reported in summary Table 11.8.9.

From these results, it was determined that the variation in axial pitch between 0.010 and 0.020 inch did not adversely affect the measurement of the disbond extent. The 0.015 inch axial pitch data was used to determine the 95%LCL values for the circumferential and axial extent results for Table 11.10.2. The standard deviation values, reported in Table 11.10.2, are averages of the reported summary standard deviations. The population standard deviation values were used to determine the reported 95%LCL values.

Table R22-7. Analysis Deltas vs. Actual Extent, Disbond Extent Sizing

	circ. 0.015 pitch	axial 0.015 pitch
	0.013	0.009
	-0.005	0.022
	0.022	0.016
	0.003	0.013
	0.000	0.003
	-0.014	-0.006
	-0.002	0.005
	-0.001	-0.002
	-0.012	0.015
	0.012	-0.013
	0.008	-0.012
	0.014	-0.007
	0.001	0.008
	-0.008	0.005
	-0.003	0.009
	0.008	0.014
	0.001	0.003
	0.004	0.004
	-0.004	-0.011
	-0.005	-0.013
	-0.006	-0.016
	0.009	0.017
	0.000	-0.001
	0.003	-0.003
	-0.002	-0.007
	0.005	-0.006
	0.006	-0.001
	0.005	-0.012
	-0.005	-0.012
	0.000	0.003
	0.001	0.006
	-0.015	-0.010
	-0.016	-0.011
	-0.012	0.004
	-0.019	-0.007
	-0.017	-0.011
max:	0.022	0.022
min:	-0.019	-0.016
ave:	-0.001	0.000
stdev:	0.009	0.010

UT techniques/data analysis

RAI # 23. Please provide the "UT Examination Technique Specification Sheets" for the EPRI peer reviews: ETSS # 98300, 98301, 98302, 98303, 98400, 98401, 98402, 98403, 98404, and 98405. (Question from the 6/7/01 meeting held with UE, FTI, and the NRC staff)

Response:

ETSS 98-300, 98-301, 98-405 are not Framatome ANP procedures for the Electrosleeve Inspection. ETSS 98-303 and 98-402 have been submitted for information.

RAI # 24. The staff would like to understand the capability of the UT to detect flaws relative to the structural integrity limits. It is the staff's understanding that this information was contained in the viewgraph presented in the 6/7/01 meeting that derived from Table 12.4.4. Please clarify the conclusions to be drawn from the viewgraph derived from Table 12.4.4 presented at the meeting. (Question from the 6/7/01 meeting held with UE, FTI, and the NRC staff)

Response:

The Bar Chart presented in the 6/7/01 meeting was a non-proprietary visual representation (specific proprietary data not included) of the Minimum Repair Limit for each postulated flaw type compared to the UT accuracy. The comparison was used to demonstrate that the UT uncertainty is significantly less than the minimum repair limit, which includes UT system variability and postulated growth (see answer to Question #12). In addition, the chart provides the qualitative evaluation that "uniform thinning" governs the plugging margin. The specific proprietary data is presented in Tables 12.4.3 and 12.4.4, BAW-10219P-Rev.4.

RAI # 25. Please provide details on the data collected during your RF-11 inspection of 26 Electrosleeves. In particular, please provide the parameters inspected and a summary of the data collected from using the seven following techniques: UT-360 Electrosleeve Disbond Analysis Procedure, UT-360 Inner Diameter Profilometry Analysis Procedure, UT-360 Outer Diameter Pit Analysis Procedure, UT-360 Electrosleeve Inner Diameter Pit Analysis Procedure, UT-360 Electrosleeve Outside Diameter Pit Analysis Procedure, UT-360 Crack Detection and Extent Sizing Analysis Procedure, UT-360 Crack Depth Sizing Analysis Procedure. (Question from the 6/7/01 meeting held with UE, FTI, and the NRC staff)

The meeting handout from the June 7, 2001 meeting states that based on the April 2001 RF-11 inspection of the Electrosleeves, there were "no detectable changes."

Please expand on this statement (e.g., was there any change in sleeve/tube thickness, were any new flaws or indications detected (regardless of whether they were in the pressure boundary or non-pressure boundary portion of the sleeve or tube), did any of the original parent tube flaws change with respect to length, depth, etc.). If any of the above changes were identified, identify how these indications were dispositioned and the basis for the disposition. (Question from the 6/7/01 meeting held with UE, FTI, and the NRC staff)

Response:

The ultrasonic data collected for the 26 Electrosleeves (SG C) consisted of acquisition with the same three channel probe used during the RF-10 outage. Zero degree thickness data was acquired and analyzed to the following procedures: UT-360 Electrosleeve Disbond Analysis Procedure, UT-360 Inner Diameter Profilometry Analysis Procedure, UT-360 OD Pit Analysis Procedure, UT-360 Electrosleeve ID Pit Analysis Procedure, UT-360 Electrosleeve OD Pit Analysis Procedure. Axial shear wave (circumferential crack detection) and circumferential shear wave (axial crack detection) data was acquired and analyzed to procedures: UT-360 Crack Detection and Extent Sizing Analysis Procedure, UT-360 Crack Depth Sizing Analysis Procedure.

Since RF-11 was an in-service inspection, as opposed to the RF-10 pre-service inspection, the inspection focused on combined wall thickness (sleeve thickness), disbond, sleeve OD pitting (none expected since no deep volumetric parent tube defects were present during RF-10), detection of ODSCC crack extents and depths. The techniques used were also sensitive to sleeve ID flaws, as indicated in the responses to Questions 6 (ID cracking) and 19 & 20 (ID pits).

In comparing the results of the RF-10 inspection to that performed in RF-11, the following conclusions were drawn:

1. There were no detectable changes in sleeve thickness.
2. There were no detectable changes in the extent or depth of parent tube indications identified in RF-10.
3. No new indications were identified in RF-11 (parent tube or sleeve).

RAI # 26. Since the 5/21/99 NRC safety evaluation was based on Rev. 3 of BAW-10219P, explain in detail how shifting the criteria to EPRI Appendix J for Rev. 4 affects the conclusions made in Rev. 3.

Response:

The "shift in criteria" is one of utilization of the EPRI Appendix J qualification program and industry UT qualified analysts to review the Framatome ANP ultrasonic system and procedures as opposed to placing the review burden entirely on NRC. (This is the same process as the EPRI Appendix H qualification for eddy-current procedures.) Completion of the EPRI Appendix J qualifications, and filing ETSS procedures demonstrates that a team of industry UT experts (peers) have reviewed the sample sets, procedures, and analysis techniques and have concluded that the techniques deliver the presented detection and sizing capabilities. The repair criteria presented in Section 12 of BAW-10219P-Rev 4 reflect the inspection uncertainties as documented in Section 11.

Unlike the EPRI guideline (G.4.2.2.2.(2)), where in "Personnel shall be considered qualified for performing sizing measurements on a specific damage mechanism if a root-mean-square error (RMSE) of less than or equal to 10% is demonstrated", personnel qualifying to the ultrasonic techniques referenced in the topical must be within the average error and standard deviation as presented in Table 11.10.2. This requirement is reasonable in that the analyst attempting qualification is being required to perform as well as the two analysts from which the values in Table 11.10.2 were determined. The analyst attempting qualification will be tested against the DE ("truth") values instead of against an "expert" as presented in Appendix G of the EPRI guidelines. By including the results of multiple analysts in the qualification program, the sizing performance values given in Table 11.10.2 include the system (technique and analyst) uncertainties without the need to perform a separate performance demonstration. All analysts qualifying to these procedures must demonstrate that they can achieve results within the average error and standard deviation values of Table 11.10.2, which supports the application of the repair criteria given in the tables in chapter 12.

RAI # 27. Appendix J (PWR Steam Generator Examination Guidelines: Revision 5) only contains minimum acceptance criteria for flaws that are $\geq 60\%$ through-wall for both performance demonstration detection and sizing. What acceptance criteria was assumed for the 20-59% through-wall flaws, considering that the Technical Specifications contain a plugging limit of 20% through wall, which is much less than 60% through wall?

Response:

The 20% plugging criteria in the Tech Spec and the 60% TW criteria in the EPRI guidelines are two different criteria and are not directly comparable. The 60% TW "criteria" in EPRI Rev. 5 is based on a structural integrity limit, reduced for growth, between cycles for the alloy 600 parent tube material. This is the ACTUAL flaw depth that must be detected with a high level of confidence in order to assure that the flaw does not grow past the maximum acceptable depth during the subsequent cycle. The plugging limit must always be less than the detection limit, because it must be reduced to account for depth sizing uncertainties. In region B of the sleeve, the plugging criteria is plug on detection and the UT technique has demonstrated acceptable detection of outer diameter flaws after addition of the sleeve material.

The 60%TW EPRI criteria is a "generic" detection limit, in that it does not account for specific flaw morphologies or plant loading conditions. The comparable detection limit for Electrosleeves can be derived from the data presented in Table 12.4.4, BAW-10219P-Rev 4, by subtracting the growth from the allowed structural degradation. This would result in detection limits ranging from 40% TW for uniform thinning to []^{b,c,e} TW for axial cracks $\leq 3/4$ ". The NDE technique used for Electrosleeve ISI must reliably detect degradation of a given morphology at these detection limits to be considered acceptable for this application.

The 20% TW plugging limit is an ADMINISTRATIVE limit on the UT MEASURED flaw depth, imposed by Callaway. (This is 20% TW of the sleeve). This cannot be compared to the 60% TW detection limit in the EPRI guidelines, because the 60% limit does not have an allowance for NDE sizing uncertainty. The actual repair limit given in the topical ranges from 37% TW to []^{b,c,e} TW depending on the flaw morphology (Table 12.4.4, BAW-10219P-Rev 4). These values account for growth and sizing inaccuracies. The 20% plugging limit imposed by Callaway represents an additional margin of 17% TW over the lowest repair limit given in the topical report.

In region C or the sleeve, the Callaway 20% through wall depth is in addition to the 100% through wall depth in the parent tube material. This is considerably greater depth than 60% through wall. The premise has always been propagation of the parent tube flaw into the sleeve material and that the propagation would take the form of pitting since SCC has never been established as a defect mechanism for the Nickel Sleeve Material. The $>59\%$ through wall acceptance criterion is for detection only. Any detected flaw must be depth sized to the average error and standard deviation, as reported as the 95%LCL, in Table 11.10.2 since this is the basis for the repair criteria presented in chapter 12 of the topical.

All of the sample sets, Table 11.10.1, meet the EPRI Appendix J, section J2.3.1 Detection

Acceptance Criteria at a 95%LCL versus the specified 90%LCL. Except for the ID pit sample set, no allowances were taken for missed flaws based upon sample set population in that all flaws were detected without regard to process step (pre-sleeve or post-sleeve) or geometry (expansion transition or dent). Thus, detection of the flaws less than 60%TW was required in order to demonstrate detection at the required statistical confidence level. In addition, the ID Pit POD is conservatively biased in that the ID pit 112396-02-1 could have been removed from the detection set because it is less than 0.006 inch deep and should not be detected by the technique.

The depth sizing sets meet the requirements of EPRI Appendix J, section J2.2.3. For the ODSCC depth sizing set, a reasonable effort was made to include cracks with maximum depths between 20% and 59%. The difficulty arises in that while a crack average depth maybe less than 60%, a localized maximum depth ultimately determines the value used for technique qualification. The set does include flaws that were not detectable by eddy-current, the technique that will be used in practice to select tube repair candidates. The decision to include such flaws bounds the range of defects that would be found in-situ.

RAI # 28. How was the correction factor of 1.6 for the mode conversion method determined? Is the correction factor of 1.6 the same for the full range of crack depths? If not, how would the correction factor be determined on a crack depth basis? (Page 11-27, BAW-10219P, Rev. 4)

Response:

As discussed in the section for Mode Converted Signal Method, page 11-24 to 11-27, the 1.6 correction is the only value that accounts for the 'sound traveling along the crack face and consequently being zero degree incident at the outer diameter surface'. The presence of the mode converted signal was verified in an experiment where in an external transducer was used to detect the longitudinal waves generated by the conversion of the traverse (shear wave) sound energy incident on the crack face. The 1.6 value is the only value used in the analysis technique. The 1.6 factor was used during the crack depth sizing qualification for those cracks that presented sufficient criteria for an MCS determination in accordance with the procedure.

RAI # 29. What is the basis for computing the crack depth by using the regression and averaging with the tip and mode converted signal depth values to determine the reported crack depth? Why would this averaging process provide the optimum crack depth? (Page 11-30, BAW-10219P, Rev. 4)

Response:

The averaging resulted in more accurate and repeatable depth determination when compared with the DE results. Not all waveforms yield a TIP result, MCS result, and a FSN result. For those that have more than one result, there is no physical (physics) criteria for selecting one result over the others. From the procedure development, the only criterion established was that if the FSN result exceeded a value of 1.0, the depth would be assigned through wall and the reported depth of penetration would be equal to the UT measured wall thickness.

The depth sizing procedure specifies the following order of precedence for assigning the final crack depth.

- a) If the FSN result is greater than 1.0 and less than 1.3, the crack depth will be reported as through wall and the recorded depth will be equal to the wall thickness.
- b) If the FSN result is less than 1.0, the crack depth will be reported as the average of the available depths from the three techniques.
- c) If the full skip signal was not detected, the reported depth will be the maximum depth determined by the Tip/CT or MCS/CT techniques.

RAI # 30. The report states that “UT techniques have been shown to be effective in the detection and sizing of fatigue cracks propagated into the sleeve material.” Please provide data to support this assertion. (Page 11-57, BAW-10219P, Rev. 4)

Response:

For the non-structural sleeve program, UT was used to monitor fatigue propagation of ODSCC into the sleeve. The generation of the fatigue crack was determined by measuring FSN values in excess of 1.0. The tubes were examined prior to fatigue cycling and FSN values were calculated for locations along the crack extent (length) where full skip reflections were present in addition to the two outer diameter skip reflections (half skip and one & one-half skip). During the cycling process, the tubes were periodically examined to determine if the FSN values had increased to a value greater than 1.0. After the through-wall determination was made, the cycling process was concluded and pressure testing was performed to ascertain the pressure associated with a leak through the fatigue flaw and the original parent tube ODSCC flaw.

The pages that follow present the C-Scan and A-Scan plots for the pre-fatigue and post fatigue flaw ultrasonic examinations of ENSA sample TST4-072-1. The sample underwent fatigue cycling after the deposition of ~0.013 inch of nickel sleeve material. The first plot is the forward scan of the sample prior to fatigue cycling. The second plot is the post-cycling forward scan plot.

The UT measured combined wall thickness at the crack site (4.4 inches x 190 degrees) is 0.062 inch. The UT measured parent wall thickness (8.0 inches x 190 degrees) is 0.050 inch.

FSN ratios and regression depths were calculated, at various locations along the crack extent, to determine crack depth propagation. The table below presents a comparison of the FSN determinations before and after fatigue cycling. The depth results indicate that the crack depth has increased along the extent of the crack and that the crack has propagated through wall along the crack extent near the 200 degree circumferential location.

Table R30-1. Crack FSN Results, Before and After Fatigue Cycling

circ. Location (degree)	Before	Fatigue	After	Fatigue
	FSN result	FSN depth by regression (inch)	FSN result	FSN depth by regression (inch)
120			0.40	0.043
140	0.41	0.044	0.63	0.050
160	0.38	0.043	0.55	0.048
180	0.81	0.056	0.87	0.058
200	0.79	0.055	1.10	0.065
220	0.44	0.045	0.57	0.049
240	0.23	0.038	0.47	0.045
260			0.30	0.040

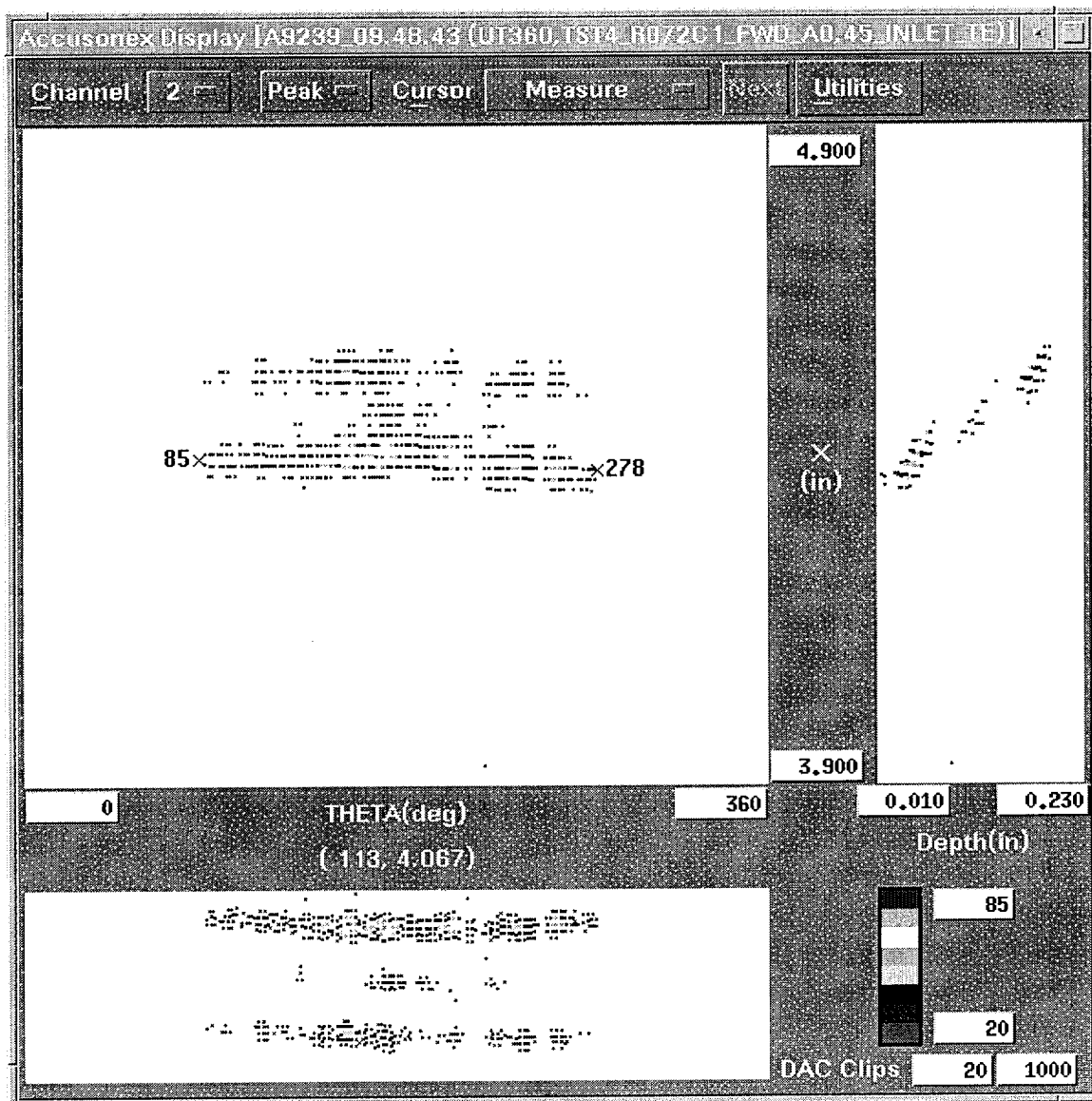


Figure R30-1

This is the pre-fatigue crack C-Scan plot of the ODSCC circumferential crack in tube TST4-072-1. The crack extent (length) can be estimated from the C-Scan plot as $(278 - 85)$ or 193 degrees. The plot shows the presence of a half skip response, a one and one half skip response and some full skip reflections.

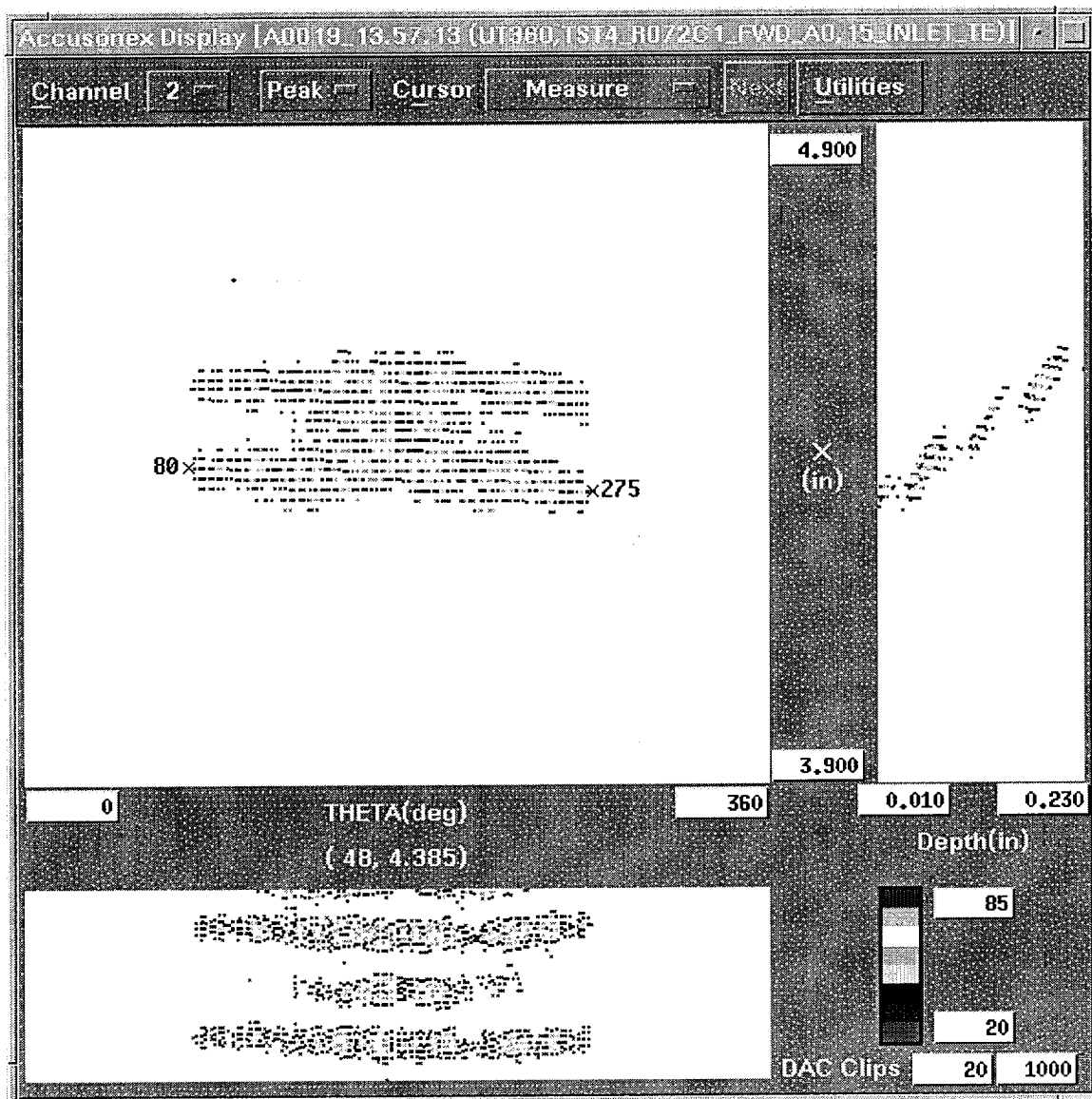


Figure R30-2

This is the post-fatigue crack C-Scan plot of the ODSCC circumferential crack in tube TST4-072-1. The crack extent (length) can be estimated from the C-Scan plot as $(275 - 80)$ or 195 degrees. The fatigue cycling has not significantly increased the crack extent (length). The plot shows the presence of a half skip response, a one and one half skip response and an increase in the full skip response.

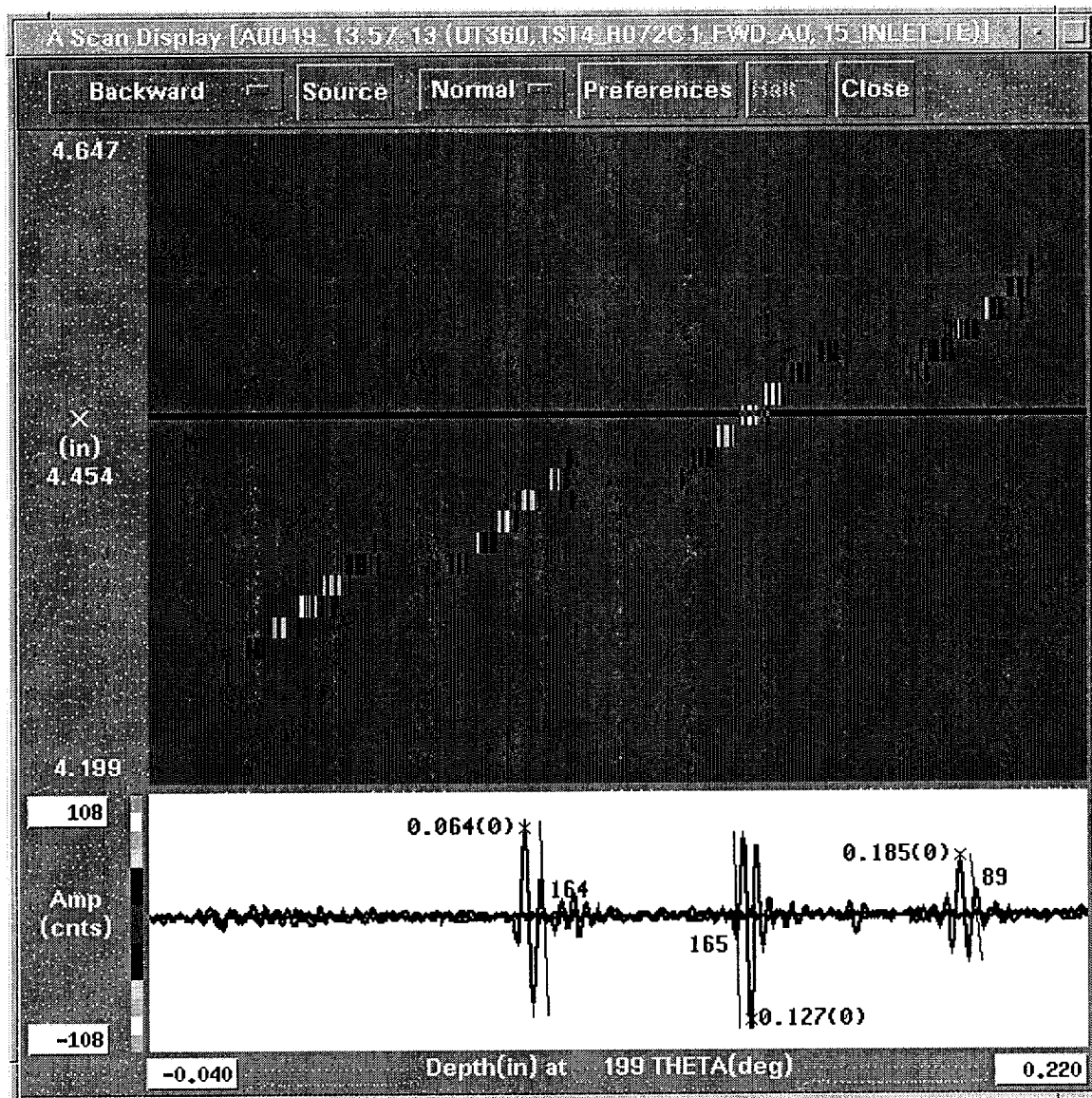


Figure R30-3

This is an A-Scan plot that presents the three waveforms that would be used for a FSN calculation. The half skip (first outer diameter reflection) is the waveform 0.064 with a 164 count amplitude. The full skip (first inner diameter reflection) is the waveform 0.127 with a 165 count amplitude. The one and one half skip (second outer diameter reflection) is the waveform 0.185 with a 89 count amplitude. The calculated FSN value is $165 / ((164 + 89) * .5)$ or 1.3. The regression equation would be solved as $(0.062 - (0.031 - 0.031 * 1.3))$ or 0.071 inch. This result would be considered through wall. The target motion to the left of the half skip target motion is caused by a near surface creeping wave detection of the fatigue crack and the inner diameter surface dimple which developed from the excavation of the ODSCC crack during deposition.

The pages that follow present the C-Scan and A-Scan plots for the pre-fatigue, post fatigue flaw and post final plating ultrasonic examinations of ENSA sample TST4-052-1. The sample underwent fatigue cycling after the deposition of ~0.008 inch of nickel sleeve material. After generation of a through wall fatigue crack, the sample received a final deposition of ~0.010 for a final combined wall thickness of ~0.068 inch. The first set of plots consists of the C-Scan of the sample prior to fatigue cycling along with two A-Scan plots associated with the FSN calculations at this process step. The second set of plots consists of the post-cycling C-Scan plot along with two A-Scan plots associated with the FSN calculations at this process step. The third set of plots consists of the post final deposition C-Scan plot along with two A-Scan plots associated with the FSN calculations at this process step.

The UT measured combined wall thickness at the crack site after the initial deposition is 0.058 inch. The UT measured combined wall thickness at the crack site after the final deposition is 0.068 inch. The UT measured parent wall thickness (8.0 inches x 210 degrees) is 0.050 inch.

To determine crack depth propagation, FSN ratios and regression depths were calculated, at two locations along the crack extent,. The table below presents a comparison of the FSN determinations at each process step. The depth results indicate that the fatigue crack penetrated the first deposition layer and was subsequently plated over during the final deposition.

Table R30-2

circ. location (degree)	After	Initial	After	Fatigue	After	Final
	FSN result	FSN depth by regression (inch)	FSN result	FSN depth by regression (inch)	FSN result	FSN depth by regression (inch)
~206	0.75	0.050	1.08	0.060	0.65	0.057
~220	0.48	0.042	0.85	0.053	0.71	0.059

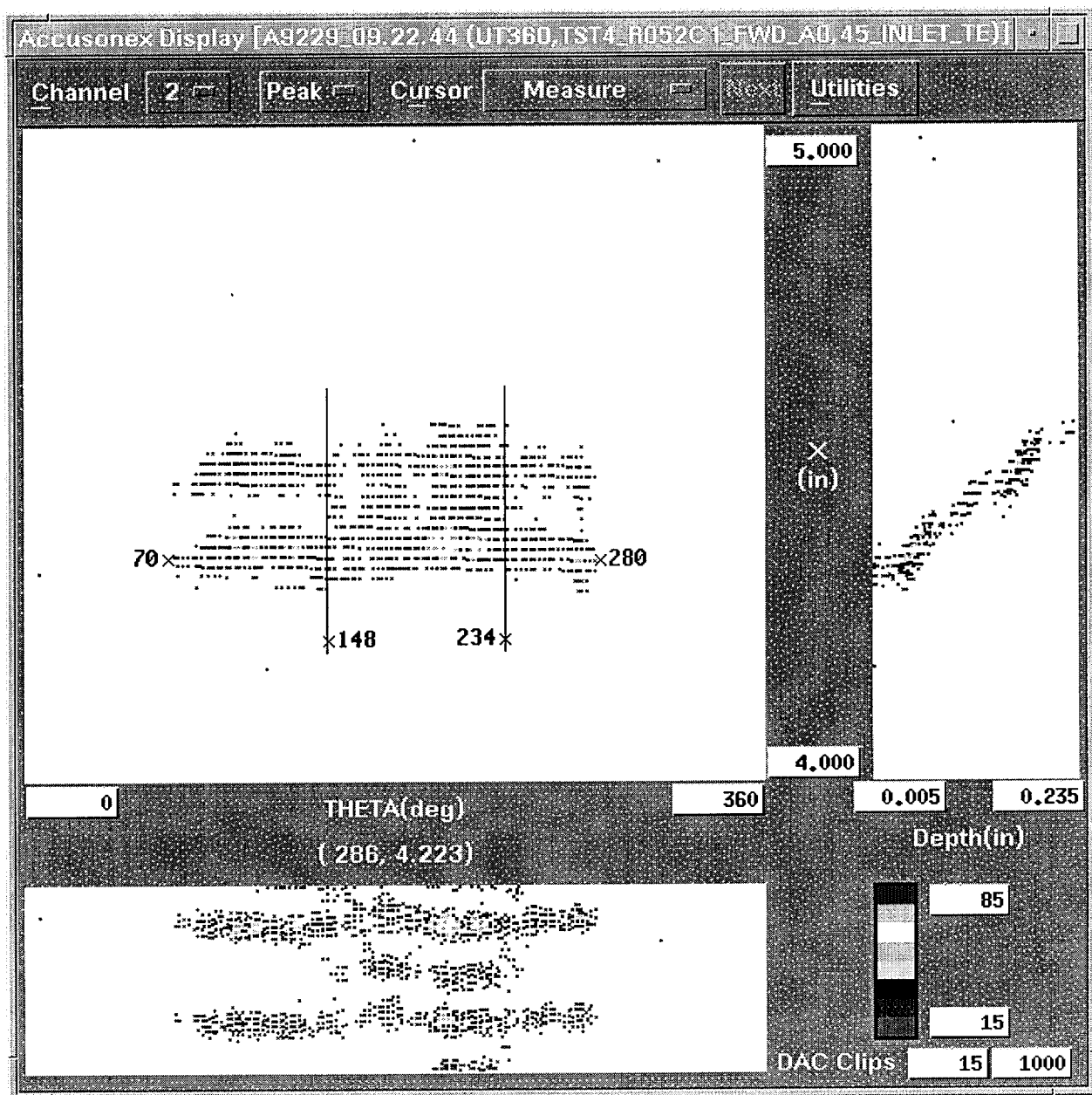


Figure R30-4

This is the pre-fatigue crack C-Scan plot of the ODSCC circumferential crack in tube TST4-052-1. The crack extent (length) can be estimated from the C-Scan plot as $(280 - 70)$ or 210 degrees. The plot shows the presence of a half skip response, a one and one half skip response and some full skip reflections between the 148 degree and 234 degree locations along the crack extent.

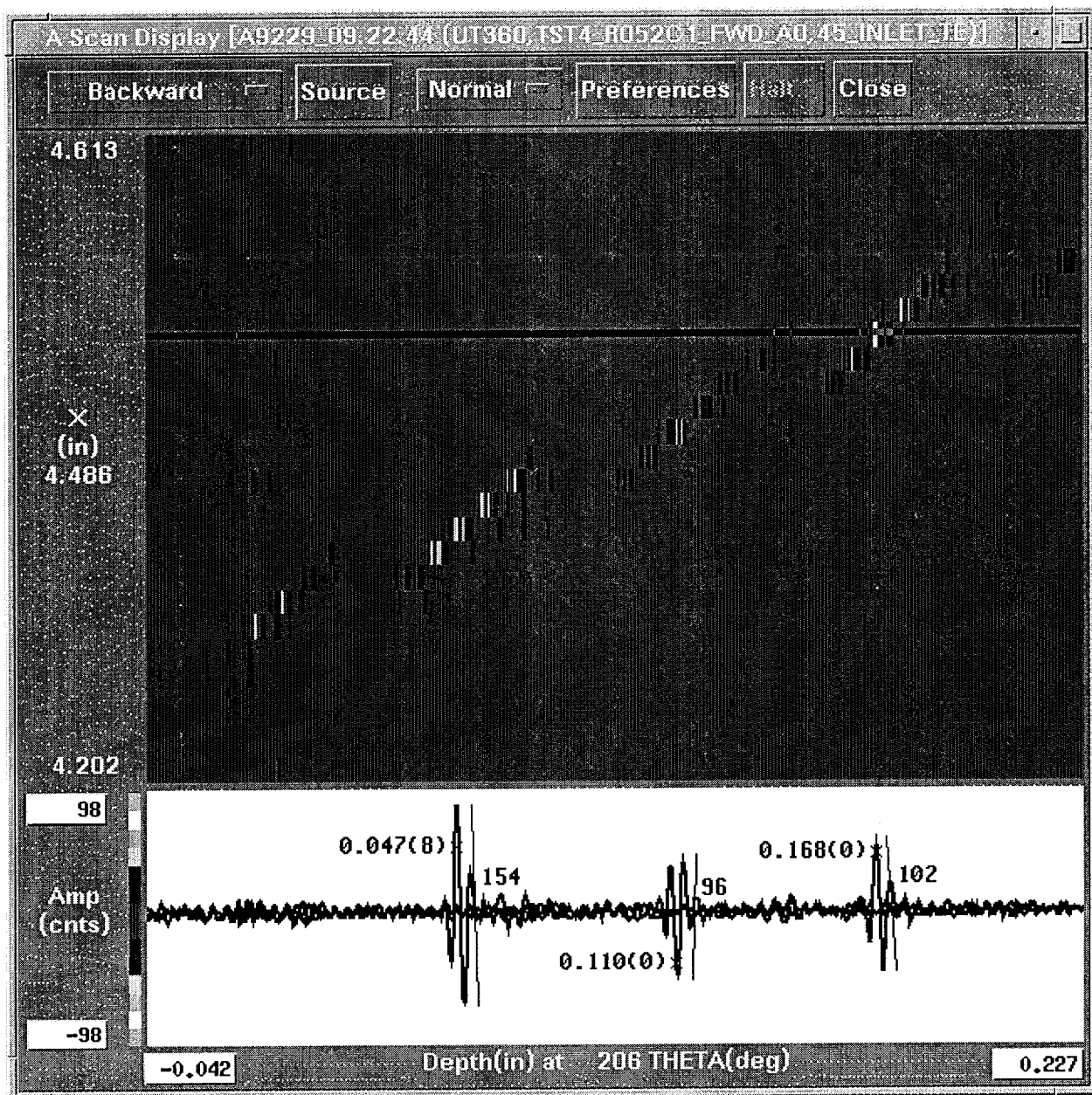


Figure R30-5

This is an A-Scan plot that presents the three waveforms that would be used for a FSN calculation at the 206 degree location. The half skip (first outer diameter reflection) is the waveform 0.047 with a 154 count amplitude. The full skip (first inner diameter reflection) is the waveform 0.110 with a 96 count amplitude. The one and one half skip (second outer diameter reflection) is the waveform 0.168 with a 102 count amplitude. The calculated FSN value is $96 / ((154 + 102) * .5)$ or 0.75. The regression equation would be solved as $(0.058 - (0.031 - 0.031 * 0.75))$ or 0.050 inch. The DE measured depth at the 204 degree location was 0.049 inch.

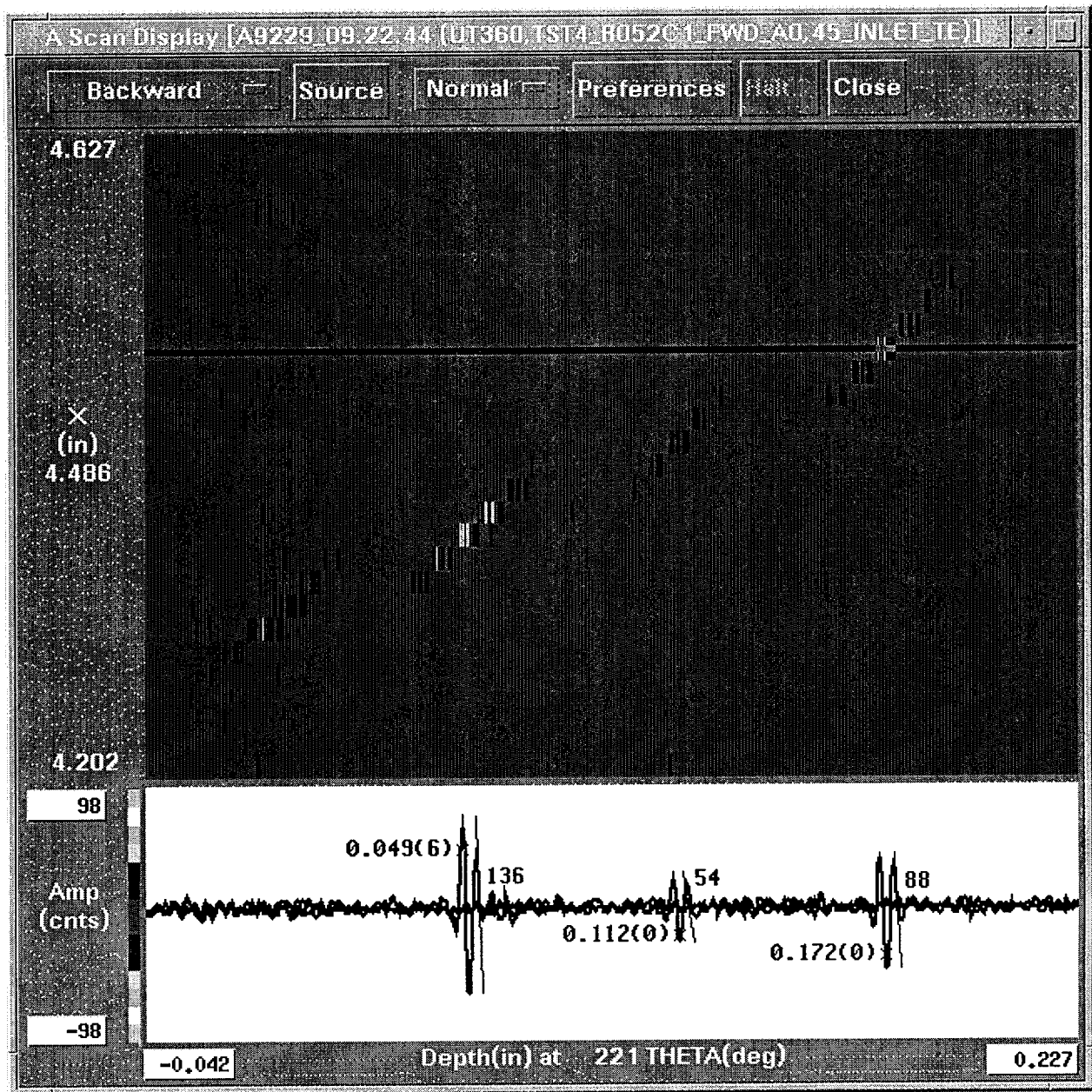


Figure R30-6

This is an A-Scan plot that presents the three waveforms that would be used for a FSN calculation at the 221 degree location. The half skip (first outer diameter reflection) is the waveform 0.049 with a 136 count amplitude. The full skip (first inner diameter reflection) is the waveform 0.112 with a 54 count amplitude. The one and one half skip (second outer diameter reflection) is the waveform 0.172 with a 88 count amplitude. The calculated FSN value is $54 / ((136 + 88) * .5)$ or 0.48. The regression equation would be solved as $(0.058 - (0.031 - 0.031 * 0.48))$ or 0.042 inch. The DE measured depth at the 220 degree location was 0.049 inch.

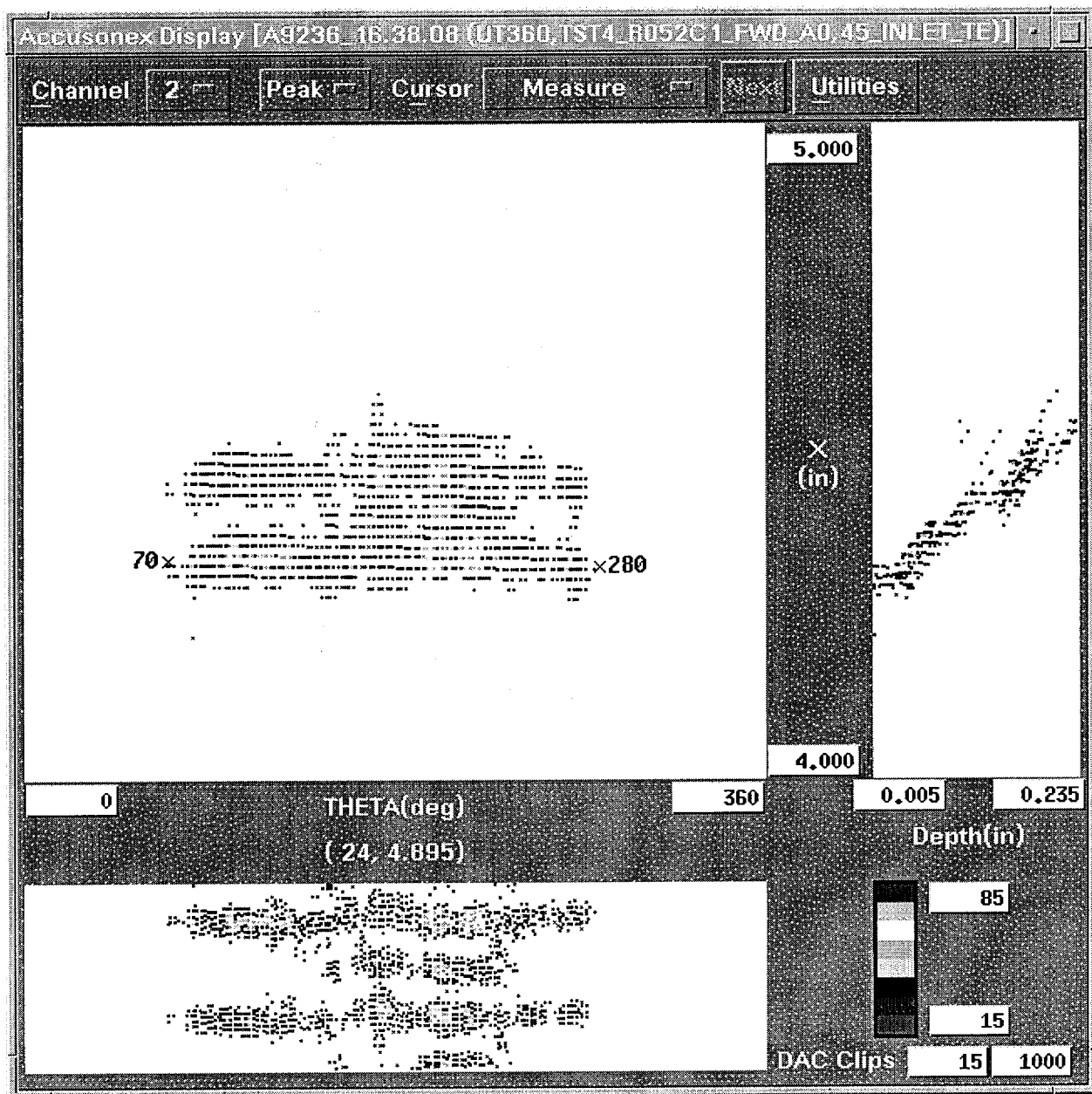


Figure R30-7

This is the post fatigue crack C-Scan plot of the ODSCC circumferential crack in tube TST4-052-1. The crack extent (length) can be estimated from the C-Scan plot as (280 – 70) or 210 degrees. The plot shows the presence of a half skip response, a one and one half skip response and an increase in the full skip response between the 200 degree and 230 degree locations along the crack extent.

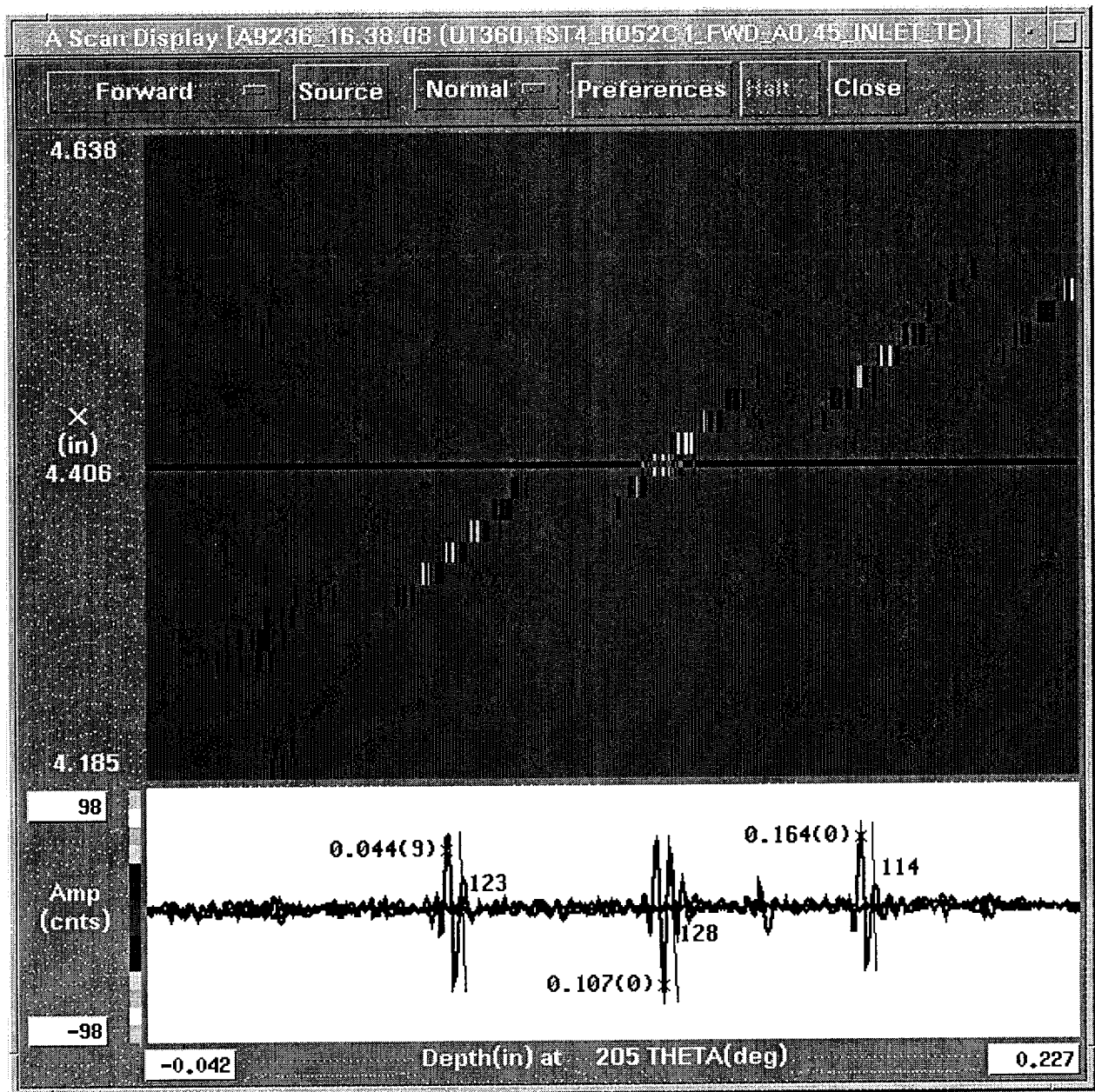


Figure R30-8

This is an A-Scan plot that presents the three waveforms that would be used for a FSN calculation at the 205 degree location. The half skip (first outer diameter reflection) is the waveform 0.044 with a 123 count amplitude. The full skip (first inner diameter reflection) is the waveform 0.107 with a 128 count amplitude. The one and one half skip (second outer diameter reflection) is the waveform 0.164 with a 114 count amplitude. The calculated FSN value is $(128 / ((123 + 114) * .5))$ or 1.08. The regression equation would be solved as $(0.058 - (0.031 - 0.031 * 1.08))$ or 0.060 inch. The DE measured depth at the 204 degree location was 0.054 inch.

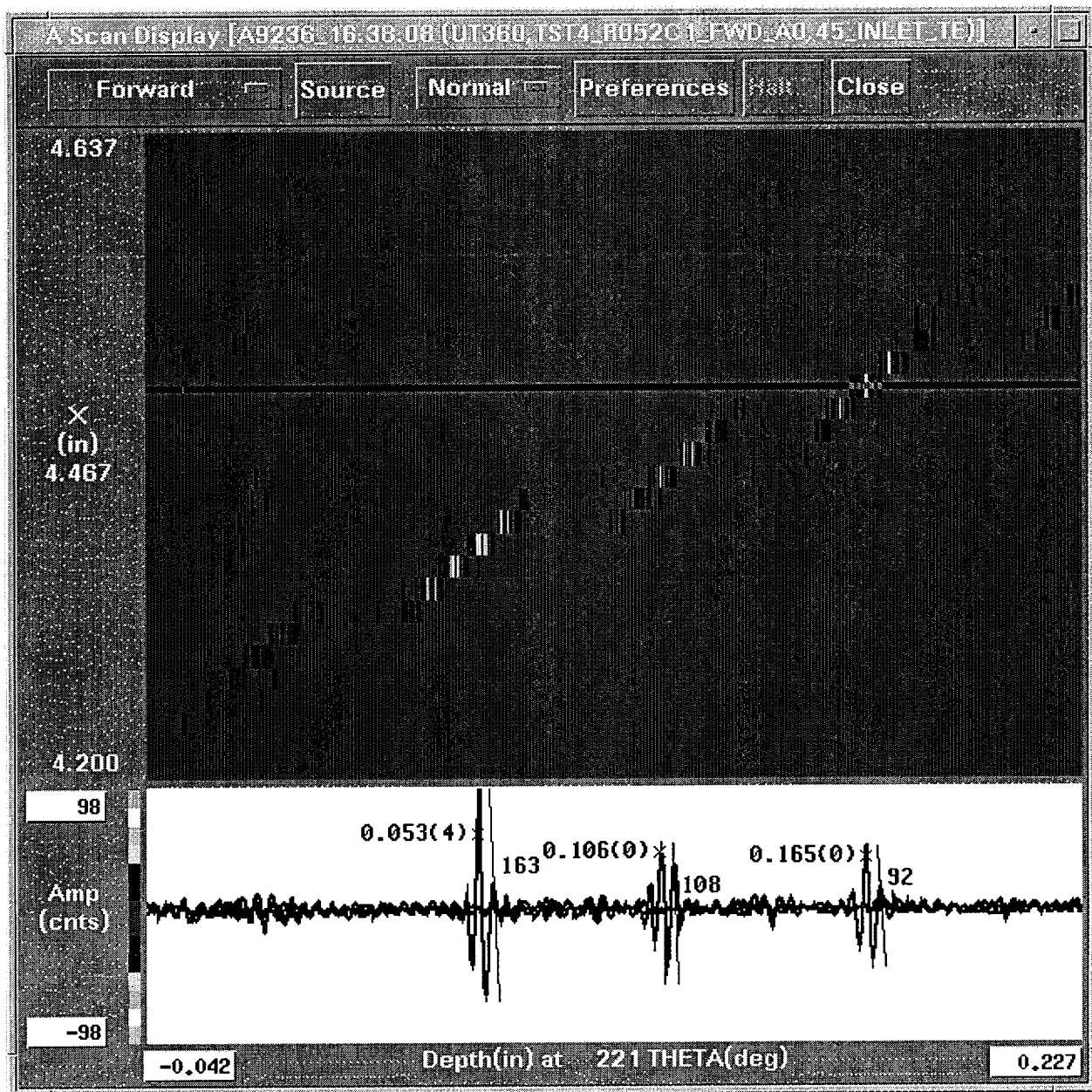


Figure R30-9

This is an A-Scan plot that presents the three waveforms that would be used for a FSN calculation at the 221 degree location. The half skip (first outer diameter reflection) is the waveform 0.053 with a 163 count amplitude. The full skip (first inner diameter reflection) is the waveform 0.106 with a 108 count amplitude. The one and one half skip (second outer diameter reflection) is the waveform 0.165 with a 92 count amplitude. The calculated FSN value is $(108 / ((163 + 92) * .5))$ or 0.85. The regression equation would be solved as $(0.058 - (0.031 - 0.031 * 0.85))$ or 0.053 inch. The DE measured depth at the 220 degree location was 0.057 inch.

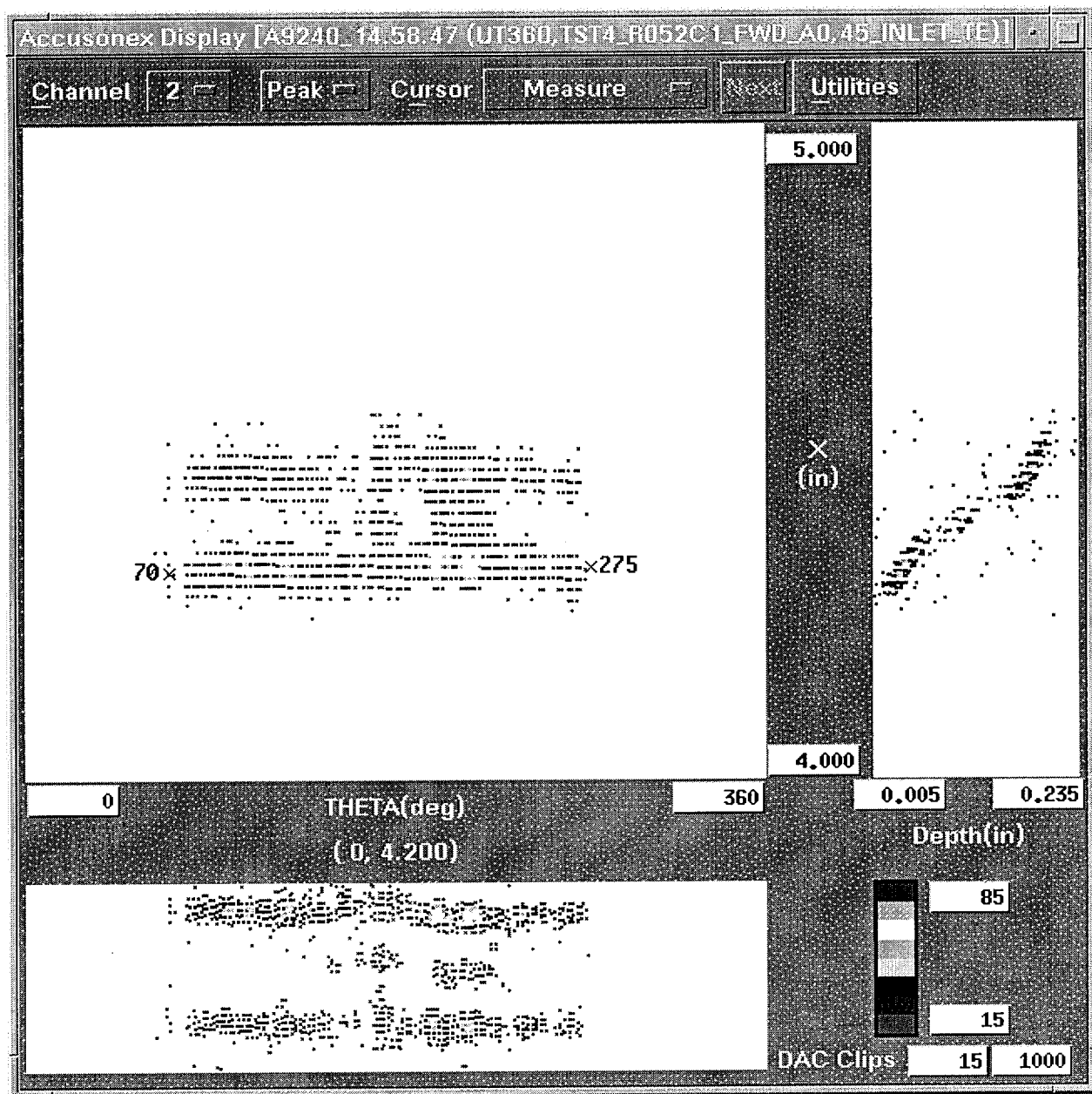


Figure R30-10

This is the post final deposition C-Scan plot of the ODSCC circumferential crack in tube TST4-052-1. The crack extent (length) can be estimated from the C-Scan plot as (275 – 70) or 205 degrees. The plot shows the presence of a half skip response, a one and one half skip response and the diminished amplitude of the full skip response.

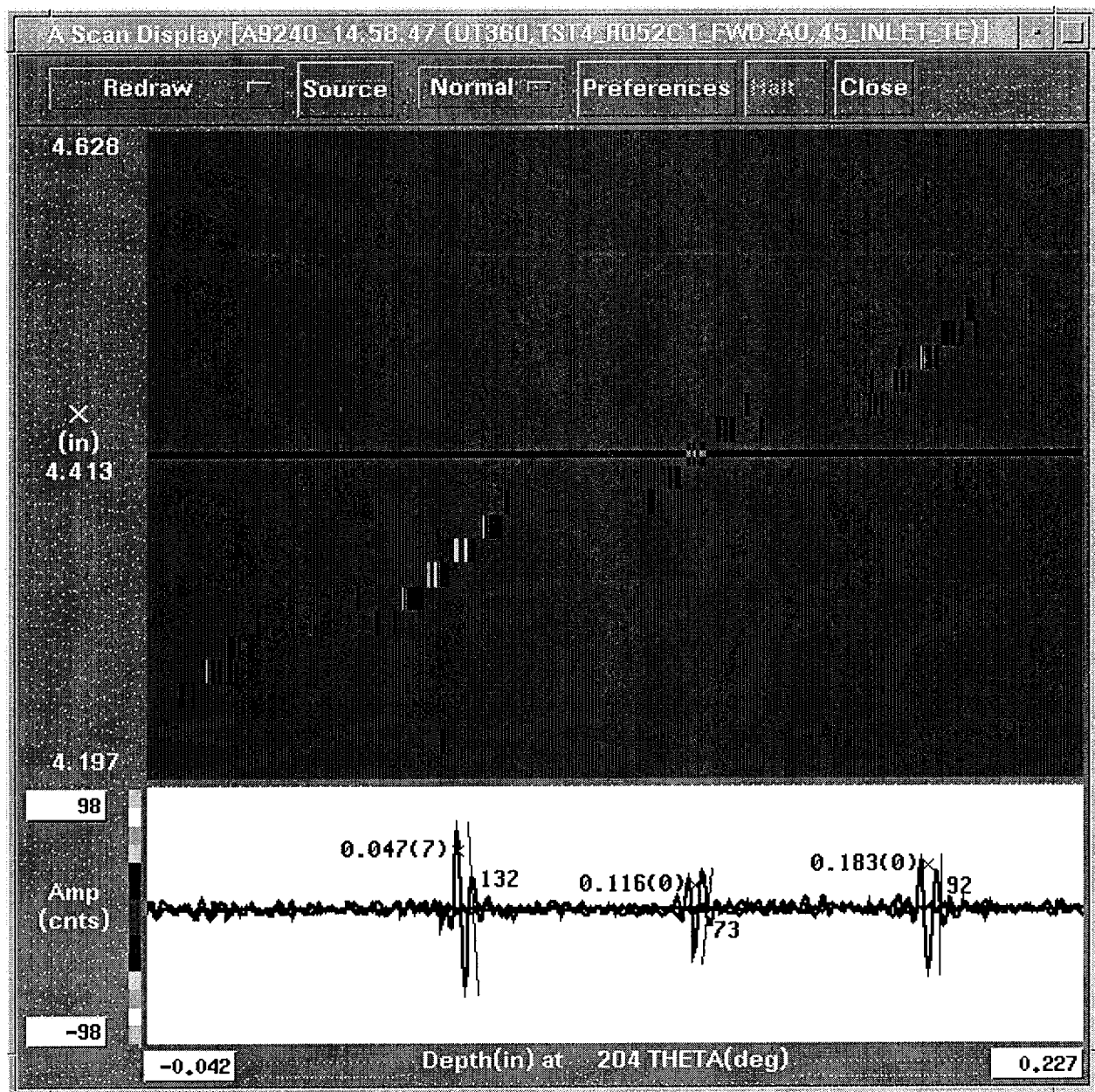


Figure R30-11

This is an A-Scan plot that presents the three waveforms that would be used for a FSN calculation at the 204 degree location. The half skip (first outer diameter reflection) is the waveform 0.047 with a 132 count amplitude. The full skip (first inner diameter reflection) is the waveform 0.116 with a 73 count amplitude. The one and one half skip (second outer diameter reflection) is the waveform 0.183 with a 92 count amplitude. The calculated FSN value is $73 / ((132 + 92) * .5)$ or 0.65. The regression equation would be solved as $(0.068 - (0.031 - 0.031 * 0.65))$ or 0.057 inch. The DE measured depth at the 204 degree location was 0.054 inch.

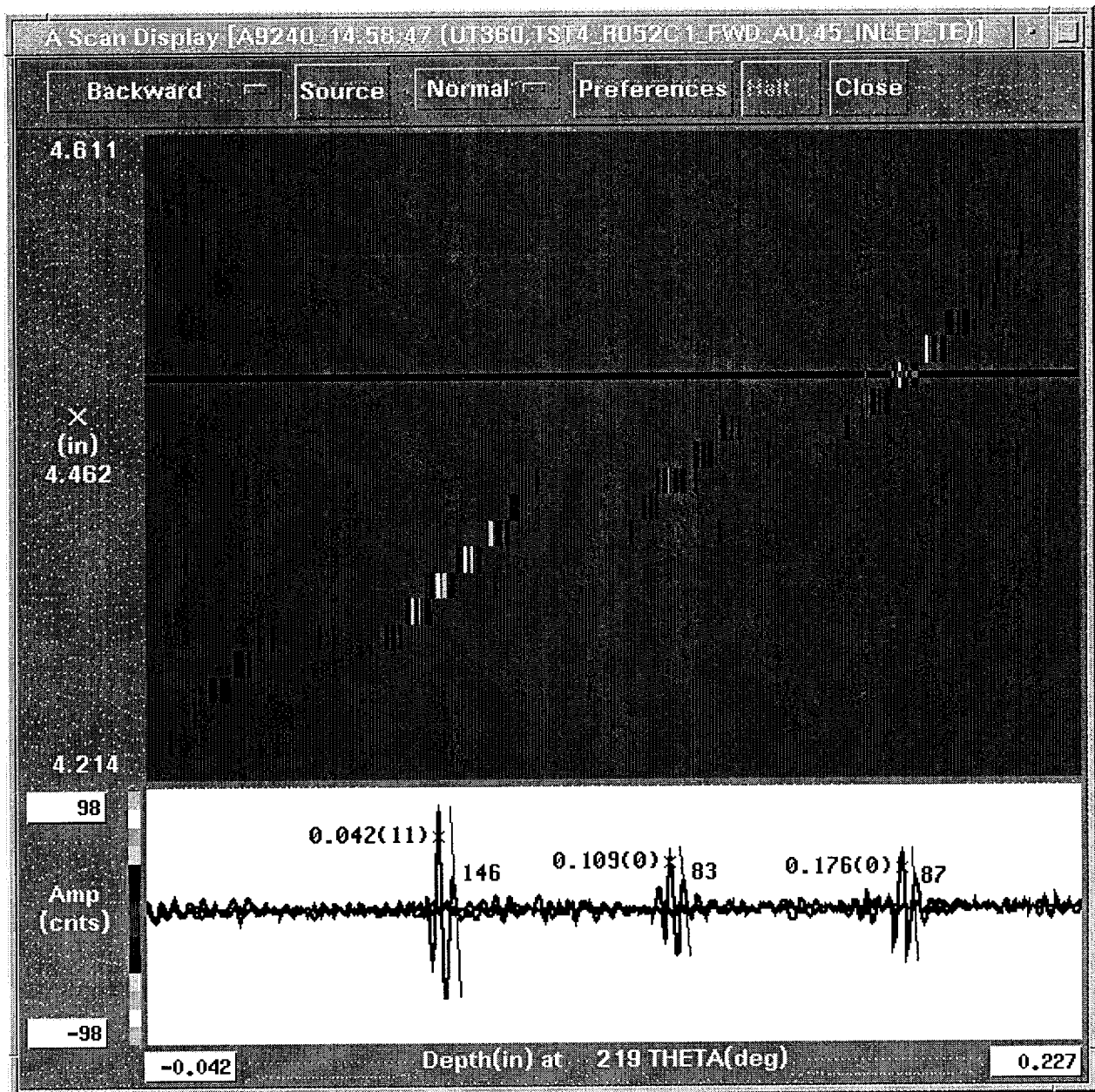


Figure R30-12

This is an A-Scan plot that presents the three waveforms that would be used for a FSN calculation at the 219 degree location. The half skip (first outer diameter reflection) is the waveform 0.042 with a 146 count amplitude. The full skip (first inner diameter reflection) is the waveform 0.109 with a 83 count amplitude. The one and one half skip (second outer diameter reflection) is the waveform 0.176 with a 87 count amplitude. The calculated FSN value is $83 / ((146 + 87) * .5)$ or 0.71. The regression equation would be solved as $(0.068 - (0.031 - 0.031 * 0.71))$ or 0.059 inch. The DE measured depth at the 220 degree location was 0.057 inch.

Summary for TST4-052-1

This sample is an ODSSC circumferential flaw propagated by internal pressure plus bending to produce tensile stresses and grow a fatigue flaw. The depth and extent of the "Flaws" were measured by scanning electron microscope (SEM) after the remaining tube/sleeve material was ruptured by application of an axial load.

Table R30-3

UT @ 206°	0° UT Thickness inches	Shear UT FSN Flaw Depth, in.	DE Flaw Depth, in. (SEM)(1)	UT Flaw in Sleeve inches	DE Flaw in Sleeve inches	Delta UT - DE Inches
Parent Tube	0.050	0.050	0.049	NA	NA	NA
+ 8 mils and Fatigue	0.058	0.060	204° 0.054	0.008	0.005	+0.003
+10 mils	0.068	0.057	204° 0.054	0.007	0.005	+0.002
UT@ 220°						
Parent Tube	0.050	0.042	220° 0.049	NA	NA	NA
+ 8 mils and Fatigue	0.058	0.053	220° 0.057	0.003	0.008	-0.005
+10 mils	0.068	0.059	220° 0.057	0.009	0.008	+0.001

Notes:

1. DE of sample was performed after both layers of sleeve material were installed. An axial pull, to fail the sample, was used to open up the flaw for SEM examination. The SEM fracture analysis contains the corrosion-induced flaw depth, the fatigue flaw depth, and the tensile rupture of the remaining wall.

Conclusion:

Therefore UT correctly tracked a fatigue flaw that was less than 100% through wall.

RAI # 31. In Table 11.8.12, how was the “actual dent” measured for each tube? (Page 11-51, BAW-10219P, Rev. 4)

Response:

The actual dimensional values (dent deformation) were determined by two physical measures. The first method used a micrometer to determine the minimum and maximum values of the outer diameter at the dent location. The difference between the nominal outer diameter and the minimum diameter is a measure of the dent deformation from the outer diameter. The second method used graduated pin gauges, 0.001 inch steps, to determine the maximum inner diameter free path. A series of pins were inserted into the tube until two pins were identified such that one pin would pass and the next larger pin would not pass. The outer diameter dimension of the larger pin was assigned as the maximum inner diameter free path. These two physical measurements compared well with a 0.001 inch standard deviation. Either of these two physical measurements can be used to determine the dent deformation. The ultrasonic dent deformation measure was compared to the pin gauge results since both of the methods (UT and pin) are measures of inner diameter deformation.

RAI # 32. The report states that the “results listed in Table 11.8.15 show that the maximum error and the RMSE are sufficient to meet the requirements for sleeve thickness examination.” Table 11.8.15 provides error measurements specific to the combined wall thickness, and doesn’t contain any sleeve thickness measurements. Is it reasonable to infer that the error for measuring sleeve thickness would be identical to that of the combined wall thickness? Provide the basis for why the values would be the same. (Page 11-56, BAW-10219P, Rev. 4)

Response:

Thickness measurement is a basic use of UT. The passage of sound in a material is a linear function in which the velocity of sound is the slope. The error in sleeve thickness is consistent with the combined wall thickness measurement error. An expansion of the data in Table 11.8.15 shows that the sleeve thickness is calculated by subtracting the parent tube thickness from the combined wall thickness. The parent tube thickness is measured in the tube at the same circumferential location just above the sleeve. This is conservative in that the excavation of the parent tube during the activation phase of the deposition process is not taken into account. This excavation typically results in removing approximately 0.0015 inch from the tube ID, which results in the sleeve being 0.0015 inch thicker than calculated.

The table on the following page shows that the standard deviation of the error in computing the sleeve wall thickness is comparable to the standard deviation of the error in computing the combined wall thickness given in Table 11.8.15.

Table R32-1. Comparison of Calculated vs. Actual Sleeve Wall Thickness

crack	DE measured parent tube wall thickness (inch)	DE measured sleeve wall thickness (inch)	DE calculated combined wall thickness (inch)	UT measured combined wall thickness (inch)	UT measured parent tube wall thickness (inch)	UT calculated sleeve wall thickness (inch)	velocity corrected sleeve wall thickness (inch)	difference UT vs DE uncorrected sleeve wall thickness (inch)	difference UT vs DE corrected sleeve wall thickness (inch)
A1	0.038	0.036	0.074	0.075	0.042	0.033	0.032	-0.003	-0.004
A2	0.040	0.037	0.077	0.079	0.042	0.037	0.036	0.000	-0.001
A3	0.041	0.035	0.076	0.077	0.043	0.034	0.033	-0.001	-0.002
A4	0.041	0.035	0.076	0.077	0.043	0.034	0.033	-0.001	-0.002
A5	0.042	0.033	0.075	0.076	0.043	0.033	0.032	0.000	-0.001
A8	0.041	0.036	0.077	0.078	0.042	0.036	0.035	0.000	-0.001
A9	0.041	0.037	0.078	0.080	0.042	0.038	0.037	0.001	0.000
A10	0.041	0.035	0.076	0.077	0.044	0.033	0.032	-0.002	-0.003
A11	0.042	0.035	0.077	0.078	0.044	0.034	0.033	-0.001	-0.002
C1	0.042	0.039	0.081	0.080	0.043	0.037	0.036	-0.002	-0.003
C2	0.041	0.031	0.072	0.072	0.043	0.029	0.028	-0.002	-0.003
C3	0.039	0.036	0.075	0.074	0.040	0.034	0.033	-0.002	-0.003
C4	0.040	0.035	0.075	0.075	0.041	0.034	0.033	-0.001	-0.002
C5	0.042	0.034	0.076	0.076	0.044	0.032	0.031	-0.002	-0.003
C6	0.042	0.035	0.077	0.076	0.043	0.033	0.032	-0.002	-0.003
C7	0.041	0.039	0.080	0.080	0.043	0.037	0.036	-0.002	-0.003
C8	0.042	0.037	0.079	0.079	0.044	0.035	0.034	-0.002	-0.003
C9	0.042	0.036	0.078	0.078	0.044	0.034	0.033	-0.002	-0.003
						max	(overcall)	0.001	0.000
						min	(undercall)	-0.003	-0.004
						ave		-0.001	-0.002
						stdev		0.001	0.001

Repair Limit

RAI # 33. The Rev. 4 to BAW-10219P states that the "Electrosleeve plugging limit is conservatively set at 30% through-wall of the sleeve nominal thickness." Rev. 3 to BAW-10219P states that the "Electrosleeve plugging limit is 20% through-wall of the sleeve nominal thickness." However, the Callaway Technical Specifications provided with the 2/15/01 UE submittal state that "[t]he plugging or repair limit for the pressure boundary portion of Electrosleeves is determined to be 20% through wall of the nominal sleeve wall thickness (as determined by NDE)." Please resolve this apparent discrepancy. (Page 11-64 and Section 12, beginning on 12.1, BAW-10219P, Rev. 4)

Response:

The better NDE performance resulting from the improved UT techniques presented in BAW-10219P-Rev. 4 resulted in a crack depth sizing error that supports repair limits presented in Section 12. Table 12.4.4 contains the repair limits for the different flaw morphologies of concern. Note that these range from 37% TW for uniform thinning to []^{b,c,e} TW for OD pits. The 30%TW sleeve repair limit given in Revision 4 of the topical report was selected as a conservative repair threshold that bounds all degradation types. The 20% TW sleeve plugging limit stated in the Callaway Technical Specification is an ADMINISTRATIVE limit established by Callaway for the MEASURED flaw depth. This represents an additional conservatism relative to that justified in BAW-10219P-Rev.4.

RAI # 34. The tube repair limit with respect to sleeve OD pitting is discussed in this report. The report states that the structural limit calculations defined a maximum allowed structural degradation of []^{b,c,e} of the sleeve nominal thickness for a sleeve OD pit degradation mechanism. What pit diameter is assumed? (Pages 12-3, 12-4, BAW-10219P, Rev. 4)

Response:

The assumed pit diameter is 0.250 inch, which is acceptable as shown on Figure 8.5.3 BAW-10219P-Rev.4.

Editorial remarks:

RAI # 35. Editorial remark - Rev. 3 of BAW-10219P contained a section discussing D-Scan Maps, that was subsequently removed in Rev. 4 of the topical report. However, even though it is no longer discussed in the following sections, the reference to D-scans still exists on page 11-17 of Rev. 4. (Page 11-17, BAW-10219P, Rev. 4)

Response:

D-scans are still mentioned because the analysis software still has the capability of producing them. No measurements are made from this plot, but some utilities request that it be included as part of their inspection results for completeness.

RAI # 36. Editorial remark - On page 3 of ULNRC-4391, which is Attachment 2 to the February 15, 2001 letter from UE conveying the FTI report, a typographical error exists. In the 4th full paragraph from the top of the page, the first and last sentences refer to Section 10.1.5. However, in the last sentence, the numbers are transposed, so that the Section is listed as 10.5.1. Section 10.5.1 does not exist in the FTI report.

Response:

This is a typographical error in ULNRC-4391, reference to section in the topical report. The referenced section should be 10.1.5.

Attachment 5c

Framatome ANP considers some of the information contained in attachment 5 to this letter to be proprietary. This information has been noted by enclosing it within brackets. The affidavit provided with the original submittal, ULNRC-4391, dated February 15, 2001, of the referenced topical report satisfies the requirements of 10CFR2.790(b) to support the withholding of this information from public disclosure.